Modelling and simulation of the dynamic behaviour of the automobile

Raffaele Di Martino

Università degli Studi di Salerno

UHA Université de Haute Alsace

FACULTY OF ENGINEERING

Course of degree in Mechanical Engineering

Thesis of degree

Modelling and Simulation of the Dynamic Behaviour of the Automobile

Author:

Di Martino Raffaele

Matr. 165/000101

Supervisor:

Professor Gérard Léon Gissinger

Co-Supervisor:

Professor Gianfranco Rizzo

Dr. Eng. Ivan Arsie

Academic year 2004/2005

Title of degree

Modelling and Simulation of the Dynamic Behaviour of the Automobile

by

Di Martino Raffaele

Thesis submitted to the Faculty of Engineering,

University of Salerno

in partial fulfilment of the requirements for the degree of

DOCTOR IN MECHANICAL ENGINEERING

Author:

Di Martino Raffaele
Matr. 165/000101

Supervisor:

Professor G. L. Gissinger

Co-Supervisor:

Professor G. Rizzo

Dr. Eng. Ivan Arsie

Modelling and Simulation of the Dynamic Behaviour of the Automobile

Raffaele Di Martino

G. L. Gissinger Supervisor and *G. Rizzo* Co-Supervisor

Mechanical Engineering

Abstract

This study, carried out in cooperation with ESSAIM, Ecole Supérieure des Sciences Appliquées pour l'Ingénieur, Mulhouse in France, was aimed at developing accurate mathematical models of some types of tyre, in order to analyze their influence on vehicle dynamics. The complete vehicle was studied under dynamic conditions, to quantify the influence of all factors, such as rolling forces, aerodynamic forces and many others, acting on their components on torque distribution and vehicle dynamics. Mathematical models for two common types of vehicle, namely front and rear wheel drive, each ones equipped with the different types of tyre, were developed. Both models were used to simulate the behaviour of a real vehicle, developing complete simulation software, developed in Matlab-Simulink environment at MIPS, Modélisation Intelligence Processus Systèmes. Therefore, this car model, running on a straight and curve track, was also developed, to get a qualitative insight of the influence of these kinds of interactions on traction capabilities. The software, used to simulate some dynamics manoeuvres, shows up the basic behaviour of vehicle dynamics.

Dedicated to my grandmother, who, with her love, patience, and encouragement during my studies, made this aim possible.

Acknowledgements

I would like to express my gratitude to some of the people who contributed to this work. First, I would like to thank my Professor G. Rizzo for his guidance and direction in the development and conduct of this research. I would like to thank Professor G.L. Gissinger, my advisor for the duration, for supporting me during my time here at ESSAIM, Ecole Supérieure des Sciences Appliquées pour l'Ingénieur, Mulhouse in France. During these six months they have also been friendly and I sincerely hope we find opportunities in the future to work together once again. Conteins

Professor Michel Basset and Assistant Professor Jean Philippe Lauffenburger must also be mentioned for their insightful comments that have exemplified the work during the development of my thesis.

I would also like to extend my thank to Doctor Engineer Ivan Arsie and Professor Cesare Pianese for their encouragement and invaluable assistance.

Anyone who was around when I began my work knows that I have to express my gratitude to Engineer Eduardo Haro Sandoval, for his patience, expertise, and support during my six moths in the Research Laboratory. Many thanks must be given to Ing. Julien Caroux, for his assistance in developing and programming the software dedicated to study about the behaviour of the vehicle. Both, friendship have made the last six months very enjoyable.

Above anyone else I would like to thank, Engineer Alfonso Di Domenico and Engineer Michele Maria Marotta, who, trough their assistance have made some moments could be overcome easily.

Lastly, I would like to thank my parents, and other people close to me for giving me the opportunity to come to the University of Haute-Alsace. They have been a tremendous emotional and psychological support to me throughout these few months and for that I am eternally thankful. I sincerely believe that this work would not exist without their guidance and support.

Table of Contents

List of Figures

List of Tables

List of Symbols

l_1, l_2	CG location	m
l_3	Vertical drawbar load location	m
l	Wheelbase of the vehicle	m
t	Track of the vehicle	m
W	Weight of vehicle	N
g	Gravitational acceleration	m/s^2
m_v	Mass of vehicle (W/g)	Kg
I_z	Yawing moment of inertia	Kg m^2
ψ	Rotation angle of the vehicle	rad
X_G	Longitudinal displacement of the vehicle	m
Y_G	Lateral displacement of the vehicle	m
(x_0, y_0, z_0)	Coordinate system "*ground axis*"	
(x, y, z)	Fixed coordinate system "*body axis*"	
$(\boldsymbol{i}, \boldsymbol{j}, \boldsymbol{k})$	Versors axis	
(X, Y, Z)	Resultant of totally forces acting on the vehicle	N
(L, M, N)	Resultant of totally moments acting on the vehicle	N
$\boldsymbol{a_y}$	Lateral acceleration	m/s^2
$\boldsymbol{a_x}$ $(=d^2x/dt^2)$	Longitudinal acceleration	m/s^2
$\boldsymbol{A_y}$ $(=\boldsymbol{a_y}/g)$	Lateral Coefficient	/
$\boldsymbol{V}$	Vehicle absolute velocity	m/s
r	Yawing velocity	rad/s
u	Longitudinal velocity (or Feed velocity)	m/s
δ	Steer angle front wheels	rad
δ_e	External steering wheel	rad
δ_i	Internal steering wheel	rad
α_f, α_r	Slip angles	rad
β	Vehicle slip angle (or Sideslip angle)	rad
C_α	Cornering stiffness	N/rad

$J_{w,f}$	Inertia front wheels	kg m^2
$J_{w,r}$	Inertia rear wheels	kg m^2
F_{xa}	Aerodynamic force acting in forward direction	N
F_{za}	Aerodynamic force acting in vertical direction	N
M_{ya}	Aerodynamic Moment acting on pitch direction	N
h_1	Inertia-forces location	m
h_2	Aero-forces location	m
Δ_{x1}	Characteristic front length	m
Δ_{x2}	Characteristic rear length	m
$\Delta_x (=U)$	Characteristic lengths	m
R_{r1}	Rolling radius of the front wheels	m
R_{r2}	Rolling radius of the rear wheels	m
R_r	Effective rolling radius	m
F_{x1}	Rolling resistance at front tyre	N
F_{x2}	Rolling resistance at rear tyre N	
F_{y1}	Lateral force at front tyre	N
F_{y2}	Lateral force at rear tyre	N
F_{z1}	Vertical load at the front axle	N
F_{z2}	Vertical load at the rear axle	N
F_{xd}	Drawbar load in forward direction	N
F^s_{z1}	Vertical static load at the front axle	N
F^s_{z2}	Vertical static load at the rear axle	N
F_{zd}	Drawbar load in backward direction	N
p	Inflation of pressure	bar
f_i	Experimental coefficient (depending tyre)	/
f_0	Experimental coefficient (depending tyre)	/
K	Experimental coefficient (depending tyre)	/
f_s	Static friction coefficient	/
f_d	Sliding friction coefficient	/
f_r	Rolling resistance coefficient	/

μ	Adhesion transversal coefficient	/
θ	Grade	rad
i	Slope	/
H_f	Longitudinal component of the chassis-reaction	N
V_f	Vertical component of the chassis-reaction	N
$d^2\theta_f/dt^2$	Angular acceleration at the front wheels	rad/s^2
$d^2\theta_r/dt^2$	Angular acceleration at the rear wheels	rad/s^2
ω_w	Rotational velocity of the wheels	rad/s
ω_e	Rotational engine speed	rad/s
n_e	Rotational engine speed	rpm
$n_{e\max}$	Maximum value of the rotational engine speed	rpm
$n_{e\min}$	Minimum value of the rotational engine speed	rpm
P_e	Engine power	kw
T_e	Engine torque	Nm
$T_{e\max}$	Maximum value of the engine torque	Nm
$T_{e\min}$	Minimum value of the engine torque	Nm
T_l	Load torque	Nm
P_l	Load power	kw
T_{aero}	Aerodynamics torque	Nm
$T_{rolling}$	Rolling Resistent torque	Nm
T_{slope}	Slope torque	Nm
α	Throttle opening	%
I_e	Engine inertia	kg m^2
I_w	Wheel inertia	kg m^2
J	Moment of inertia	kg m^2
I_{eq}	Equivalent inertia	kg m^2
$I_{chassis}$	Chassis Inertia	kg m^2
I_{wheel}	Wheel Inertia	kg m^2
I_{cgi}	Crank gear inertia	kg m^2
I_{fw}	Flywheel inertia	kg m^2
τ_c	Transmission gear ratio	/

τ_d	Transmission final drive ratio	/
η_c	Efficiency of the gear box	/
η_d	Efficiency of the final drive	/
τ	Kinetic Energy of the vehicle	J
m_c	Crank mass	kg
m_{cr}	Connecting Rod Big End mass	kg
R_c	Crank radius	m
n_{cyl}	Cylinder number	/

Chapter 1

1 Introduction

This chapter illustrates the ground vehicle development which has traditionally been motivated by the need to move people and cargo from one location to another, always with the intent of having a human operator.

1.1 Historical Notes on Vehicles

Since the inception of the wheel as a viable means of ground transportation, man has been on a never-ending quest to optimize its use for the transport of people and cargo. Vehicles of all shapes, sizes, and weights have been built to accomplish one task or another. Although vastly different in design and intended application, we could classify most ground vehicles in terms of a single design feature; the number of wheels. This classification does not predicate advantages of one vehicle over another. However, it does provide a metric against which the designer may estimate of a vehicle's potential performance characteristics and general capabilities. Therefore, it stands to reason that the historical record should demonstrate mankind's quest to classify the dynamic characteristics and performance advantages of vehicles with every conceivable number of wheels. This is in fact the case. Simply by examining the design and use of ground transportation throughout history, we can see both experimentation and refinement in the design of everything from vehicles having no wheels (tracks or legs) to those containing hundreds of wheels (trains). Figure 1.1 presents the best known single-wheel

Figure 1.1: One-Wheel Vehicle (Rousseau-Workshops, France,wheel radius 2 m, without steer, 1869)

vehicle, the unicycle. Although this would have been the only possible configuration at the moment of the wheel's inception, the design has never proven itself as an effective means in the transportation of people and cargo.

However, it remains in mainstream society as a source of entertainment and amusement. Likewise, we see in Figure 1.2 the common perception of the two-wheel vehicle, the bicycle. This design, though inherently unstable, has found widespread use and acceptance throughout the world.

Figure 1.2: Two-Wheel Vehicle (Turri and Porro, Italia, 1875)

Although the standard bicycle has met with great success in both human and engine-powered transportation its overall utility as a workhorse remains a point of debate. Millions of people all over the world rely on the standard bicycle as their primary mode of transportation.

At this point, we could make a strong argument for the correlation between how many wheels are on a vehicle and its relative usefulness to society. Indeed, we could continue this pattern by examining some of the more successful three-wheel designs. Though not as prevalent in number as bicycles and motorcycles, this design shows up in everything from toy tricycles to commercially successful off and on-road vehicles. Figure 1.3 presents a very successful three-wheel car marketed by the Morgan motor company during the late 1920's.

These types of vehicles are still highly acclaimed and sought after by both collectors and driving enthusiasts. Naturally, they also tend to be much more stable than bicycles and motorcycles, but problems still exist. In fact, it was the high-speed instability of the three-wheel all-terrain vehicle that ultimately led to its demise [Johnson, 1991]. So if we continue on the premise that more is better, we may consider several more steps in ground vehicle design.

Nothing need be said concerning the success of the four-wheel vehicle; one of the finest examples of which is presented in Figure 1.4. No other vehicle type has met with more public enthusiasm than the standard automobile.

Figure 1.3: Production Three-Wheel Vehicle (1929 Morgan Super Sports Aero)

Four wheeled vehicles are used in public, private, and industrial transportation and have become an icon of the American dream. Again we see ever-increasing numbers of people and amounts of cargo being moved over the world's roadways every year. Compared to the success of the four-wheel vehicle class, the popular two-wheelers and nearly forgotten three-wheelers are primitive in their capabilities.

Larger trucks designed specifically for cargo handling can have anywhere from 10 to 22 wheels. These examples effectively support the thesis that more wheels inherently lead to more utility when considering the transportation of people and cargo.

Finally, if we take the utility to number of wheels correlation toward the limit, we find one of the most influential vehicle types since the development of the wheel itself, the train; see Figure 1.5. Largely responsible for United States expansion in the West, the train represents to limit of the wheel-utility correlation.

Most of a train's volume is dedicated to cargo. Its efficiency in ground transport is therefore undeniable. Even today when most Americans do not travel by train, it remains at the forefront of industrial transportation.

We have made an argument supporting the idea that more wheels are better. In light of this apparent correlation, one would assume that investigation of the two-wheel concept would prove fruitless. However, what must be considered here is that the historical development of ground vehicles has focused on efficiency in business, commerce, and personal transportation.

Figure 1.4: Production Four-Wheel Vehicle (1963 Austin Healey 3000 MKII**)**

Figure 1.5: Multiple-Wheel Ground Vehicle: The Train

Further, designers of ground vehicles have in general worked under the assumption that vehicle control would ultimately fall into the hands of a human pilot. If another metric of utility is employed, we see much different results.

1.2 Thesis Outline

I will begin with a brief history of land based transportation vehicles from antiquity to the present and proceed to a thorough discussion of modern motor vehicle dynamics. Chapter 2 illustrates the motivation for studying the vehicle dynamics and so the research objective, showing with all its complexity the undefined environment of the topic. Following the same direction, Chapter 3 describes the axis system used throughout this research, which is the standardized SAE vehicle axis system. This section also explains the mechanism of pneumatic tyres, particularly the forces acting between road and wheel. Then, the longitudinal and lateral vehicle dynamics models will be presented into Chapter 4 and 5, respectively. The derivation of the three-degree-of-freedom vehicle model will be described, referring particularly attention to the dynamic behaviour of the system. In the following models which will be shown, the transformation of equations of motion to the state space form did not perform because it was not possible, owing the mathematical difficulty. The logic of the simulation program in Matlab/Simulink environment and the structure of the script code are provided in Chapter 6. Instead, in Chapter 7 some experimental tests required in order

to perforce a validation of the complete vehicle model will be presented. Definitions of some problems associated with this particular comparison between the reference, means experimental tests and the mathematical model will be also discussed. Finally, the conclusion of the research and recommendation on future research are provided in Chapter 8. Appendixes contain the major Matlab m-files used to perform the simulations.

Chapter 2

2 Vehicle Dynamics

This chapter describes a general overview of this research. Background information related to the topic of vehicle dynamics and modelling along with research objectives are introduced. Related literature is reviewed in this section, linking relevant topics to the research presented here. Finally, an outline of the thesis and a brief description on the contents of each chapter are also presented.

2.1 Motivation for Studying Vehicle Dynamics

Research in vehicle dynamics has been an on-going study for decades, ever since the invention of automobiles. Engineers and researchers have been trying to fully understand the dynamic behaviour of vehicles as they are subjected to different driving conditions, both moderate daily driving and extreme emergency manoeuvres. They want to apply this finding to improve issues such as ride quality and vehicle handling stability, and develop innovative design that will improve vehicle operations. With the aid of fast computers to perform complicated design simulations and high speed electronics that can be used as controllers, new and innovative concepts have been tested and implemented into vehicles [1]. This type of research is mainly conducted by automotive companies, tyre manufacturers, and academic institutions.

Automotive companies are constantly improving on their chassis design and development by re-engineering their suspension systems through new technology. For

example, the recent developments of traction control systems show that a marriage of vehicle dynamics and electronics can improve handling quality of vehicle [1]. Examples of such systems are anti-lock braking systems (ABS) and automatic traction systems. They use a sensor to measure the rotational speed of the wheels and a micro-controller to determine, in real time, whether slipping of the tyre is present. This results in full traction and braking under all road conditions, from dry asphalt to icy conditions [2]. Another example of the benefit of joining vehicle dynamics with electronics is in controllable suspensions, such as those using semi-active damper [3]. Semi-active dampers enable damping characteristics of the suspension system to be set by a feedback controller in real-time, thus improving the ride quality of the vehicle on different types of road conditions [3].

A more advanced concept that is currently under research and development by automotive companies is an autonomous vehicle [4, 5, 6]. This concept will enable the vehicle to get from one point to another without constant commands from the driver.

The idea is to relieve the burden of vehicle control and operation from the driver and also to reduce the number of accidents associated with driver operating error.

Tyre manufacturers also perform a variety of research on vehicle dynamics. They are interested in characterizing the performance of their tyres as function of the tyre construction component [7, 8]. Their goal is to be able to predict or design tyres for any type of applications efficiently, and to reduce the cost associated with prototyping and testing. Their efforts require developing more accurate tyre models; specifically models that can predict how changing the tyre compound affects the tyre performance. The use of predictive models is particularly important in applications where the tyre performance is crucial, such as in race cars. The functions of tyres are to support the vertical load of the vehicle, to generate the forces and moments necessary to keep the race car on the track, and to generate traction against the ground. Formula-One race cars are the most highly advanced vehicles in the world, where millions of dollars are spent on their research and development. The performance between different race vehicles are relatively the same, about the same amount of horsepower, the same amount of braking ability, and the same suspension systems. Most races, however, are decided by the tyres each team puts on their car and the skills of the driver to push the car to the limits. Tyre

manufacturers spent tremendous amount of money and time developing the best tyres for different types of racing conditions. Still, it is often difficult for the racing teams to select the tyre compound that is most suitable for a particular racetrack. As a result, tyre manufacturers in conjunction with racing teams are developing a simulation tool to predict the best tyres for a particular racing condition [9].

Universities and research institutions are interested in vehicle dynamics for the same reasons as mentioned above. Most of their projects are often funded by the automotive industry. Another financial contributor may be the government agencies where their interest is preserving the road surface due to different driving conditions. In this way, it may be possible to reduce the road damage caused by heavy trucks. The latter is a major concern in trying to keep the cost of infrastructure maintenance to a minimum [10].

2.2 Motivation for this Research

Currently track testing is conducted by using test drivers to perform repetitive manoeuvres on the track; specifically to characterize the handling, ride, and other vehicle related performance of the vehicle. The objective of the test may be to do performance comparison between old and new designs of shock absorbers, suspension geometries, or tyres. Unfortunately, all these track tests are expensive and it is required so much time to equip the test vehicle. Having a simulation model these processes could be avoided, the simulation results could be equivalent with real tests.

In fact, the simulators are much utilized in all industrial fields such as aero spatial, aeronautic, motor and many others. Their principal goal is to understand, whether to expect the physical behaviour of the system. In many applications it is necessary to understand the phenomena which come from the external working conditions, because it would be too much dangerous, such as the landing/takeoff and vehicle collisions. Other applications have only an educational purpose such as the flight simulators.

Sometimes, there is no other way to study the phenomenon, understood as the behaviour of a system, owing to the dynamic develops. For example, this happens while one studies the evolution of the universe. Also a lot of simulators are used to predict the behaviour of a system, such as the meteorological and seismic ones.

2.2.1 Research Objective

The objective of this research is to evaluate the mean characteristics of the vehicle dynamics. Specifically a complete vehicle model, without vertical dynamics investigation, will be evaluated, considering the tyre behaviour. A mathematical model according to a physical system will be developed, under Matlab/Simulink environment. Particular attention will be placed about the tyre forces, in order to investigate on the mean phenomena which lead into critical conditions.

The philosophy of the simulation work is always to use simple models, it means with few degrees of freedom models, in order to understand more aspects possible about the physical system. This study, which uses a relatively simple vehicle and tyre model, is intended as a preliminary study of an undefined field, such as vehicle dynamics. More complete studies could be included in the future.

2.2.2 Literature Review

At the beginning of this research, an extensive literature search in the area of vehicle dynamics and optimal control of vehicle was conducted. The database *CiteSeer.IST* (Scientific Literature Digital Library), a leading source of engineering research, science, and electronics articles, the database has an index of articles from nearly 700,000 documents. Moreover, a database of conference publications was used to complete the search.

Keyword search was referenced on the following terms; modelling, vehicle, vehicle dynamics, longitudinal, lateral, tyre, vehicle, and behaviour. Figure 2.1 shows the results of the literature search.

The following sections, divided into optimal paths, vehicle, and tyre modelling sections, briefly describe the papers that were found most relevant and complimentary to this research.

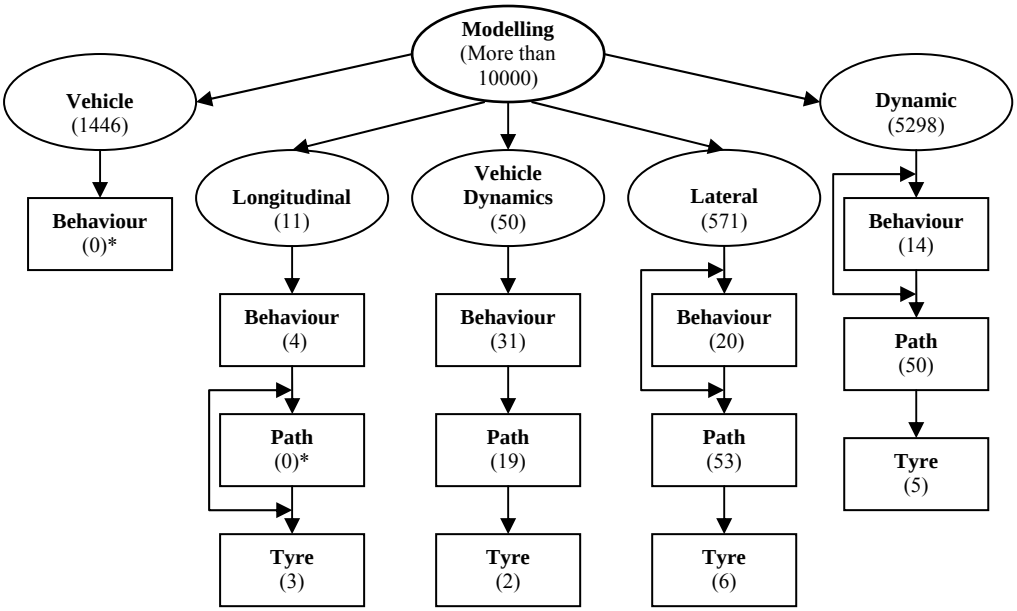

Figure 2.1: Literature Review Keyword Search Diagram.
(* Irrelevant topic)

2.2.2.1 Optimal Path

The research by of Hatwal, et al. [11] generated the time histories of steer angle, traction, and braking forces required to track a desired trajectory, for a lane-change manoeuvre.

Hatwal, et al. also made a comparison of different handling performances between a front wheel drive (FWD) vehicle and a rear wheel drive (RWD) vehicle using a five-degree-of freedom model for the vehicle. The system control variables were steer angle of the front wheel, longitudinal force of the front wheel for FWD vehicle, and longitudinal force of the rear wheel for RWD vehicle. Hatwal, et al. used optimal control approach to determine the system control vectors with an objective of minimizing time. They first assumed a free final time optimal control formulation, and concluded that it was complex. Next, they used a fixed final time formulation by deriving the differential equations with respect to forward distance using the relationship between distance, velocity, and time. They noticed that the fixed final time formulation reduces the number of equations needed to be solved. They used a penalty cost function and the weighting factors tuning approach to find the desired trajectory.

They concluded that FWD and RWD require similar steering angle input and longitudinal force input during low speed lane-change manoeuvre. At higher speeds, however, they concluded that there was a significant difference in trajectory between the two types of vehicle.

Another study by Hendrikx, et al. [12] was to determine a time optimal inverse model of a vehicle handling situation. They were interested in the driver actions, time histories of the steering rate and the longitudinal force at the road/tyre contact. This optimal control problem was calculated using the Gradient Method [13]. The vehicle was modeled as a two-dimensional four-wheel model where the tyre model was nonlinear.

Their objective was to determine the vehicle trajectory for a lane-change manoeuvre, with minimum time. A parametric study comparing the optimal trajectories between FWD and RWD vehicles was also performed. As a result, they concluded that optimal control could be applied to optimize car handling for a specific lane-change manoeuvre by means of inverse vehicle model simulation, and FWD and RWD vehicles required different driving strategies.

2.2.2.2 Vehicle and Tyre Modelling

Smith, et al. [14] performed a study on modelling accuracy between different vehicle models and tyre models. Specifically, they compared three models; the first was a bicycle model with yaw and side-slip degrees of freedom using a linear tyre model. The second model was a five-degree-of-freedom model with additional longitudinal and wheel rotational degrees of freedom, using a nonlinear tyre model. The third was an eight degree-of-freedom model, with additional roll and wheel rotational degrees of freedom for the other two tyres using a nonlinear tyre model. The equations of motion were integrated using the Runge-Kutta method. The results shown in their paper indicated variations in accuracy between these models. They suggested that the bicycle vehicle model could not be used accurately in the high lateral acceleration manoeuvres due to the lack of lateral load transfer and body roll dynamics. With these results, they concluded that the tyre lag information must be included in a lateral controller for high speed manoeuvres, in order to accurately predict the desired and safe trajectory.

Maalej et al. [7], performed a study on various types of tyre models which were used to characterize the effects of slip ratio and slip angle on lateral force. They investigated four different models, Dugoff, Segel, Paceijka, and proposed polynomial, comparing the accuracy and the computational time between them. For the comparison, they investigated the lateral force, longitudinal force, alignment moment, and combined braking and steering performance of each model. They found that each model had its own advantages and disadvantages, Paceijka scored highest in the accuracy category while Segel scored the highest in the computational time category.

2.2.2.3 Basic Structure of vehicle system dynamics

In general, the characteristics of a ground vehicle may be described in terms its performance, handling, and ride. Performance characteristics refer to ability of the vehicle to accelerate, to develop drawbar pull, to overcome obstacles, and to decelerate. Handling qualities are concerned with the response of the vehicle to the driver's command and its ability to stabilize the external disturbances. Ride characteristics are related to the vibrations of the vehicle excited by the surface irregularities and its effects on the passengers. The theory of the ground vehicles is concerned with the study of the performance, handling, and ride and their relationships with the design of the ground vehicles under various operating conditions

The behaviour of the ground vehicles represents the results of the interactions among the driver, the vehicle, the environment, as illustrated in Figure 2.2 [22].

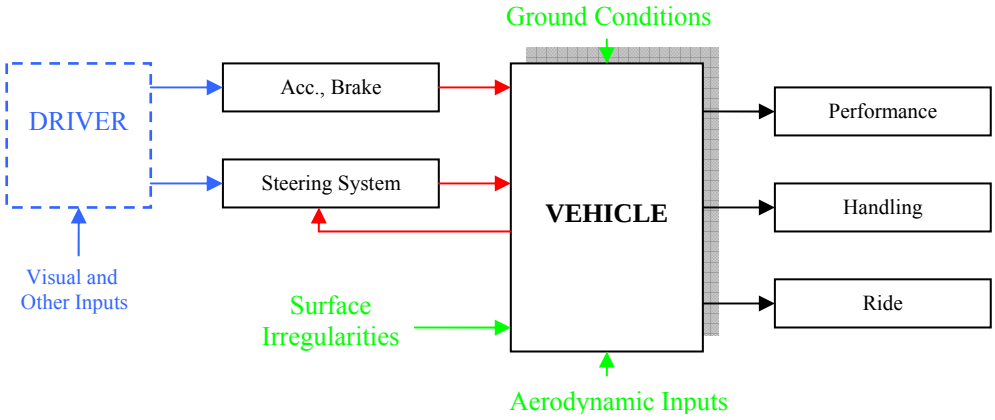

Figure 2.2: The Driver-Vehicle-Ground System [22].

An understanding of the behaviour of the driver, the characteristics of the vehicle, and the physical and geometric properties of the ground is, therefore, essential to the design and evaluation of the ground vehicle systems.

According to this configuration, the vehicle dynamics can be introduced. The latter can be subdivided into longitudinal, lateral and vertical one, Figure 2.3 [15, 16]. Obviously, these subsystems are not independent of each other but mutually interconnected.

While vertical dynamics are experienced by the driver in a more or less passive manner, horizontal dynamics comprising longitudinal and lateral dynamics are actively controlled by the human driver.

Numerous approaches to dynamics vehicle modelling are documented in the literature. Two simple ones are adopted here to describe longitudinal and lateral Behaviour, as in the following chapters will be presented.

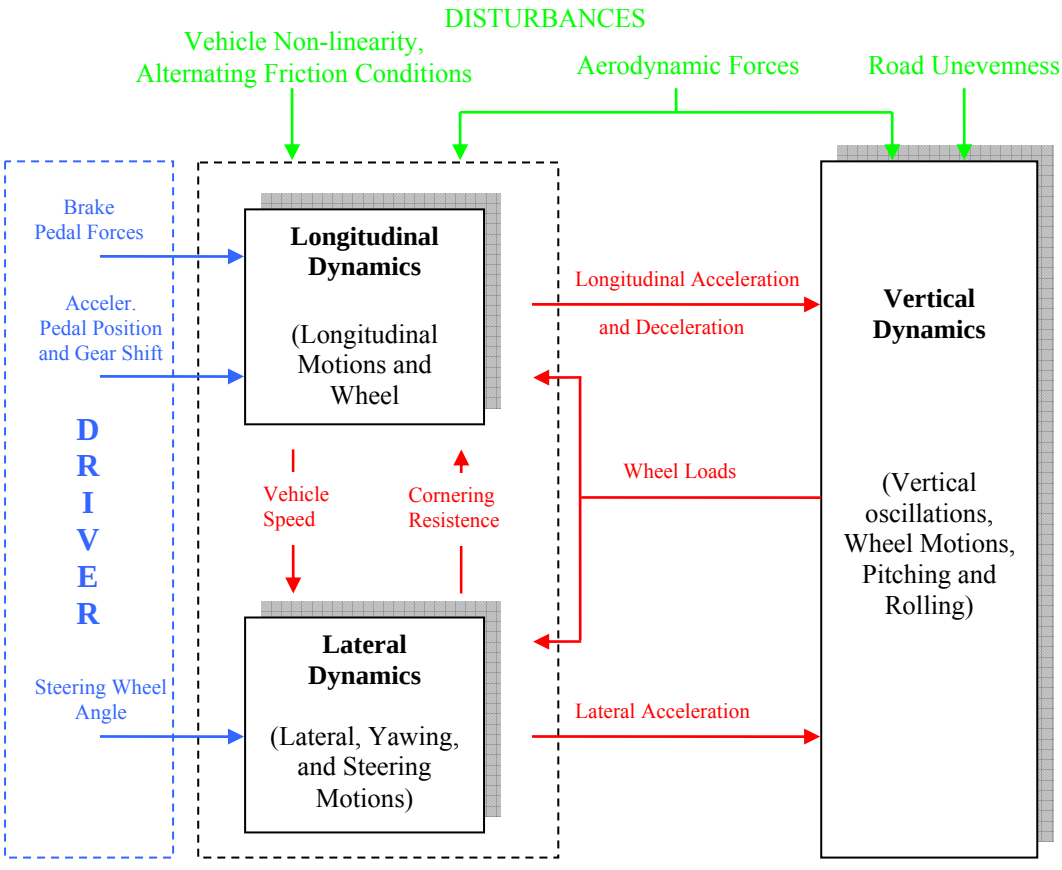

Figure 2.3: Basic Structure of Vehicle System Dynamics[1]

1 For the meaning of few variables mentioned to see 4th and 5th chapters.

Chapter 3

3 Vehicle Dynamics Modelling

This chapter provides information on dynamics modelling of the vehicle. The vehicle axis system used throughout the simulation is according to the SAE standard, as described in SAE J670e [17]. As well a research study of typical forces acting at wheels of each vehicle will be used in this research in order to construct a complete vehicle model.

3.1 Axis System

At any given instant of time, a vehicle is subjected to a single force acting at some location and in some direction. This so-called external or applied force maintains the velocity or causes an acceleration of the vehicle. This force is made up of tyre, aerodynamic, and gravitational components. These different components are governed by different physical laws ant it is not convenient to deal with this single force. Furthermore, these various components act at different locations and in different directions relative to the vehicle chassis.

In order to study the vehicle performance it is necessary to define axis systems to which all the variables, such as the acceleration, velocity and many other can be referred. Throughout this thesis, the axis systems used in vehicle dynamics modelling will be according to SAE J670e [17]. These two axis systems are used as required for the

complete representation of the system. Both are described in the following sections, as shown in Figure 3.1.

3.1.1 Earth-Fixed Axis System

The coordinate system is fixed to the ground and the letters *(x_0, y_0, z_0; O_0)*, are used to denote the three principal directions, namely "*Ground Axis*[2]"; x_0 and y_0 are in the horizontal plane (the former orthogonal to the sheet), z_0 is vertical upward; see Figure 3.1 (a).

3.1.2 Vehicle Axis System

On the analogy of ground-axis, an axis system (*x, y, z; G)* behind the vehicle, so called "*Body Axis"*, can be fixed. Its origin is situated in the centre of gravity of the vehicle, and the directions are characterized with the versors ***(i, j, k)***. As shown in Figure 3.1 (b), *x*-axis is defined parallel to road and forward direct, *z*-axis is orthogonal to the road and *y*-axis is perpendicular to ones and left direct. The *x*-axis points to the forward direction or the longitudinal direction, and the *y*-axis, which represents the lateral direction, is positive when it points to the right of the driver. The *z*-axis points to the ground satisfying the right hand rule. In most studies related to handling and directional control, only the *x*-*y* plane of the vehicle is considered. The vertical axis, *z*, is often used in the study of ride, pitch, and roll stability type problems.

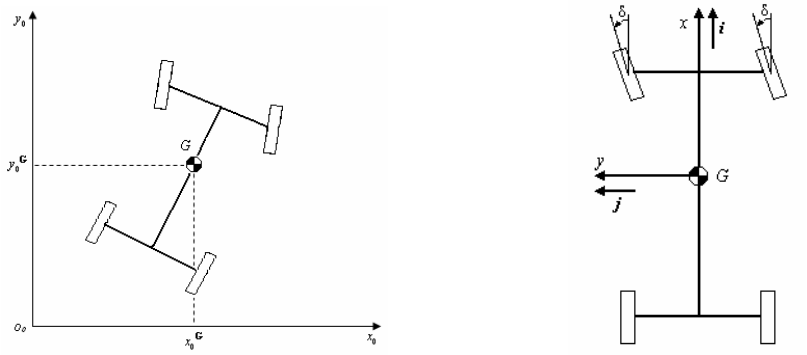

(a) (b)

Figure 3.1: Axis Systems after Guiggiani [20]

2 This reference can be considered an inertial system because the earthly rotation is irrelevant as regard to the vehicle one.

The following list defines relevant definitions for the variables associated with this research:

Longitudinal direction: forward moving direction of the vehicle. There are two different ways of looking at the forward direction, one with respect to the vehicle body itself, and another with respect to a fixed reference point. The former is often used when dealing with acceleration and velocity of the vehicle. The latter is used when the location information of the vehicle with respect to a starting or an ending point is desired.

Lateral direction: sideways moving direction of the vehicle. Again, there are two ways of looking at the lateral direction, with respect to the vehicle and with respect to a fixed reference point. Researchers often find this direction more interesting than the longitudinal one since extreme values of lateral acceleration or lateral velocity can decrease vehicle stability and controllability.

Sideslip angle: is the angle between the *x*-axis and the velocity vector that represents the instantaneous vehicle velocity at that point along the path, as shown in Figure 3.2. It should be emphasized that this is different from the slip angle associated with tyres.

Even though the concept is the same, each individual tyre may have a different slip angle at the same instant in time. Often the body slip angle is calculated as the ratio of lateral velocity to longitudinal velocity.

Tyre slip angle: This is equivalent to heading in a given direction but walking at an angle to that direction by displacing each foot laterally as it is put on the ground as shown in Figure 3.3. The foot is displaced laterally due to the presence of lateral forces. Figure 3.4 shows the standard tyre axis system that is commonly used in tyre modelling. It shows the forces and moments applied to the tyre and other important parameters such as slip angle, sideslip angle, and others.

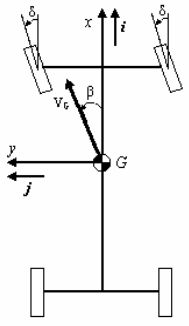

Figure 3.2: Sideslip Angle after Guiggiani [20].

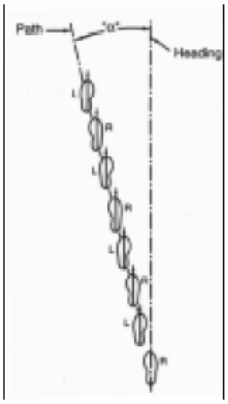

Figure 3.3: Walking Analogy to Tyre Slip Angle after Milliken [18].

In order to simplify the vehicle model so that results of the integration can be quickly calculated, the effects of camber angle are not included in this study.

3.2 Mechanism of Pneumatic Tyres

3.2.1 Force Acting Between Road and Wheel

The wheels of all modern motor vehicles are provided with pneumatic tyres, which support the vehicle and transfer the driving power (power tractive) through the wheel-ground contact. Therefore in all modern vehicles all the disturbance forces which are applied to the vehicle, with the exception of aerodynamic force, are generated in the same contact surface.

This interaction determines how the vehicle turns, brakes and accelerates. As our purpose is to understand the principal aspects of the vehicle dynamics, the tyre behaviour is an essential part of this work, and in the following section its characteristics will be explained.

In the study of the behaviour of the wheel, it is essential to evaluate the forces and the moments acting on it. Consequently, to describe its characteristics, it is necessary to define an axis system that serves as a reference for the definition of various parameters. Again, one of the common axis systems used in the vehicle dynamics work has been defined recommended by the Society of Automotive Engineers is shown in Figure 3.4

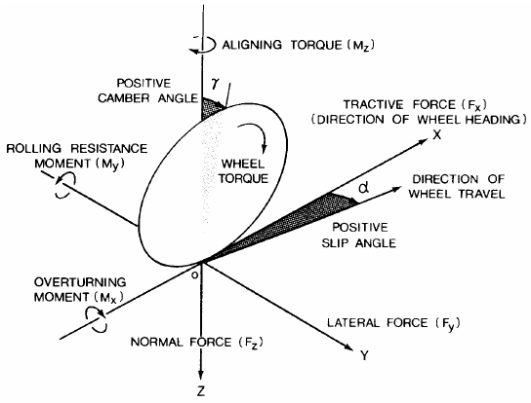

Figure 3.4: SAE Tyre Axis System after Gillespie [19].

[17, 18]. The origin of the axis system is in the centre of the tyre contact and the *x*-axis is the intersection of the wheel plane and the ground plane with positive direction forward. The *z*-axis is perpendicular to the ground plane with a positive. Consequently, the *Y*-axis is in the ground, and its direction is chosen to make the system axis orthogonal and right hand.

Assuming all the forces to be located at the centre of contact area, we can individuate three forces and three moments acting on the tyre from the ground. Tractive force (or longitudinal force) F_x is the component in the x direction of the resultant force exerted on the tyre by the road. Lateral force F_y is the component in the y direction, and normal force F_z is the component in the z direction. Similarly, the moment M_x is the moment about the X axis exerted from the road to the tyre. The rolling resistent moment M_y is the moment about the Y axis, and the aligning torque M_z is the moment about the z-axis. The moment applied to the tyre from the vehicle, exactly by powertrain, about the spin axis is referred to as wheel torque T_w.

There are two important angles associated with a rolling tyre: the slip angle and the camber angle. Slip angle α is the angle formed between the direction of the velocity of the centre of the tyre and the plane x-z. Moreover, the camber angle γ is the angle formed between the x-z plane and the wheel plane. How the lateral force will be shown at the tyre-ground contact patch is a function of the slip angle and the camber angle [22].

3.2.1.1 Rolling Radius

Consider a wheel rolling on a level road with no braking or tractive moment applied to it, with its plane perpendicular to the road. Therefore, remembering the known relationship between the angular velocity of a rigid wheel and the forward speed as being $u=\omega R$, for a tyre an effective rolling radius R_r can be defined as the ratio between the same velocity but referring to the wheel:

$$u = \omega_w R_r \qquad \textbf{(3.1)}$$

where R_r is the effective rolling radius and ω_w the velocity of the wheel. See references [22, 23].

This relationship comes from an important assumption, called *Low of Coulomb*. In accordance to this relation (called rolling without drifting), no drift between the two parts is assumed. The behaviour of the tyre comes from this assumption and being a point of contact[3]. For this reason, as shown in Figure 3.5 the centre of instantaneous rotation R is not coincident with the centre of contact *A*.

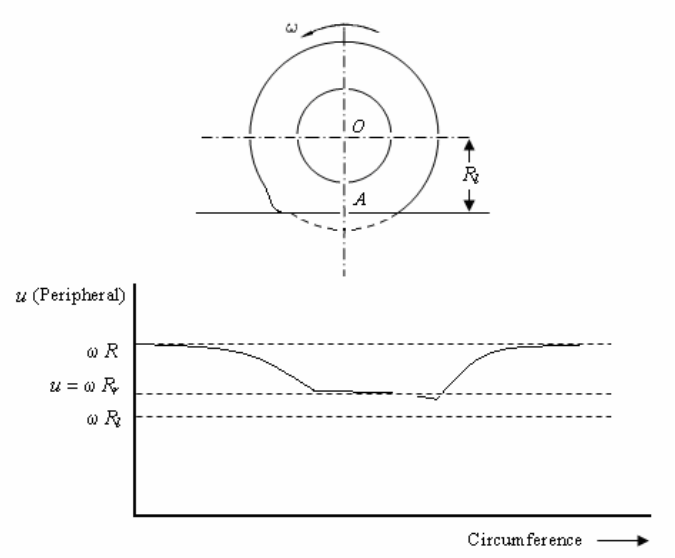

Figure 3.5: Geometrical Configuration and Peripheral Speed in the Contact Zone.

3 Actually, when two surfaces make contact, the local deformation is never about a point but there is always a degeneration into a surface owing to Hertz's Deformation.

The peripheral velocity of any point varies periodically in according with the angular variation of the wheel. Analyzing the strain around the point of contact A and knowing the direct correlation between the radius and the linear velocity, it is possible to note the corresponding smaller radius, in owing of the compression and consequently the velocity decreases. In the opposite way, on the right and the left of the same point the velocity remains meanly constant.

As a consequence of this mechanism, the spin speed of the wheel with the pneumatic tyre is smaller than a rigid wheel with the same load. On account of the strain, this relationship is available:

$$R_l < R_r < R \qquad \textbf{(3.2)}$$

The effective rolling radius depends on many factors, some of which are determined by the tyre structure and others by the working conditions such as inflation pressure, load, speed, and others [22, 23].

In the following work, an estimation of the resistent rolling radius will be made, in accordance with the geometrical values assumed for the test vehicle.

3.2.1.2 Rolling Resistent

Consider a wheel rolling freely on a flat surface. If both the wheel and the road were perfectly undeformable, there would be no resistance and consequently no need to exert a tractive force. In the real world, as shown in the former section, perfectly rigid bodies do not exist and both the road and the wheel are subject to deformation with the contact surface.

During the motion of the system, how in all mechanical real system subject to strains, the material behaviour is never perfectly elastic, but it includes at least a small plastic strain in owing to the hysteresis of material and other phenomena. For this reason to every turn of the wheel in according with this macroscopic deformation it is necessary to spend some energy. This energy dissipation is what causes rolling resistent. Obviously it increases with the tyre deformation, stiffness of the tyre and many others parameters.

Other mechanisms, like small sliding between road and wheel and aerodynamic drag are responsible for a small contribution to the overall resistent, of the order of a small percentage.

The distribution of the contact pressure, which at standstill was symmetrical with respect to the centre of contact zone, becomes unsymmetrical when the wheel is rolling and the resultant F_z moves forward producing a torque $M_y=-F_z\Delta x$ with respect to the rotation axis.

Rolling resistance is defined by the mentioned SAE document J670e as the force which must be applied to the centre of the wheel with a line of action parallel to the *x*-axis so that its moment about a line through the centre of tyre contact and parallel to the spin axis of the wheel will balance the moment of the tyre contact force about this line.

Consider a free rolling wheel on level road with its mean plane coinciding with *x-z* plane ($\gamma=0$, with γ *camber angle*), as shown in Figure 3.6.

Assuming that no traction or braking moment other than M_f due to aerodynamic drag is applied to the wheel, the equilibrium equation about the centre of the wheel in steady state rolling, solved in the rolling resistance F_x, is

$$F_x = \frac{-F_z \Delta x + M_f}{R_l} \tag{3.3}$$

where it must be noted that both rolling resistance, F_x, and drag moment M_f are negative. Equation (3.3) is of limited practical use, as Δx and M_f are not easily determined.

For the practical purposes, rolling resistance is usually expressed as

$$F_x = f_r F_z \tag{3.4}$$

where the rolling resistance coefficient f_r should be determined experimentally. The latter depends on many parameters, as the traveling speed (or longitudinal linear velocity of the wheel), the inflation of pressure *p*, the normal force F_z, the size of the

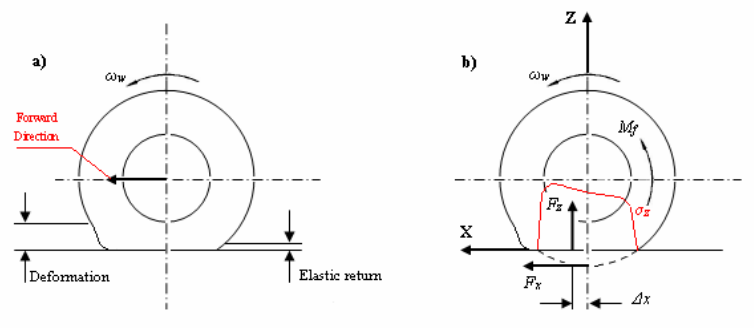

Figure 3.6: (a)Wheel Deformation in owing to Rolling Resistent (Ground Deformation and Elastic Return); (b) Forces and Contact Pressure σ_z in a Rolling Wheel.

tyre, the working temperature, the road conditions and finally, the forces F_x and F_y exerted by the wheel[4].

The most important effect on the rolling resistance coefficient is the longitudinal velocity of the centre of the wheel[5]. Generally, this coefficient increases with the velocity of the vehicle, at the beginning very slowly and then at an increased rate.

This functional dependence can be approximated with a polynomial of the type

$$f_r = \sum_{i=0}^{n} f_i u^i \qquad \textbf{(3.5)}$$

Where u^i is the longitudinal velocity of the vehicle with i which denotes the degree of the polynomial used and f_i a coefficient valuated by experimental tests.

Generally a polynomial with second order is preferred. In this work the latter approximation will be used.

$$f_r = f_0 + Ku^2 \qquad \textbf{(3.6)}$$

4 The complex relationships between the design and operational parameters of the tyre and its rolling resistance make it extremely difficult, if not impossible, to develop an analytic method for predicting the rolling resistent. To provide a uniform basis for collecting experimental data, the Society of Automotive Engineers recommends rolling resistent measurement procedures for various types on different surfaces, which may be found in SAE Handbook.

5 For a vehicle seen as a single rigid body and in presence of rigid driveline the velocity of the centre of the wheel (or peripheral one)can be approximated with the velocity of the vehicle.

Particularly the values of f_0 and K must be measured on any particular tyre. The values assumed by these coefficients will have chosen according with Reference [22]; for more details see [23, 24] too.

3.2.1.3 Adherence Condition of Tyre

According with Coulomb Hypothesis, before illustrated, the contact between the wheel and the ground is without drift if this relationship is satisfied:

$$|F_x| \leq f_s |F_z| \tag{3.7}$$

where F_x and F_z are the component of tangential and normal force transferred in the contact point respectively; as well f_s represents the static friction coefficient which depends on the surfaces of materials.
Moreover, if the former relationship (3.7) is not satisfied between both surfaces the drift will have produced. During this critical condition, it is available in the following one

$$|F|_x = f_d |F_z| \tag{3.8}$$

where f_d represents the sliding friction coefficient which depends on the surfaces of the materials.
Therefore it is introduced an important parameter, longitudinal feed U which is able to describe the imperfect elasticity through the bodies

$$\Delta x_1 = U = f_r R_r \tag{3.9}$$

where the symbol f_r had just defined.
This kind working hypothesis is able to investigate with a good approximation the principal aspects of the dynamics behaviour of the tyre, for all its simplicity.

3.2.1.4 Slope Resistance

Not taking into account a level road (banked surfaces) but a slope surface, an additional contribution will be presented. In fact, the road grade will contribute directly to the braking effort, either in a positive sense (uphill) or negative (downhill).

Grade is defined as the ratio of the vertical distance to the horizontal one. The additional force on the vehicle arising from the slope, F_s, is given by:

$$F_s = W_x = W \sin\theta \qquad \textbf{(3.10)}$$

For small angles typical of most grades, it is assumed that:

$$\begin{aligned} &\cos\vartheta = 1 \\ &\sin\vartheta = \tan\vartheta = i \end{aligned} \qquad \textbf{(3.11)}$$

Thus, a grade of 4% (i=0.04) will be equivalent to a deceleration of ±0.04g (with g means the acceleration of gravity) [19].

3.2.1.5 Force Acting on the vehicle

Determining the axle loadings on a vehicle under general conditions can be performed through the Newton's Second Law. It is an important step in analysis of the dynamic behaviour of the vehicle because the axle loads determine the tractive effort obtainable at each axle, affecting the acceleration, gradeability, maximum speed, and many other factors. The major external forces acting on a two-axle vehicle are shown in Figure 3.7. References [22, 23, 24, 25].

In the longitudinal direction, the typical forces acting on the vehicle are caused by different nature. For this reason, most of these forces do not act at the centre of gravity of the vehicle, and thus create moments.

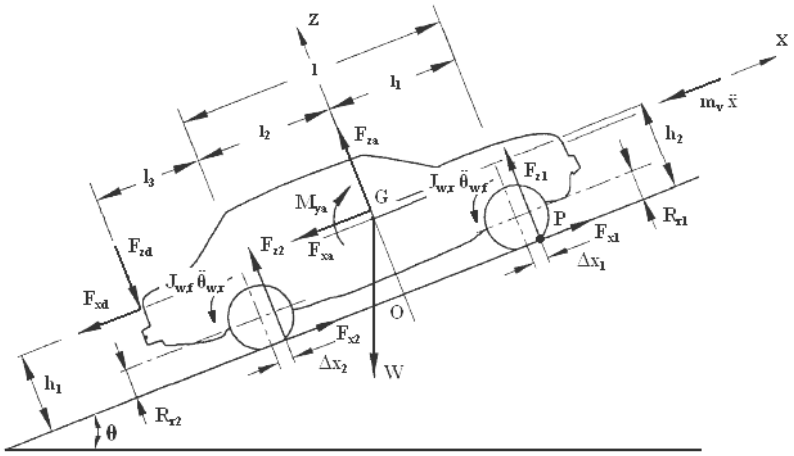

Figure 3.7 Generalized Forces Acting on the Vehicle.

Referring to the same figure, the forces can be justified in the following manner:

W: weight of the vehicle acting at its centre of gravity, G, with a magnitude equal to its mass times the acceleration of gravity. On a grade it may have two components, a longitudinal component which is proportional to the sine of the slope and parallel to the road, and a vertical component which is proportional to the cosine of the slope and perpendicular to the road surface;

m_v: mass of the vehicle;

$J_{w,f}$ and $J_{w,r}$: Inertia of the front and rear wheels;

d^2x/dt^2: linear acceleration of the vehicle along the longitudinal axis;

$d^2\theta_f/dt^2$ and $d^2\theta_r/dt^2$: angular accelerations of the vehicle along the spin z-axis at the front and rear wheels; Formally, they are equal and fixed to d^2x/dt^2 times R_r;

l: wheelbase of the vehicle, that means the length between the two spin axles;

l_1 and l_2: centre of gravity location, referring to both axles;

l_3: distance between the vertical drawbar load and rear axle;

F_{xa}, F_{za} and M_{ya}: Aerodynamic forces acting on the body of the vehicle. ; the former, in x direction, may be represented as acting at a point above the ground indicated by the height, h_2, or by a longitudinal force of the same magnitude in the ground plane with an associate moment equivalent to F_{xa} times h_2; Instead M_{ya} represent the aerodynamic pitching moment;

h_1 and h_2: lengths between the line of action of the inertia force and the aerodynamic one, respectively;

Δ_{x1} and Δ_{x2}: characteristic lengths between the line of action of the inertia force and the aerodynamic one, respectively;

R_{r1} and R_{r2}: Rolling radius of the front and rear wheels, respectively. However, their magnitude is always equal and so, it is fixed as R_r;

F_{x1}, F_{x2}: Rolling resistance of the front and rear tyres;

F_{z1}, F_{z2}: Vertical load of the vehicle at the front and rear tyres;

F_{xd}, F_{zd}: Drawbar loads. Exactly, they are the longitudinal and vertical forces acting at hitch point when the vehicle is towing a trailer;

To valuate the normal components of the contact ground-tyre at both axis of the vehicle two equations of dynamics equilibrium are required. Always referring to the same figure, taking into account that at each axle there are two wheels, an rotational equilibrium about the point P and a global one in forward direction have been made:

$$\begin{aligned} m_v\ddot{x}h_1 + 2J_{w,f}\ddot{\theta}_{w,f} + 2J_{w,r}\ddot{\theta}_{w,r} - 2F_{z2}\left(l - \Delta x_1 + \Delta x_2\right) + F_{zd}\left(l + l_3 + \Delta x_1\right) + F_{xd}h_1 + F_{xa}h_2 + \\ - F_{za}\left(l_1 + \Delta x_1\right) - M_{ya} + W_x h_1 + W_z\left(l_1 + \Delta x_1\right) = 0 \end{aligned} \quad \textbf{(3.12)}$$

Where, for simplicity it is assumed null the contribution of the aerodynamic forces F_{za} and M_{ya}, different from the x-direction:

$$\begin{aligned} F_{za} &= 0 \\ M_{ya} &= 0 \end{aligned} \quad \textbf{(3.13)}$$

Analogy for the both drawbar forces, that is the vehicle is running without trailer (F_{xd}= F_{xd}=*0*); Therefore, it is assume that the inertia of the wheels have the same magnitude, like as the characteristic lengths:

$$\begin{aligned} J_{w,f} &= J_{w,r} = J_w \\ \Delta x_1 &= \Delta x_2 = U \end{aligned} \quad \textbf{(3.14)}$$

Finally, like working hypothesis the elementary rotation of the wheels at the same axle assumes equal values:

$$\theta_{w,f} = \theta_{w,r} = \theta_w \tag{3.15}$$

Thus, the equation of equilibrium around the point *P* becomes:

$$m_v \ddot{x} h_1 + 4J_w \ddot{\theta}_w - 2F_{z2} l + F_{xa} h_2 + W_x h_1 + W_z \left(l_1 + U\right) = 0 \tag{3.16}$$

where W_x and W_z represent the both components of the vehicle weight that, supposing the vehicle moving on roads with small slope we have:

$$\begin{aligned} W_x &= W \sin\theta = m_v g i \\ W_z &= W \cos\theta = m_v g \end{aligned} \tag{3.17}$$

Finally, the equation which is able to provide the rear load transfer on the tyre is:

$$F_{z2} = \frac{1}{2l}\left[m_v \ddot{x} h_1 + 4J_w \ddot{\theta}_w + F_{xa} h_2 + m_v g h_1 i + m_v g \left(l_1 + U\right)\right] \tag{3.18}$$

Analogously, performing an equilibrium into vertical direction it is possible to obtain the front load[6] transfer:

$$2F_{z2} + 2F_{z1} - F_{zd} + F_{za} - W_z = 0 \tag{3.19}$$

where, for the same considerations about the drawbar and aerodynamic forces:

$$F_{z1} = \frac{m_v g - 2F_{z2}}{2} \tag{3.20}$$

6 The same expression for the front load transfer could be obtained performing the same rotational equilibrium about the point of contact ground-tyre at the rear wheel. Evidently, it would be more industrious, mathematically.

To note how the front and rear vertical loads are constituted by two parts, first *"Static Load"* and *"Dynamic Load"*. In fact, examining the Equations (3.16) and (3.18), they can be written as:

$$\begin{aligned} F_{z1} &= F_{z1}^{s} - \frac{1}{2l}\left[m_v \ddot{x} h_1 + 4J_w \ddot{\theta}_w + F_{xa} h_2 + m_v g h_1 i + m_v g U \right] \\ F_{z2} &= F_{z2}^{s} + \frac{1}{2l}\left[m_v \ddot{x} h_1 + 4J_w \ddot{\theta}_w + F_{xa} h_2 + m_v g h_1 i + m_v g U \right] \end{aligned} \qquad \textbf{(3.21)}$$

where the terms F^{s}_{z1} and F^{s}_{z2} represents the front and rear static loads transfer, respectively; expressly they assume the following form[7]:

$$\begin{aligned} F_{z1}^{s} &= m_v g \frac{l_2}{2l} \\ F_{z2}^{s} &= m_v g \frac{l_1}{2l} \end{aligned} \qquad \textbf{(3.22)}$$

Instead, to valuate the longitudinal components of the contact forces another two dynamic equation of equilibrium are required. First, taking care a single axle, and rearranging all the forces acting at its we have the Figure 3.8.

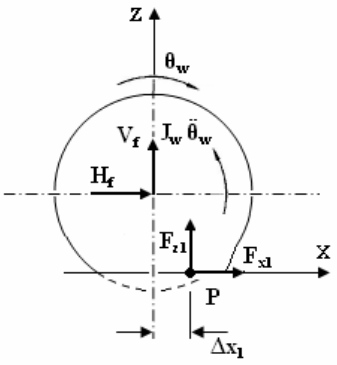

Figure 3.8: Generalized Forces Acting on the Vehicle.

7 To note that in many books concerning the Vehicle Dynamics, the static load is characterized by a proportionality respect to the semi-wheelbase, but the latter is reported only on the wheelbase total. The reason why the static load transfer is referred to the double wheelbase is corresponding to have considered on the same axle both wheels.
Exactly, if the variation of the rolling resistance is considered invariant with the velocity, in the load transfer could be added this latter term.

Performing an equilibrium about the spin axle of the front wheel, the relation assumes the following form:

$$J_w\ddot{\theta}_w + F_{z1}U + F_{x1}R_r = 0 \qquad (3.23)$$

and, rearranging to have the value of the normal rear force:

$$F_{x1} = -\frac{J_w\ddot{\theta}_w + F_{z1}U}{R_r} \qquad (3.24)$$

Consequently, the global equilibrium at the vehicle in forward direction gives the following relation:

$$m_v\ddot{x} - 2F_{x1} - 2F_{x2} + F_{xa} - F_{xd} + W_x = 0 \qquad (3.25)$$

But, with the same observations made for the former equations, we obtain:

$$F_{x2} = \frac{1}{2}\left(m_v\ddot{x} + m_v gi + F_{xa}\right) + F_{x1} \qquad (3.26)$$

where H_f and V_f are the horizontal and vertical components of the reactions exerted on the chassis by the tyre.

Finally, since the principal purpose of the model is to investigate the response of the dynamic behaviour of the vehicle with the interaction of the powertrain, the Equations from (3.16) to (3.22) need to be rearranged in respect of the angular engine velocity, variable obtained from the longitudinal model. To do this it required recalling various terms which are compared in these equations. Simplifying into the following sentences, they can be reported.

$$\begin{aligned} u^2 = \dot{x}^2 &= \omega_e{}^2 R_r{}^2 \left(\frac{\eta_c\eta_d}{\tau_c\tau_d}\right)^2 \\ a_x = \ddot{x} &= \dot{\omega}_e R_r \frac{\eta_c\eta_d}{\tau_c\tau_d} \\ \ddot{\theta}_w &= \frac{\ddot{x}}{R_r} = \dot{\omega}_e \frac{\eta_c\eta_d}{\tau_c\tau_d} \end{aligned} \qquad (3.27)$$

Obviously, it is reported the square velocity because the aerodynamic force is proportional to its. Therefore, the final equation which describes the tyre behaviour is:

$$
\begin{aligned}
F_{z2} &= \frac{1}{2l}\left[\frac{1}{2}\rho SCxh_2R_r^2\left(\frac{\eta_c\eta_d}{\tau_c\tau_d}\right)^2\omega_e^2+\left(m_v h_1 R_r+4J_w\right)\frac{\eta_c\eta_d}{\tau_c\tau_d}\dot{\omega}_e+m_v g\left(h_1 i+l_1+U\right)\right] \\
F_{z1} &= -\frac{1}{2l}\left[\frac{1}{2}\rho SCxh_2R_r^2\left(\frac{\eta_c\eta_d}{\tau_c\tau_d}\right)^2\omega_e^2+\left(m_v h_1 R_r+4J_w\right)\frac{\eta_c\eta_d}{\tau_c\tau_d}\dot{\omega}_e+m_v g\left(h_1 i-l_2+U\right)\right] \\
F_{x1} &= -\frac{1}{2l}\left[\frac{1}{2}\rho SCxh_2R_r^2\left(\frac{\eta_c\eta_d}{\tau_c\tau_d}\right)^2\omega_e^2+\left(m_v h_1 R_r+\left(\frac{l}{R_r}+2\right)2J_w\right)\frac{\eta_c\eta_d}{\tau_c\tau_d}\dot{\omega}_e+m_v g\left(h_1 i-l_2+U\right)+2lf_r\right] \\
F_{x2} &= -\frac{1}{2l}\left[\left(\frac{h_2}{2}-\frac{l}{2}\right)\rho SCxR_r^2\left(\frac{\eta_c\eta_d}{\tau_c\tau_d}\right)^2\omega_e^2+\left(\left(h_1-l\right)m_v R_r+\left(\frac{l}{R_r}+2\right)2J_w\right)\frac{\eta_c\eta_d}{\tau_c\tau_d}\dot{\omega}_e+m_v g\left(\left(h_1-l\right)i-l_2+U\right)+2lf_r\right]
\end{aligned}
\qquad \textbf{(3.28)}
$$

3.2.2 Constitutive Equations

In order to analyze completely the dynamic behaviour of the vehicle, it is necessary to define the tyre behaviour at each wheel in lateral direction too. In this way other two relations, able to define the lateral behaviour of a tyre, will be found [20, 21]. From a general point of view the lateral forces F_{yij} are a function of slip angle α, camber angle γ, longitudinal force F_{xij} and load transfer F_{zij}. Formally, the former dependence is written:

$$F_y = Y_p\left(\alpha,\gamma,F_x,F_z\right) \qquad \textbf{(3.29)}$$

where, Y_p represents the *"characteristic function of the tyre"*. However, the influence of the longitudinal force and the camber angle are neglected, and thus, depending on the variability of the lateral force F_{yij} by the slip angle and load transfer, we will have different kinds of tyre model.

3.2.2.1 Linear Tyre Model

Taking into account only the functional variation about the slip angle we will formulate the tyre model able to integrate the equation of motion, shown in Chapter 5. For this elementary model, considering constant the vertical load, the following relation is available:

$$F_y = Y_p\left(\alpha\right) \qquad \textbf{(3.30)}$$

In the following section we propose most simplified model, the linear tyre model. This latter describes the lateral force as a linear function of the slip angle [20, 21]. This functional link is expressed into the following relation:

$$F_{y_{ij}} = C_{\alpha_{ij}} \alpha_{ij} \tag{3.31}$$

where, being $\alpha_{i1}=\alpha_{i2}=\alpha_i$, we have:

$$F_{y_i} = C_{\alpha_i} \alpha_i \tag{3.32}$$

and $C_{\alpha i}$ is the tyre "*cornering stiffness*", defined formally by the relation:

$$C_\alpha = C_\alpha \left(F_z \right) = \left. \frac{\partial Y_p}{\partial \alpha} \right|_{\alpha=0;F_z=\text{cost}} \tag{3.33}$$

From the dimensional point of view it represents a force per unit angle. For convention is always positive. Generally, its magnitude for passenger vehicle is 10^5 N/rad and is two or four times as the previous one for the formula 1 tyres. The working field is characterized by small slip angle, which means the order of magnitude is equal to 15÷20 degrees on dry road. Figure 3.9 shows the front and rear lateral force in function of the slip angle. Obviously, increasing the magnitude of the cornering stiffness, the inclination of the line will increase too.

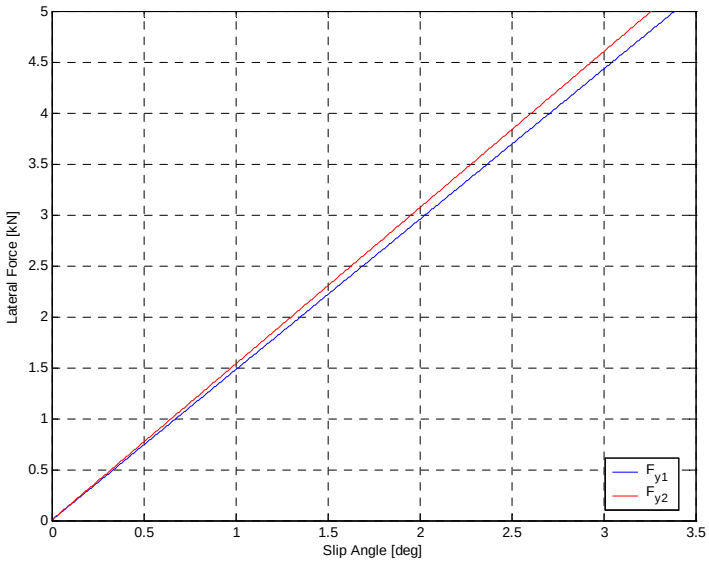

Figure 3.9: Lateral Force versus Slip Angle.

3.2.2.2 Linear Tyre Model with Relaxation Length

To study the behaviour of the tyre during the transient condition, it cannot be utilized the algebraic function, shown in the former section, but a differential equation is required. From experimental tests it is appeared that the lateral force is an increasing monotonic function which begins from zero and moves in asymptotic way to the permanent condition. From a general point of view, once a slip angle in different to zero, the instantaneous increasing of the lateral force is not possible [20, 21].

A simple mathematical model to describe the tyre behaviour during a transient condition, can be described by the following differential equations:

$$\frac{d}{u}\dot{F}_{yi} + F_{yi} = Y_p(\alpha) \qquad \textbf{(3.34)}$$

where the length d is the *"relaxation length"* and the function $Y_p(\alpha)$, namely *"characteristic function"*, represents the lateral force in function of the slip angle during the steady-state condition.

It is a ordinary differential equation, non homogenous, first order, linear and with constant coefficients8. The unknown variable of this equation is the lateral force as function of time.

Making same considerations about the former relationship, it is possible to calculate immediately the analytical solution:

$$F_{yi}(t) = F^{h}{}_{yi} + F^{p}{}_{yi} \qquad \textbf{(3.35)}$$

where, $F^{h}{}_{yi}$ and $F^{p}{}_{yi}$ are the particular integral and the homogenous associated solution (with i which assumes the value 1 for the front wheel and 2 for the rear ones). They assume the values, respectively

8 Strictly, this happens only if the longitudinal velocity does not change. However, as first approximation its variability is neglected.

$$F^{h}_{yi}(t) = A\exp\left(-\frac{u}{d}t\right)$$
$$F^{p}_{yi} = Y_p(\bar{\alpha}) \quad \textbf{(3.36)}$$

where, $\bar{\alpha}$ is the value assumed by the slip angle during the permanent conditions and A is integration constant. To note the dependence of the particular from the slip angle α(t). In order to calculate the value of the constant it can be imposed the following condition:

$$F_{yi}(0) = 0 \quad \textbf{(3.37)}$$

The solution of the differential equation is presented:

$$F_{yi}(t) = A\exp\left(-\frac{u}{d}t\right) + Y_p(\bar{\alpha}) \quad \textbf{(3.38)}$$

That, substituting the initial condition, gives:

$$A = -Y_p(\bar{\alpha}) \quad \textbf{(3.39)}$$

And finally, the solution is:

$$F_{yi}(t) = Y_p(\bar{\alpha})\left(1-\exp\left(-\frac{u}{d}t\right)\right) = Y_p(\bar{\alpha})\left(1-\exp\left(-\frac{s}{d}\right)\right) \quad \textbf{(3.40)}$$

where it is imposed $s=ut$, with s which indices the displacement covered of the wheel. Obviously this function is an increasing monotonic function which begins from zero and moves in asymptotic way up to the permanent condition $\bar{\alpha}$.

The relaxation length can be obtained by some geometrical considerations, as shown in Figure 3.10, considering the permanent value equal to 2.4 kN. Imposing $s=d$ the relation available is:

$$F_{yi}(t) = \left(1-\exp(-1)\right)Y_p(\bar{\alpha}) = 0.6321\ Y_p(\bar{\alpha}) \quad \textbf{(3.41)}$$

Therefore, the length *d* represents the wheel displacement required to obtain a lateral force equal to 63 percent of the steady-state value.

Another method to obtain the relaxation length observing the following property:

$$\left.\frac{dF_y}{ds}\right|_{s=0} = \frac{Yp(\bar{\alpha})}{d} \qquad \textbf{(3.42)}$$

Normally, the magnitude of the relaxation length is about the rolling radius of the tyre. Synthetically, the table 3.1 shows the cornering force influence (steady-state value) on the relaxation length. To note its influence is very small, nearly insignificant.

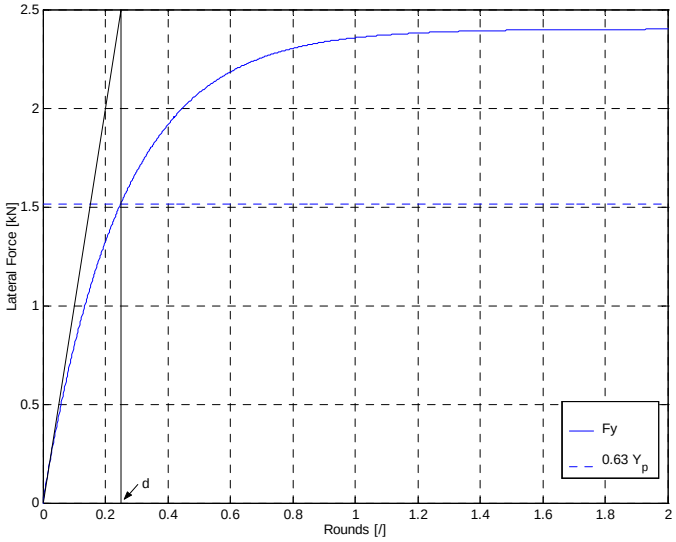

Figure 3.10: Lateral Force versus Wheel Rounds in Transient Condition with Permanent Value equal to 2.4 kN.

$F_y(\bar{\alpha})$	*d*
2.00	0.248
2.20	0.250
2.40	0.248

Table 3.1: Distance assumed with variation of Steady-State Cornering Force.

3.2.2.3 Non Linear Tyre Model with Relaxation Length

To describe the tyre behaviour, it is possible to use some empirical formulas which may not have any physical correlation with the effective behaviour of the tyre, such as the Magic Formula [20, 21, 22, 24, 25] and other experimental tendency traduced into a mathematical form. These empirical formulas come used to develop the mathematical model in order to study the complete vehicle dynamics. From a general point of view the tyre description could be just an approximation problem of an unknown analytical function. But, anyway there will have further constraints to respect. First, the first derivative may have some fluctuations that do not really exist. Real is the same as saying that the second derivative will be constrained too. This aspect produces the approximation more delicate. Another important aspect is to consider how many parameters will have to take into account, which of these will have to be constant and their physical meanings.

Still, the general trend is been to investigate some transcendental functions which are depending on a finite number of parameters. The function taken into account is:

$$F_y\left(\alpha, F_z\right) = \mu F_z\left(1 - \exp\left(-\frac{C_\alpha \alpha}{\mu F_z}\right)\right) \qquad \textbf{(3.43)}$$

where μ represents the ratio between the normalized tyre friction and the lateral force. Even if the lateral force depends on many factors, such as the road surface conditions, the curves shown in Figure 3.11 and Figure 3.12 illustrate how the normal force influences the shape of F_{yi} for the front and rear wheels.

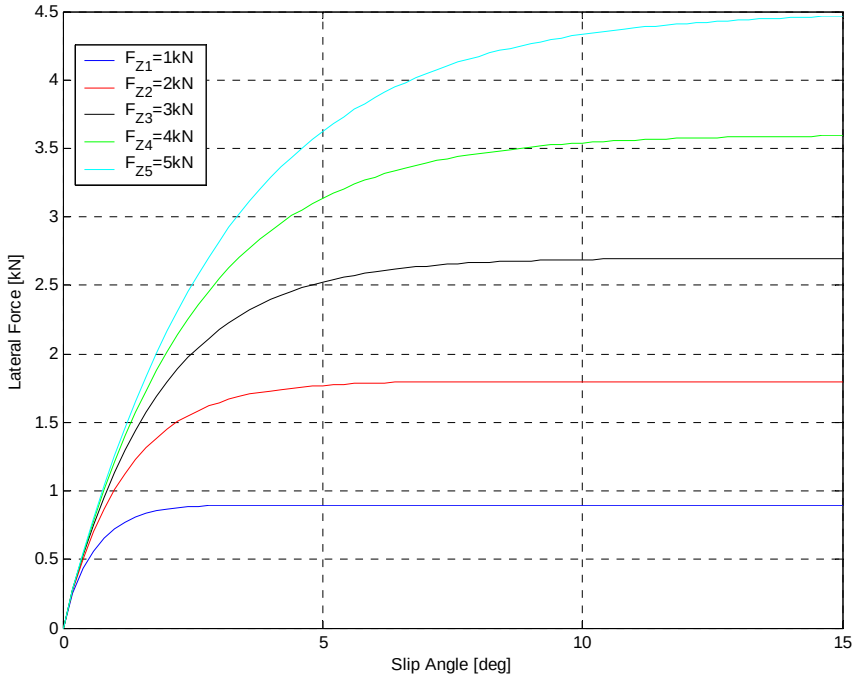

Figure 3.11: Front Lateral Force versus Slip Angle with Different Normal Load.

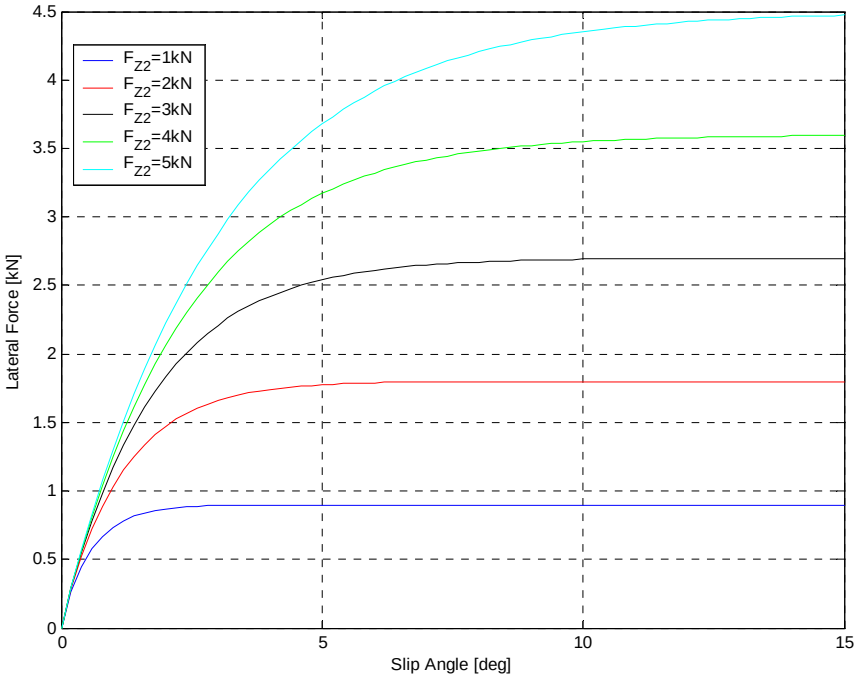

Figure 3.12: Rear Lateral Force versus Slip Angle with Different Normal Load.

Chapter 4

4 Longitudinal Dynamics Model

Modelling an vehicle in all its parts requires good knowledge of the components involved and their physics. The first step in the study of the longitudinal behaviour of the vehicle is to create a mathematical model that must represent the physical system with good approximation. This chapter describes the modelling of the dynamics longitudinal. In the field of vehicle lateral dynamics field, the feed velocity is kept constant in order to investigate the behaviour of the rest of the system. In this vehicle model, the speed and torque variability have been added.

4.1 Physical Model

From a mechanical point of view, a vehicle can be mainly presented as a numerous set of rotating and translating parts. Initially, to identify its dynamic behaviour we will model the whole system, basically composed of the propulsion system called "*powertrain*" and the set including the suspension, wheel and road links, called "*chassis*".

According to the aim to reach, vehicles can be modeled in many different ways. In fact, in this work we are going to analyze the dynamic development of the vehicle speed from a known throttle opening.

That is the reason why we will consider engine modelling only, and not driveline modelling [19], as shown in Figure 4.1.

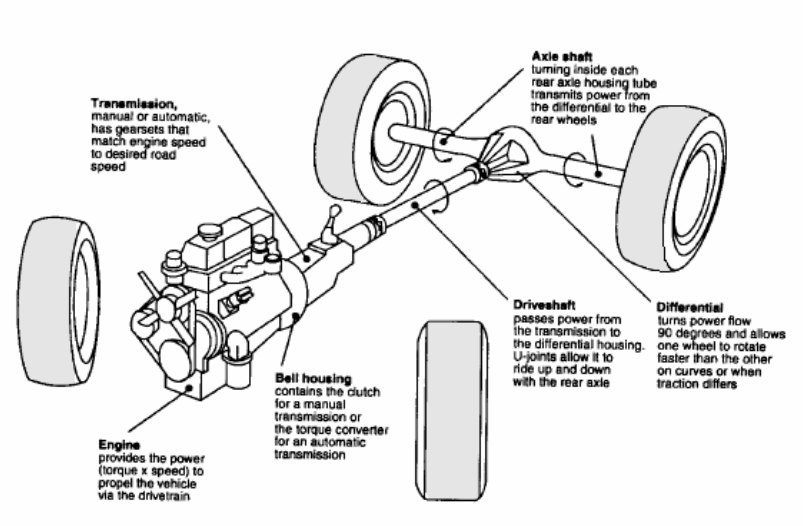

Figure 4.1: Primary Elements in the Powertrain

Schematically, the powertrain system can be represented as in Figure 4.2. The system-vehicle can be configured through a set of interconnected blocks; see Figure 4.3 for a description of the different powertrain components [26, 27].

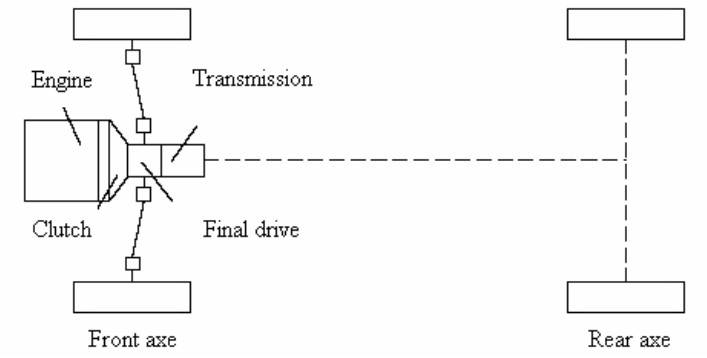

Figure 4.2: Schematization Elements in the Powertrain

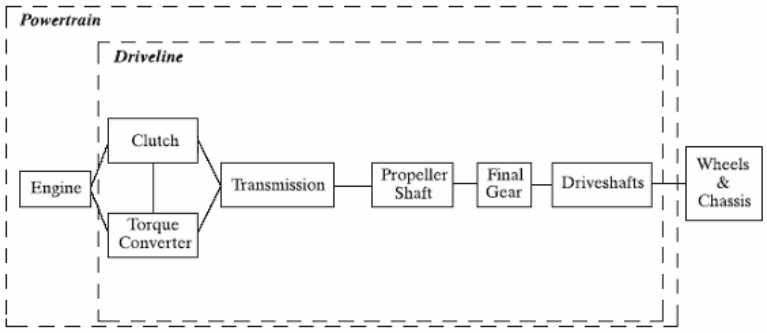

Figure 4.3: Powertrain Components and Configurations Theoretical Model

The main parts of a vehicle powertrain are the engine, clutch transmission, torque converter and shafts. This section covers the derivation of basic equations describing a complete longitudinal model. The aim of modelling is to find the most important physical effects explaining the oscillations in the measured engine speed, transmission speed, and wheel speed. The model is the combination of rotating inertia connected with damped shaft flexibilities, considered rigid.

A theoretical model of the drivetrain is introduced in form of a non linear Simulink model of the first order. The parameter values are derived from the measurement data. The model input is the throttle position of the driver; the model output is the engine speed and wheel speed [24, 25, 26, 28].

4.2 Powertrain Modelling

Modelling the powertrain requires good knowledge of the components involved and their physics. We will divide modelling into two parts: the *engine model* and the *driveline model*, including a torque converter model. The models presented in the literature are usually complex and therefore not suitable for the visualization the principal aspects of vehicle dynamics owing to long simulation time. So, we will construct some simpler models.

As mentioned previously, there are two limiting factors to the performance of a road vehicle: one is the maximum traction effort that the tyre-ground contact can stand, and the other is the traction effort that the engine torque with a given transmission can provide. The smaller of these two will give the performance potential of the vehicle.

In low gears with the engine throttle fully open, the traction stress may be limited by the nature of the tyre-road grip. Instead, in higher gears, the traction effort is usually determined by the engine and transmission characteristics. To predict the overall performance of a vehicle, the engine and transmission characteristics must be taken into consideration. In this section, the general characteristics of vehicle power and transmissions will be presented.

4.2.1 Engine Model: Characteristics of Internal Combustion Engines

As most road vehicles are powered by reciprocating internal combustion engines, their characteristics will be summarized in the present section.

Apart from the action of the throttle control, the power supplied by the engine depends mainly on the rotational speed. The performance of an internal combustion engine is usually summarized in a single map plotted in a plane whose axles are the rotational speed ω_e and the torque (or power P_e) as shown in Figure 4.4. Often the former is reported in rpm and the latter in Nm (or in kw if power); in the present text however S.I. units, i.e. rad/s will be used, according to the following relation:

$$\omega_e = \frac{2\pi n_e}{60} \qquad \textbf{(4.1)}$$

with n_e that represents the engine speed in rad/s.

The choice about the characteristic representation does not make sense because power and torque are related by the speed. Specifically,

$$P_e = T_e \omega_e \qquad \textbf{(4.2)}$$

where P_e is the engine power.

The internal combustion engine is connected to the wheels through a transmission system which includes a clutch, a gear selector (or gear box) and some joints.

The relationship between the angular velocity of the engine and the velocity of the wheels is simply given by:

$$\omega_e = \frac{\tau_c \tau_d}{\eta_c \eta_d} \omega_w \quad \textbf{(4.3)}$$

where τ_c and τ_d are the transmission ratios (defined as the ratio between the velocities of the output and the input shafts) of the gearbox and the final drive respectively. Moreover, η_c and η_d are the efficiency of the gearbox and the final drive. Note that the transmission ratio and the efficiency of the gearbox are a function of gear in. Instead, the other parameters of the final drive are constant. The efficiency of the gearbox is usually smaller than 1.

However, the relationship between the angular velocity of the wheels and the velocity of the vehicle is given from the Equation (3.1), shown in the following relationship:

$$u = \omega_w R_r \quad \textbf{(4.4)}$$

where R_r is the effective rolling radius.

This model can be considered as the first important aspect of the complete vehicle model. The characteristic curve of an internal combustion engine defines the torque supplied as function of the engine speed n_e and throttle opening α that is as function of a parameter able to show how much the throttle should be opened.

Conceptually, the throttle opening is proportional to the mass flow rate of air. In fact, the throttle opening assumes included values between 0, section completely closed and 1 (or percent value) for fully opened.

Usually, the output engine torque is measured with a test-engine linked to a brake system, in maximum and minimum admissions. During these two steady-state conditions, the corresponding characteristic curves can be pointed out . A representative characteristic of the gasoline engine is shown in Figure 4.4 and 4.5, in dimensionless form.

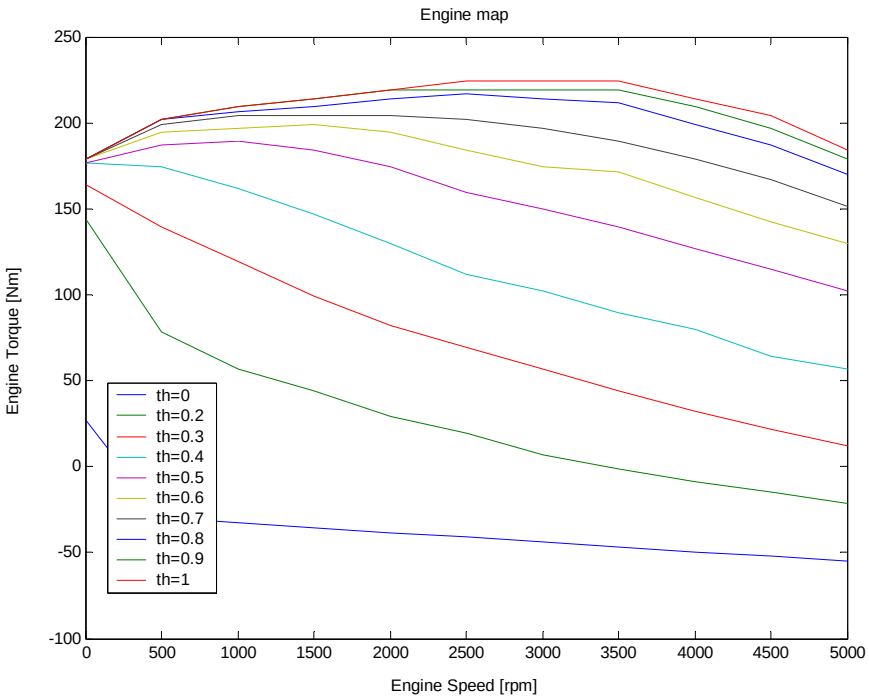

Figure 4.4: Performance Characteristic of Test-Vehicle

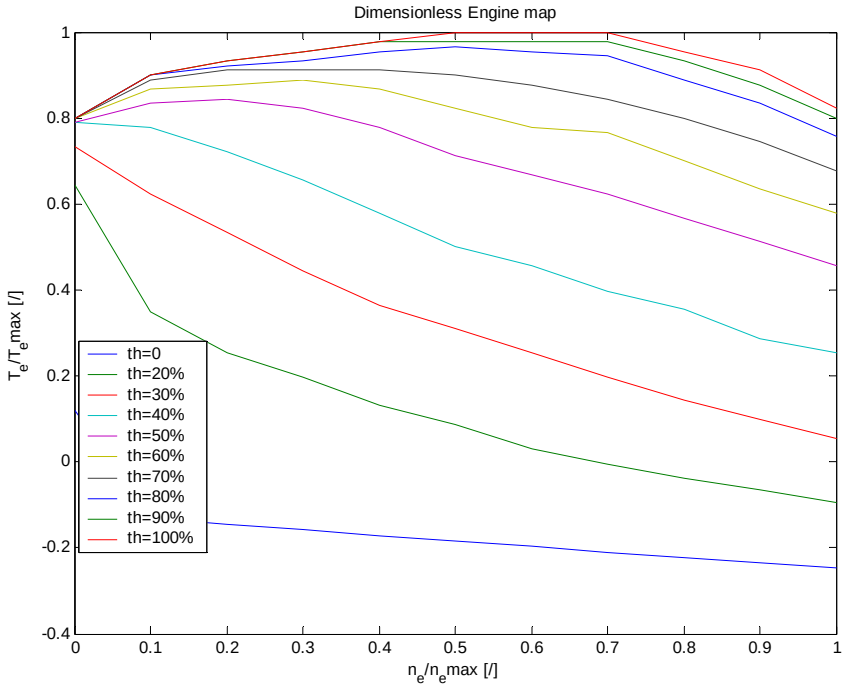

Figure 4.5: Dimensionless Performance Characteristic of Test-Vehicle

Numerically, this picture is an element matrix because it represents the engine torque as function of the engine speed for a fixed throttle opening.
In intermediate conditions, with a good approximation, the engine torque is a linear function of throttle opening, so the engine torque is expressed by the following relation:

$$T_e = T_{e\max}\alpha + T_{e\min}\left(1-\alpha\right) \quad \textbf{(4.5)}$$

where T_{emax} and T_{emin} represent the maximum and minimum value of the engine torque T_e, [24].

4.2.2 Gear Box and Torque Converter

These two models will be illustrated directly in the Chapter 6, with the main details. The complete gearbox is simulated. The presence of the clutch is neglected.

4.3 Driver Model

A driver typically control vehicle speed by depressing the accelerator pedal to request positive torque or depressing the brake pedal (not modeled) to request negative torque. In a conventional vehicle, positive torque is supplied only by the combustion engine, and negative torque is supplied only by the brakes. Perhaps, to develop the complete vehicle model, but not taking into account the brake model, the negative torque is supplied by the close-throttle manoeuvreing (as well to work with negative torque value) and the total resistent motion.

4.4 Equivalent Dynamic System

In this section, the principal aim is to reduce all the mechanical system into a reduced system in order to work with an easier vehicle model.

For this reason an equivalent dynamic system, including all vehicle parts, (rotating and translating ones) will carried out. From the mathematical point of view, the *Kinetics Energy Theorem* end *Principle of D'Alembert* will be used.

Consider a vehicle with a mechanical transmission with a number of different gear ratios. Schematically, in according to Figure 4.2, the complex system studied, before reducing, is shown in Figure 4.6. Note the new parameters introduced, τ_c, η_c, τ_d, η_d, I_e and I_w.

These parameters represent a great physical mean:

I_e: Engine Inertia;

I_w: Wheel Inertia;

τ_c: Transmission Gear box ratio;

τ_d: Final drive ratio;

η_c, η_d: Gear box and Final drive efficiency.

In order to reduce the whole mechanical system into an equivalent one, we can assume that is only a physical system (without energy transferred). The vehicle can be modeled as two moments of inertia, one to model the engine and one to model the vehicle; see Figure 4.7 (a) and (b). The first one includes the moment of inertia of the engine, up to the flywheel, while the moment of inertia of the clutch disks, of the shaft entering the gearbox, of all the rotating parts, reduced to the engine shaft, and the mass of the vehicle as "seen" from the engine are included in the second

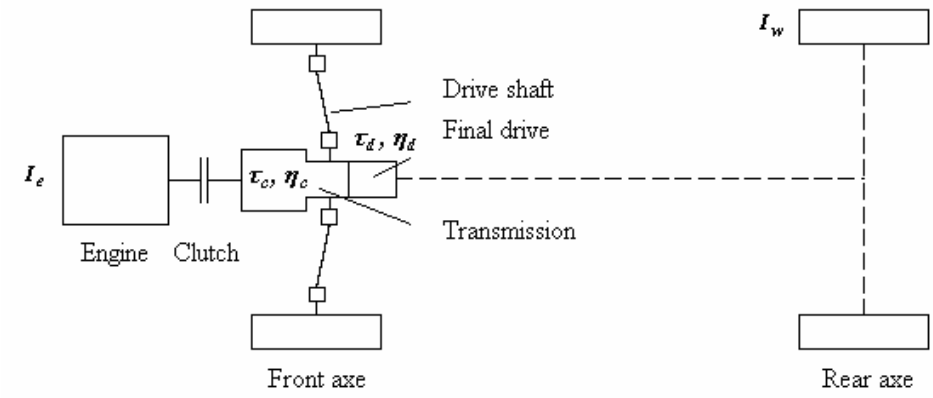

Figure 4.6: Driveline Notations

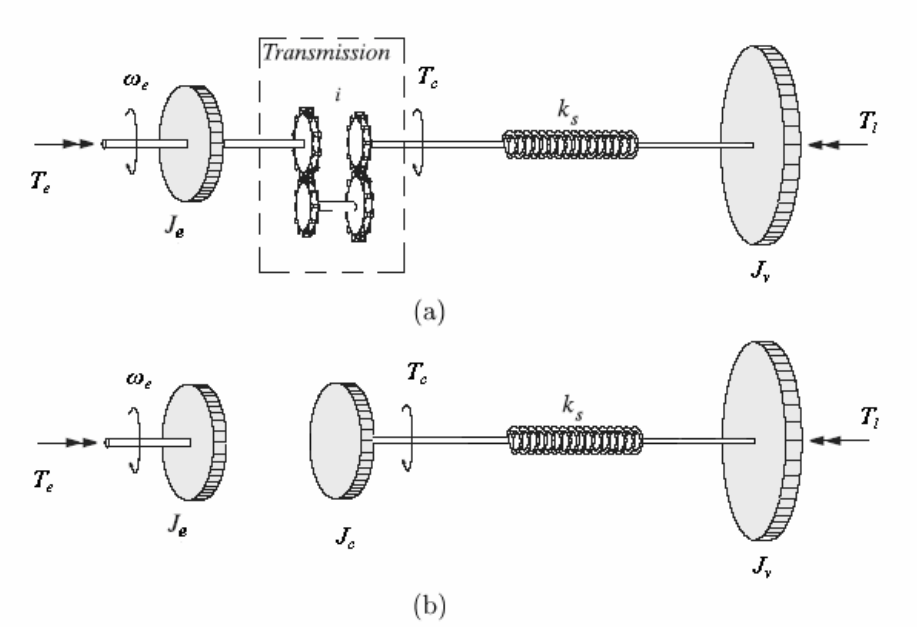

Figure 4.7: Driveline Complex Model. (a) Transmission Engaged; (b) Transmission Disengaged.

In accordance with our convention (RHL), we can note the opposite orientations of the torques applied at shaft, because the first on the left is drive and the second one is "resistent".

To simplify the theoretical model, we start from the following working hypothesis:

- Transmission shaft is rigid, as well as the stiffness k_s and has an infinite value. This makes things easier;
- Transmission is engaged-disengaged immediately, the clutch system is neglected. Actually, this working hypothesis is not satisfied; only making a good setup of the implementation model, a realistic approximation can be obtained. So, the final esteemed system is shown in Figure 4.8.

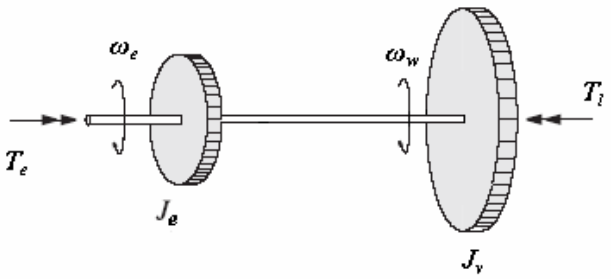

Figure 4.8: Equivalent System for a Driveline Model.

During an acceleration manoeuvre, the rotating elements (wheels, transmission, the engine itself) must increase their angular velocity. Resorting to this expedients, it is possible to write only one equation, linking the engine torque with kinetic energy of the vehicle [23, 24, 29].

Fundamental equations for the driveline will be derived by using the generalized Newton's second law of motion.

The state equation of the speed is given below:

$$P_e - P_l = \frac{d\tau}{dt} \tag{4.6}$$

where:

τ: Kinetic Energy of the vehicle;

I_{eq}: Equivalent Inertia;

T_e: Engine Power;

T_l: Load Power.

Note that the engine power *Pe* should be the one provided in non steady-state running.

The kinetic energy of the vehicle, "seen" as an equivalent system can be expressed as

$$\tau = \frac{1}{2} I \omega^2 + \frac{1}{2} \sum_{i=1}^{n} m_i v_i^2 = \frac{1}{2} I_{eq} \omega_e^2 \tag{4.7}$$

where the sum extends to all translating elements which must be accelerated when the vehicle speeds up. Making a derivate of the kinetic energy we obtain

$$\frac{d\tau}{dt} = I_{eq} \omega_e \frac{d\omega_e}{dt} + \frac{1}{2} \omega_e^2 \frac{dI_{eq}}{dt} \tag{4.8}$$

Generally, the equivalent inertia changes in time if a torque converter is used because of the transmission ratio of the gearbox. If we consider that the equivalent inertia does not

change very fast, the former equation should have the following correction. Usually this change is very small, however, so it is possible to neglect it.

$$\frac{d\tau}{dt} = I_{eq}\omega_e \frac{d\omega_e}{dt} \quad \textbf{(4.9)}$$

The term on the left of equal, net power, is quantified according to Equation (4.6)

$$P_e - P_l = \left(T_e - T_l\right)\omega_e \quad \textbf{(4.10)}$$

However, the final expression which formalizes the mechanical system is

$$I_{eq}\frac{d}{dt}\omega_e = T_e - T_l \quad \textbf{(4.11)}$$

where:

ω_e: Engine Rotational Speed;

I_{eq}: Equivalent Inertia;

T_e: Engine Torque;

T_l: Load Torque.

It is possible to obtain the same formula in terms of power and linear velocity:

$$m_{eq}u\frac{du}{dt} = P_e - P_l \quad \textbf{(4.12)}$$

Consider the vehicle shown in Figure 3.7, in which the major significant forces are shown. So, paying attention to the term on the right of equal, T_l, the latter is a sum of some contributions:

$$T_l = T_{r,aero} + T_{r,rolling} + T_{r,slope} \quad \textbf{(4.13)}$$

where:

$T_{r,aero}$: Aerodynamics Torque;

$T_{r,rolling}$: Rolling Resistent Torque;

$T_{r,slope}$: Slope Torque;

In our simulations, we assumed that only the slope torque is constant (not during time) and known by the driver behaviour. In this way, there is not a direct connection between the engine speed and the engine torque, but continuously an update for these.

In order to construct only an equation, we need an explicit form of the equivalent inertia I_{eq}; it assumes the form:

$$I_{eq} = I_{engine} + I_{r,chassis} + 4I_{r,wheel} \quad \textbf{(4.14)}$$

with:

I_{engine}: Engine Inertia;

$I_{r,chassis}$: Chassis Inertia;

$I_{r,wheel}$: Wheel Inertia;

4.4.1 Reduction of Forces Acting on the Vehicle

In order to integrate numerically Equation 4.11, an explicit form of the whole physical terms, present in it, is required. This means, to perform two operations on the effective system; see Figure 4.8, namely "Reductions of mass" and "Reduction of forces", applying the *Kinetics Energy Theorem* and *Principle of D'Alembert* respectively [23, 24, 29].

From a general point of view, a force F_e, applied to a generic point of the effective[9] system, can be reduced[10] into a force F_r, acting to the reduced system (or into a torque T_r), only fixing a "reduction axle". The equivalence is verified if the works carried out by the each forces are equal. Considering ds_e and ds_r, the displacement of the previous points, we have the following relation:

$$F_e ds_e = F_r ds_r \quad \textbf{(4.15)}$$

and so we obtain:

9 The forces acting on the effective system F_e are denoted through the pedics e.

10 Analogy with note 1 the forces and the torques acting on the reduced system F_r and T_r are denoted through the pedics r too.

$$F_r = F_e \frac{ds_e}{ds_r} \quad \textbf{(4.16)}$$

Likewise, considering the reduction of a moment T_r, acting on the normal plane to the selected axle, the elementary rotation around this latter, $d\theta$ must be considered. So, the following relationship must be satisfied:

$$F_e ds_e = T_r d\theta_r \quad \textbf{(4.17)}$$

and so:

$$T_r = F_e \frac{ds_e}{d\theta_r} \quad \textbf{(4.18)}$$

According to this concept, all the machine members can be reduced to an equivalent system, namely "*Equivalent Flywheel*".

The external forces acting on the vehicle to develop the reduced system are:

- Aerodynamics Force in straight condition (without taking account of the positive and negative lift);
- Rolling Force at tyre-ground contact;
- Grade Resistent (or slope force) acting in the centre of gravity.

The reduction of forces, considered as a general principle, is performed trough the equality of the work carried out by the effective forces (acting on the effective system) and the work carried out by the reduced ones (acting on the reduced system).

4.4.1.1 Reduction Aerodynamics Force

The aerodynamic drag is characterized by the equation:

$$F_{aero} = F_{e,aero} = \frac{1}{2} \rho_{air} S C_x u^2 \quad \textbf{(4.19)}$$

Applying the Principle of D'Alembert to reduce this force on the engine shaft:

$$T_{r,aero} = F_{e,aero} \frac{ds_e}{d\theta_r} \quad \textbf{(4.20)}$$

It is required to make the quantities ds_e and $d\theta_r$ explicit.

$$ds_e = u_e dt \quad \textbf{(4.21)}$$

and

$$d\theta_r = \omega dt \quad \textbf{(4.22)}$$

So, replacing these two expressions[11] in the former:

$$T_{r,aero} = F_{e,aero} \frac{u_e}{\omega} \quad \textbf{(4.23)}$$

From the relationship between the velocity of the vehicle and the velocity of the wheels we obtain:

$$T_{r,aero} = F_{e,aero} R_r \frac{\omega_w}{\omega_e} \quad \textbf{(4.24)}$$

Where parameter R_r represents the effective rolling radius. However, taking into account of the relation of the rotational wheel velocity and the engine velocity we have finally an expression of the reduced aerodynamics force:

$$T_{r,aero} = F_{e,aero} R_r \frac{\eta_c \eta_d}{\tau_c \tau_d} = \frac{1}{2} \rho_{air} S C_x R_r \frac{\eta_c \eta_d}{\tau_c \tau_d} u^2 \quad \textbf{(4.25)}$$

or like a function of the rotational wheel velocity:

11 To note that the angular velocity ω is the velocity of a flywheel with mass equal to I_r which is rotating around the reduction axle. Specially, this velocity corresponds to the rotational engine velocity because the engine shaft was chosen as "reduction axle".

$$T_{r,aero} = \frac{1}{2}\rho_{air} SC_x \frac{\eta_c \eta_d}{\tau_c \tau_d} R_r{}^3 \omega_w{}^2 \quad \textbf{(4.26)}$$

and a function of the engine velocity:

$$T_{r,aero} = \frac{1}{2}\rho_{air} SC_x \frac{\eta_c{}^3 \eta_d{}^3}{\tau_c{}^3 \tau_d{}^3} R_r{}^3 \omega_e{}^2 \quad \textbf{(4.27)}$$

4.4.1.2 Reduction Rolling Force

The rolling resistent force can be expressed as :

$$F_{rolling} = F_{e,rolling} = f_r W \quad \textbf{(4.28)}$$

where W represents the weight of the vehicle. We can obtain the same expression for the rolling force reduced to the engine shaft:

$$F_{r,rolling} = F_{e,rolling} \frac{ds_e}{d\theta_r} \quad \textbf{(4.29)}$$

where the terms ds_e and $d\theta_r$ do not change.
Replacing these in the rolling resistent relation:

$$F_{r,rolling} = F_{e,rolling} \frac{u_e}{\omega_e} \quad \textbf{(4.30)}$$

and so we finally obtain:

$$F_{r,rolling} = F_{e,rolling} R_r \frac{\omega_w}{\omega_e} \quad \textbf{(4.31)}$$

Therefore, using the relationship between rotational wheel velocity and the engine velocity we finally obtain an expression of the reduced rolling force too:

$$F_{r,rolling} = F_{e,rolling} \frac{\eta_c \eta_d}{\tau_c \tau_d} R_r \omega_e \quad \textbf{(4.32)}$$

and the same expression in explicit form:

$$F_{r,rolling} = W f_r \frac{\eta_c \eta_d}{\tau_c \tau_d} R_r \omega_e \quad \textbf{(4.33)}$$

Where the terms have been already defined.

4.4.1.3 Reduction Grade Force

The grade force can be expressed as follows:

$$F_{slope} = F_{e,slope} = Wi \quad \textbf{(4.34)}$$

where *i* indicates the slope road. By applying the Principle of D'Alembert to reduce this force on the engine shaft, we obtain again:

$$F_{r,slope} = F_{e,slope} \frac{ds_e}{d\theta_r} \quad \textbf{(4.35)}$$

with ds_e and $d\theta_r$ which are not chancing expression. Representing the latter quantities in explicitly we have:

$$F_{r,slope} = F_{e,slope} \frac{u_e}{\omega_e} \quad \textbf{(4.36)}$$

By considering the relationship between the velocity of the vehicle, the velocity of the engine, we can obtain:

$$F_{r,slope} = F_{e,slope} R_r \frac{\omega_w}{\omega_e} \quad \textbf{(4.37)}$$

where the parameter R_r represents the effective rolling radius. However, taking into account of the relation of the rotational wheel velocity and the engine velocity we have finally an expression of the reduced aerodynamics force:

$$F_{r,slope} = F_{e,slope} R_r \frac{\eta_c \eta_d}{\tau_c \tau_d} \quad \textbf{(4.38)}$$

and a final expression:

$$F_{r,slope} = W R_r \frac{\eta_c \eta_d}{\tau_c \tau_d} i \quad \textbf{(4.39)}$$

Note that this resistent force is a constant in opposition with the other ones, and its value changes only as function of the slope grade and not changing with the velocity.

4.4.2 Reduction of Inertias of the Vehicle

As is the case for the reduction of forces, it is possible to do the same thing, estimating the reduced inertias of our model, applying the Kinetics Energy Theorem [23, 24, 29].
Given a point or an axle belonging to the effective system, the reduction of masses can be performed, by substituting each mass m_e of the effective system for a mass m_r reduced to the point of reduction, imposing the invariance of Kinetic Energy.
By noting with u_e the velocity of the effective mass (as well the point of application of this mass) and with u_r the velocity of the reduced mass (as well the point of application), we can impose the invariance of kinetic energy:

$$\frac{1}{2} m_e u_e^{\,2} = \frac{1}{2} m_r u_r^{\,2} \quad \textbf{(4.40)}$$

therefore,

$$m_r = m_e \frac{u_e^{\,2}}{u_r^{\,2}} \quad \textbf{(4.41)}$$

The mass m_e, translating with velocity u_e, can be reduced to a rotating mass m_r, having velocity ω around a reduction axle, from which it is distant of r. This can be obtained by expressing the following relationship:

$$\frac{1}{2} m_e u_e^{\,2} = \frac{1}{2} m_r \omega^2 r^2 \qquad \textbf{(4.42)}$$

and:

$$I_r = m_r r^2 \qquad \textbf{(4.43)}$$

it is possible to obtain:

$$m_e u_e^{\,2} = I_r \omega^2 \qquad \textbf{(4.44)}$$

and we have the final expression about the reduced inertia as function of the effective parameters:

$$I_r = m_e \frac{u_e^{\,2}}{\omega^2} \qquad \textbf{(4.45)}$$

Naturally, an inertia flywheel whose moment of inertia is equal to I_e will be equivalent to a flywheel, namely I_r which is rotating with velocity ω around the reduction axle, only if the following relation is satisfied:

$$\frac{1}{2} I_e \omega_e^{\,2} = \frac{1}{2} I_r \omega^2 \qquad \textbf{(4.46)}$$

And so, the other condition can be obtained by:

$$I_r = I_e \frac{\omega_e^{\,2}}{\omega^2} \qquad \textbf{(4.47)}$$

4.4.2.1 Engine mass

The engine is constituted by rotating and translating parts. By considering only the rotating ones, we directly need just in an explicit form the engine inertia:

$$I_e = I_{cgi} + I_{fw} = \left(m_c + m_{cr}\right) R_c{}^2 n_{cyl} + I_{fw} \quad \textbf{(4.48)}$$

where:

I_{cgi}: Crank Gear Inertia;

I_{fw}: Flywheel Inertia;

m_c: Crank Mass;

m_{cr}: Connecting Rod Big End Mass;

R_c: Crank Radius;

n_{cyl}: Cylinder Number;

The Figure 4.9 shows the basic nomenclature of the correcting rod of an internal combustion engine[12]. For an accurate description of all components see [28].

4.4.2.2 Reduction Vehicle Mass

The vehicle mass (chassis), can be expressed in an inertia form using the relationship (4.45):

$$I_{r,chassis} = m_{e,chassis} \frac{u_e{}^2}{\omega^2} \quad \textbf{(4.49)}$$

where $m_{e,chassis}$ represents the effective mass of vehicle.

12 The connecting rod inertia should be to concentrated into two points, connecting rod (the mass of the piston included) and in other point situated near the connecting rod big end. For completeness, calling m_1 the former and m_2 the latter it should have $m_1=m\ h/(c+h)$ and $m_2=m\ c/(c+$h), where $h=I_{zz}/mc$ with I_{zz} the moment of inertia of the connecting rod about the orthogonal axis to the paper and m is the mass of the connecting rod which may be measured experimentally. The terms c and h represent the distant of the centre of the connecting rod and the position of m_2 to the centre of gravity of the rod. To note that the position of the mass m_2 is not defined completely; in fact it is assumed to be coincident with the big end of the connecting rod (with an opportune measuring of the relief).

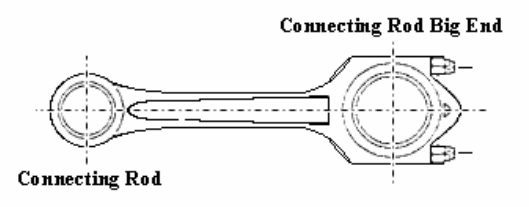

Figure 4.9: Description of Correcting Rod of Internal Combustion Engine.

As in the former section, about the reduced forces, we can have the same expression for the reduced inertia, explaining the vehicle velocity:

$$I_{r,chassis} = m_{e,chassis} R_r^{\,2} \frac{\omega_w^{\,2}}{\omega_e^{\,2}} \qquad \textbf{(4.50)}$$

where it is still the concept about the rotational velocity ω. Substituting the relationship between the angular velocity of the wheels for that of the engine:

$$I_{r,chassis} = m_{e,chassis} R_r^{\,2} \left(\frac{\eta_c \eta_d}{\tau_c \tau_d} \right)^2 \qquad \textbf{(4.51)}$$

4.4.2.3 Reduction Wheel Inertia

Each wheel mass can be considered as an inertia performing the relationship (4.47):

$$I_{r,wheel} = I_{e,wheel} \frac{\omega_e^{\,2}}{\omega^2} \qquad \textbf{(4.52)}$$

where $I_{e,wheel}$ is the effective inertia of the wheel. As was the case for the chassis mass, we have the same expression for the reduced inertia of the wheel, noting that the effective angular velocity is that of the wheel:

$$I_{r,wheel} = I_{e,wheel} \frac{\omega_w^{\,2}}{\omega_e^{\,2}} \qquad \textbf{(4.53)}$$

Therefore, by substituting the relationship between the angular velocity of the wheels and the engine one:

$$I_{r,wheel} = I_{e,wheel}\left(\frac{\eta_c \eta_d}{\tau_c \tau_d}\right)^2 \quad \textbf{(4.54)}$$

From the Equation (4.12) the maximum acceleration the vehicle is capable of at the various speeds is immediately obtained

$$\left(\frac{du}{dt}\right)_{\max} = a_x = \frac{P_e - P_l}{m_{eq} u} \quad \textbf{(4.55)}$$

where the engine power P_e is the maximum power that the engine can deliver at the speed ω_e related to speed u.

The plot of the maximum acceleration versus the speed for a vehicle with a five speed gearbox is reported in Figure 4.10, and 4.11.

The minimum time needed to accelerate from speed u_1 to speed u_2 can be computed by separating the variables in Equation (4.11)and integrating

$$T_{u_1 \to u_2} = \int_{u_1}^{u_2} \frac{m_{eq}}{P_e - P_l} u du \quad \textbf{(4.56)}$$

The integral must be performed separately for each velocity range in which the equivalent mass is constant because in this way the gearbox works with a fixed transmission ratio. Although it is possible to integrate analytically Equation (4.11) if the maximum power is a polynomial, numerical integration is usually performed.

A graphical interpretation of the integration is performed, as shown in Figure 4.12. The area under the curve:

$$\frac{1}{a_x} = \frac{m_{eq} u}{P_e - P_l} \quad \textbf{(4.57)}$$

versus u is the time required for the acceleration.

The speeds at which gear shifting must occur to minimize acceleration time are readily identified on the plot *1/a(u)*, as shown in Figure 4.13, and 4.14

As the area under the curve is the acceleration time or the time to speed, the area must be minimized and the gears must be shifted at the intersection of the various curves. If they do not intersect, the short gear must be used up to the maximum engine speed.

The areas between the dashed and the continuous lines account for the time which must be added due to the presence of a finite number of speeds: the transmission ratios, during the project phase, can be chosen in such a way to minimize this area.

By increasing the number of speeds the acceleration time is reduced, as the actual curve gets nearer to the ideal dashed line.

However, at each gear shift there is a time in which the clutch is disengaged and consequently the vehicle does not accelerate: increasing the number of speeds leads to an increase of the number of gear shifting and thus of the time wasted without acceleration. Obviously, this restricts the use of high number of gear ratios.

The characteristic curves, such as speed-time at maximum power, and many others, (which can be easily obtained by integrating the equation of motion), are reported in Figure 4.15, 4.16, 4.17, and 4.18.

Through further integration it is possible to obtain the distance needed to accelerate to any value of the speed

$$s_{u_1 \to u_2} = \int_{t_1}^{t_2} u dt \qquad \textbf{(4.58)}$$

It is however, possible to directly obtain the acceleration space.

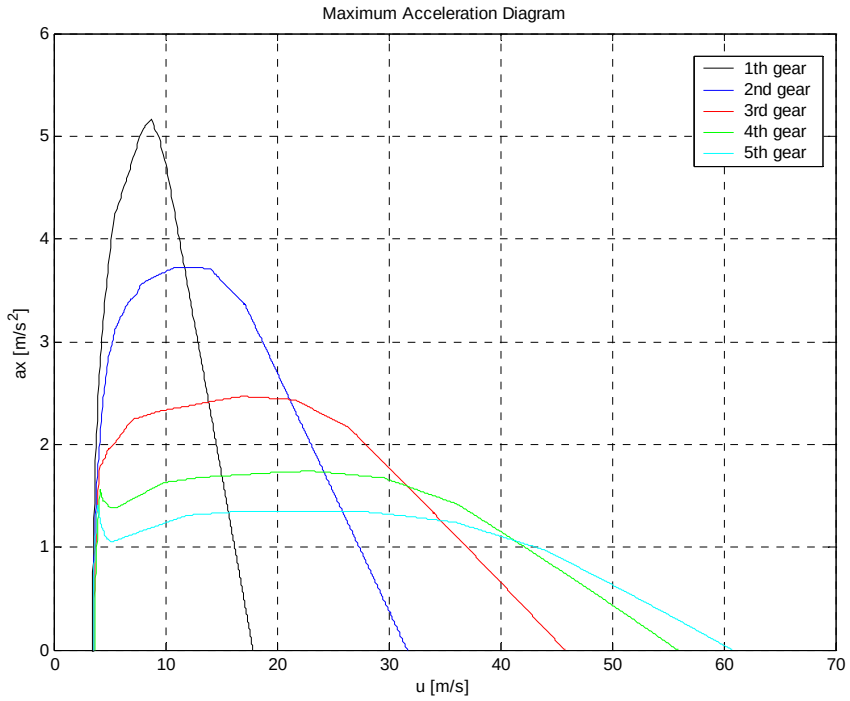

Figure 4.10: Maximum Acceleration as function of the Speed.

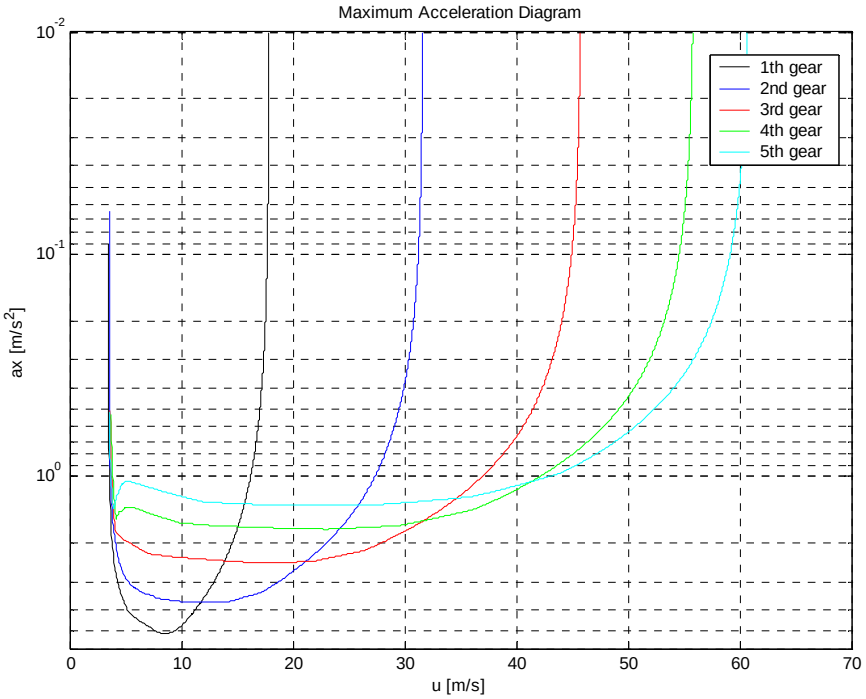

Figure 4.11: Maximum Acceleration as function of the Speed in log scale and reverse.

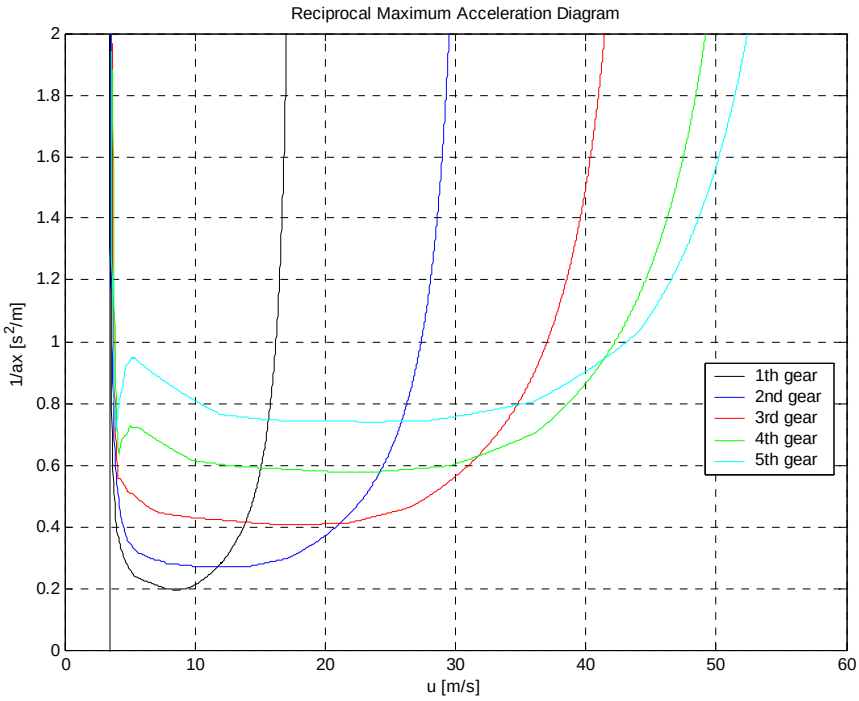

Figure 4.12: Function *1/a(u)* and Search for the Optimum Speeds for Gear Shifting.

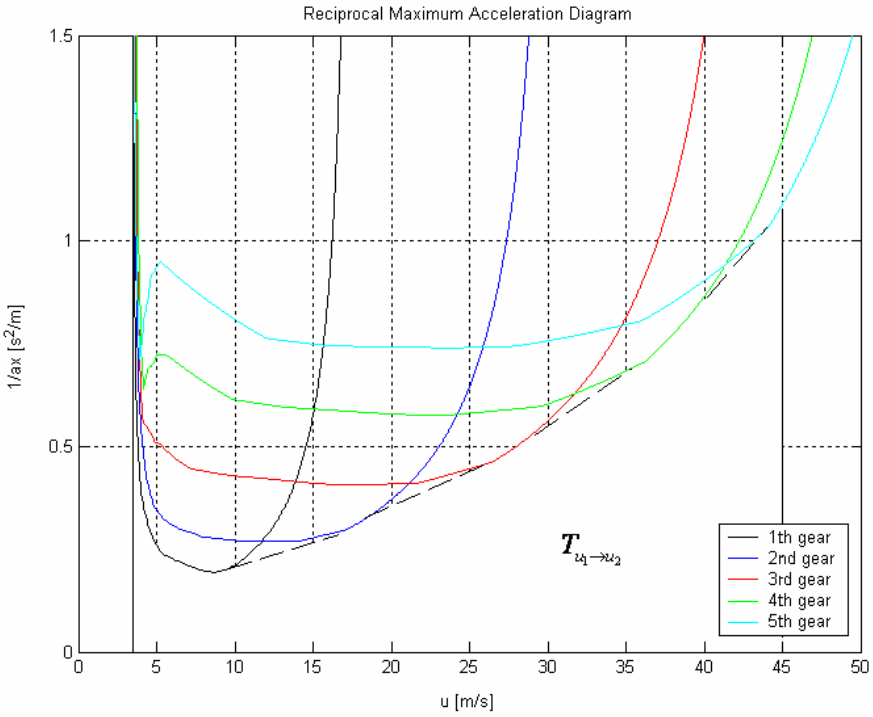

Figure 4.13: Function *1/a(u)* and Search for the Optimum Speeds for Gear Shifting; the white area is the time to speed.

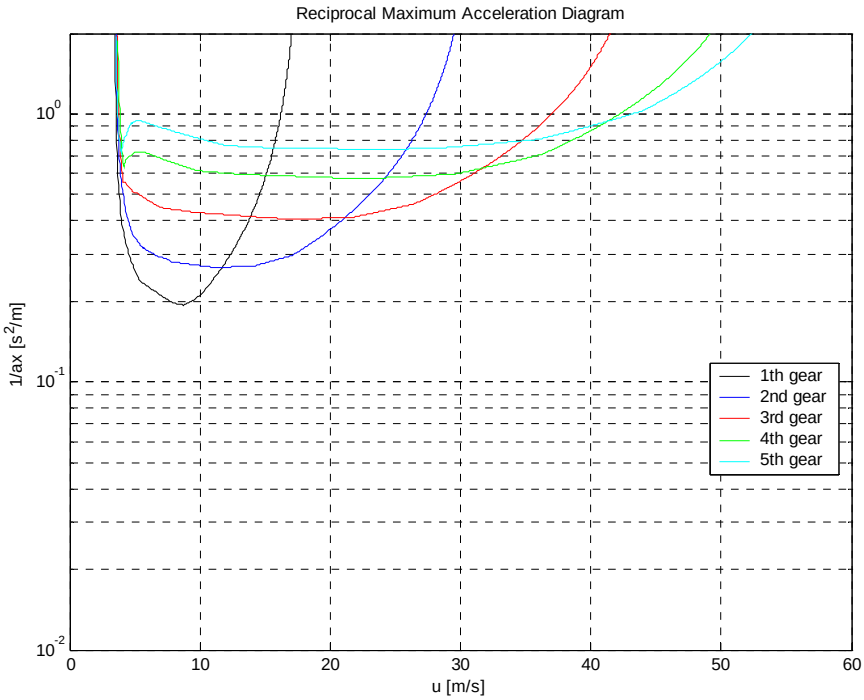

Figure 4.14: Function $1/a_x(u)$ in log scale.

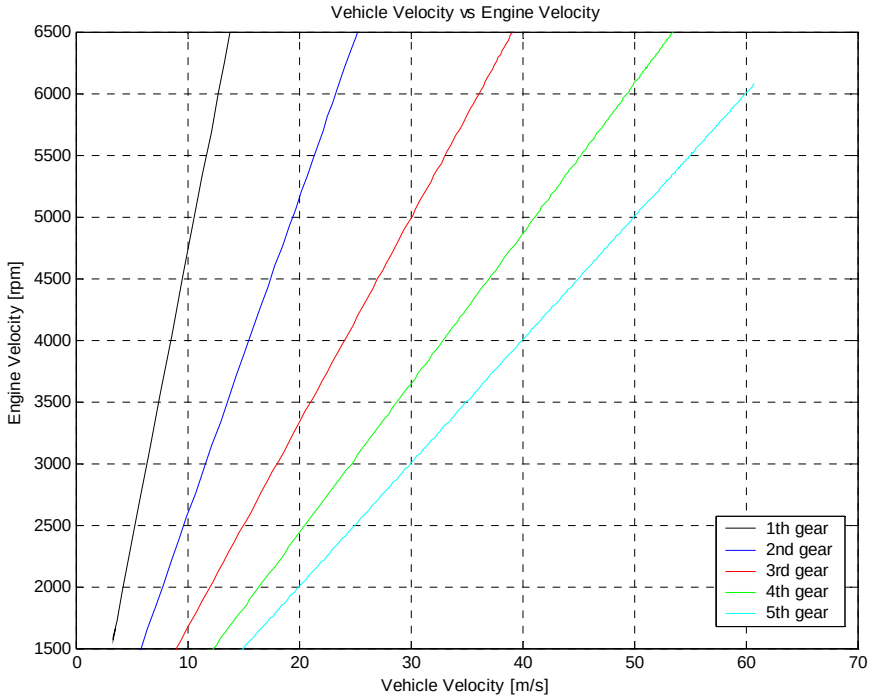

Figure 4.15: Engine Speed versus Vehicle Speed.

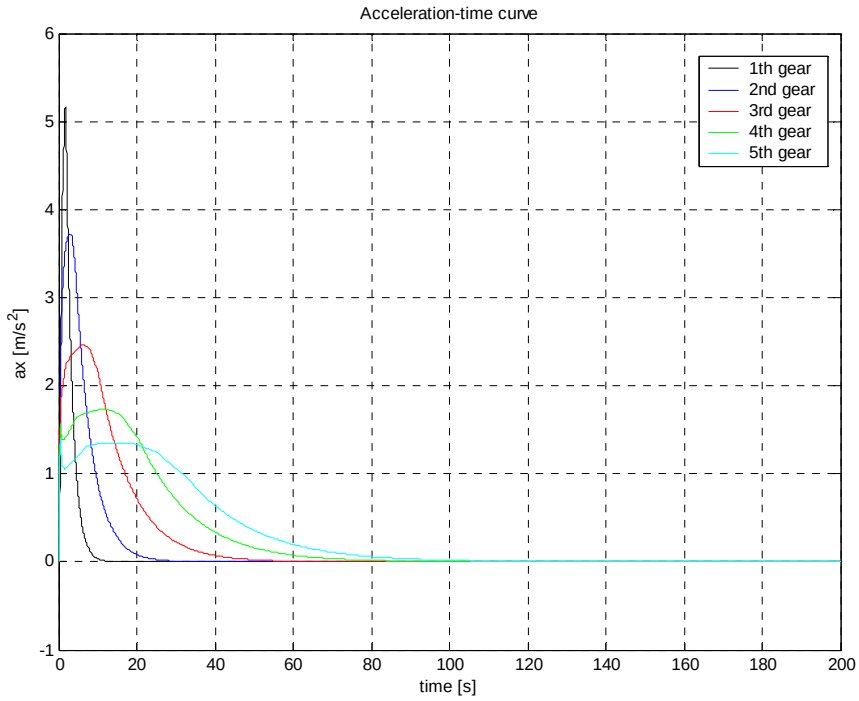

Figure 4.16: Acceleration-time curve.

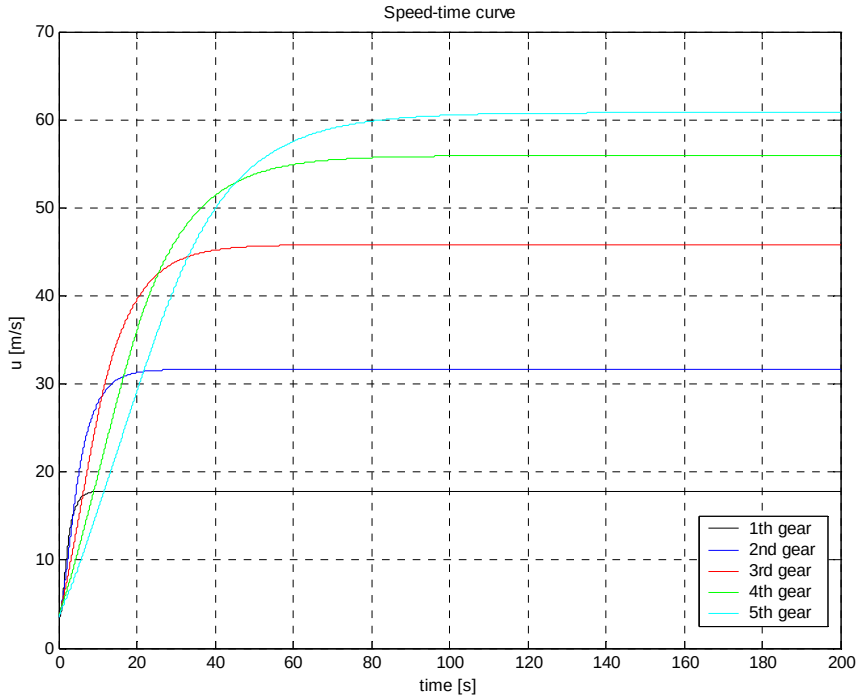

Figure 4.17: Speed-time curve.

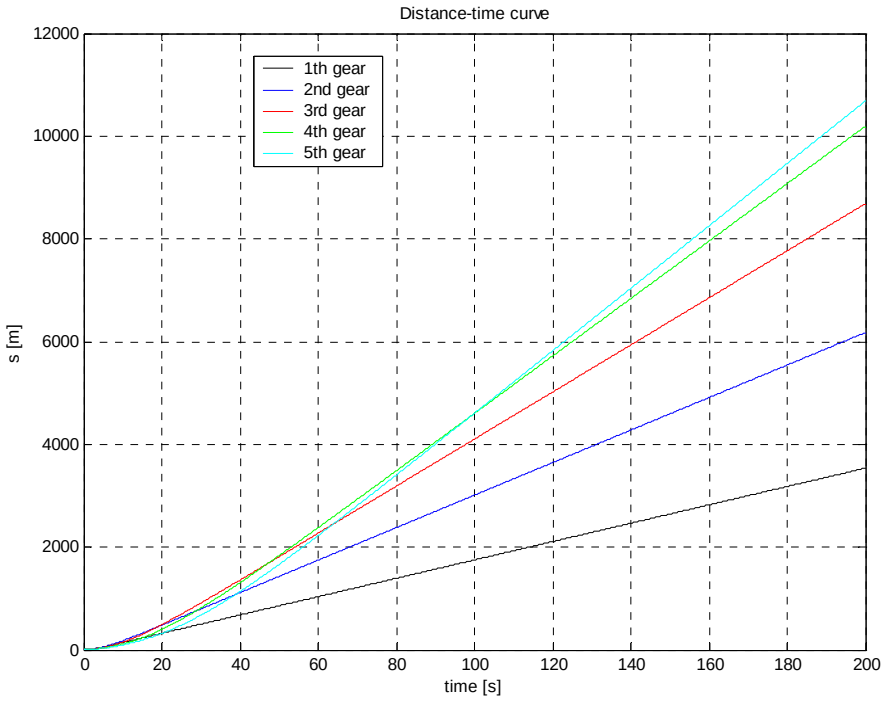

Figure 4.18: Distance-time curve.

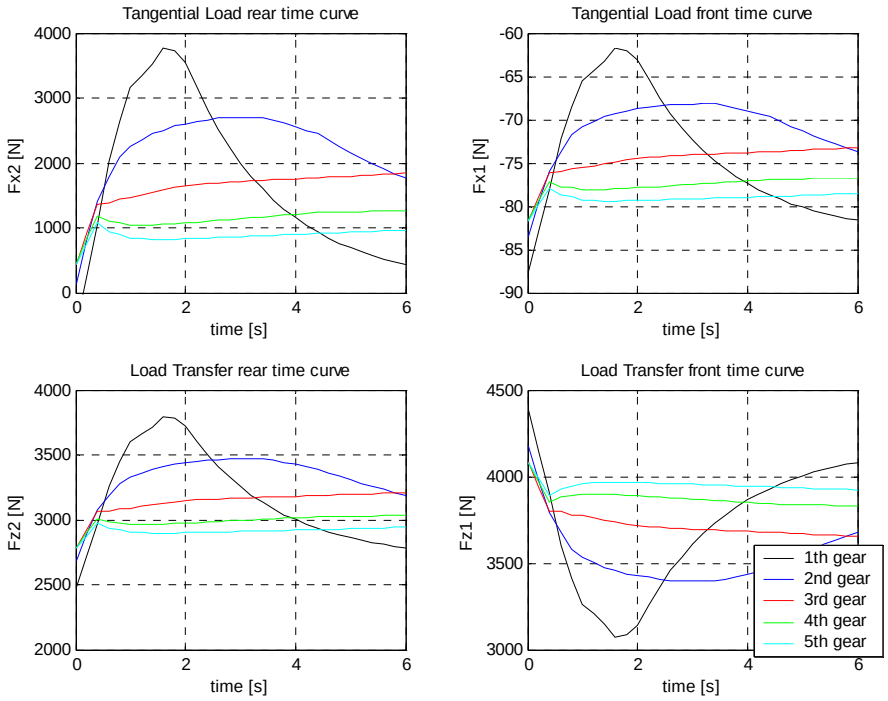

Figure 4.19: Traction tyre curve.

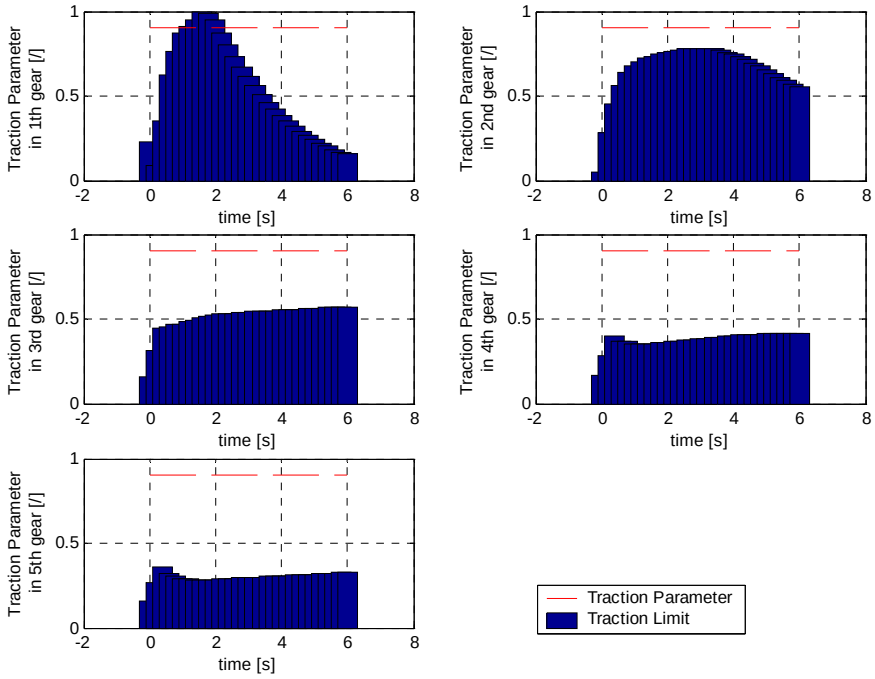

Figure 4.20: Traction Control curve.

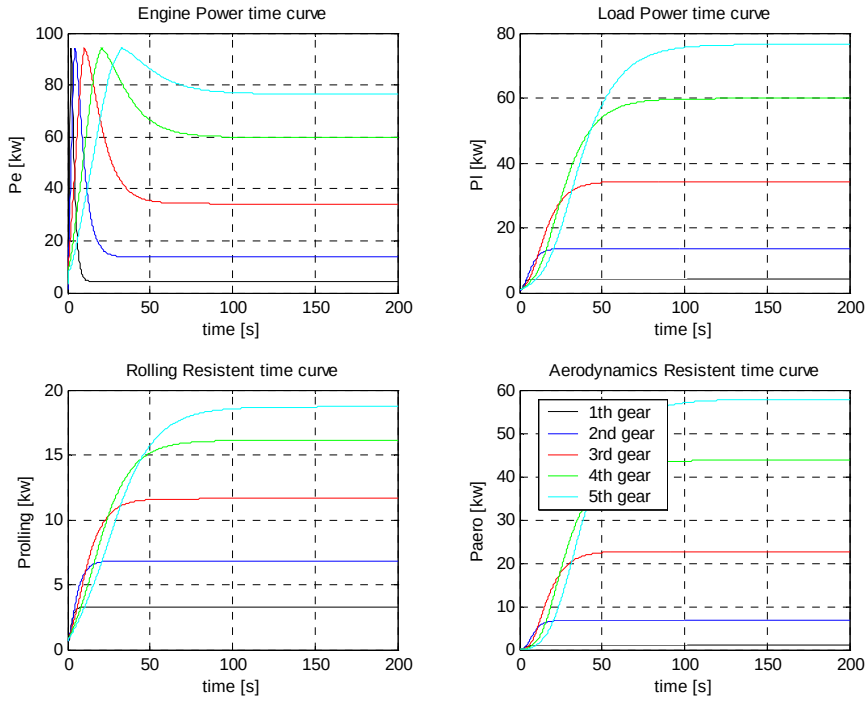

Figure 4.21: : Power-time curve.

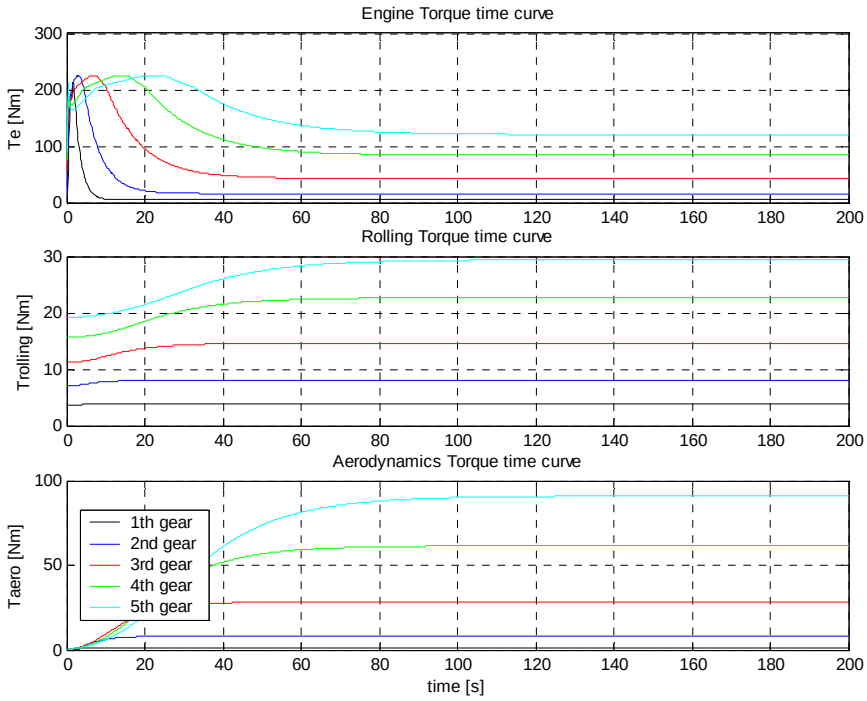

Figure 4.22: Torque-time curve.

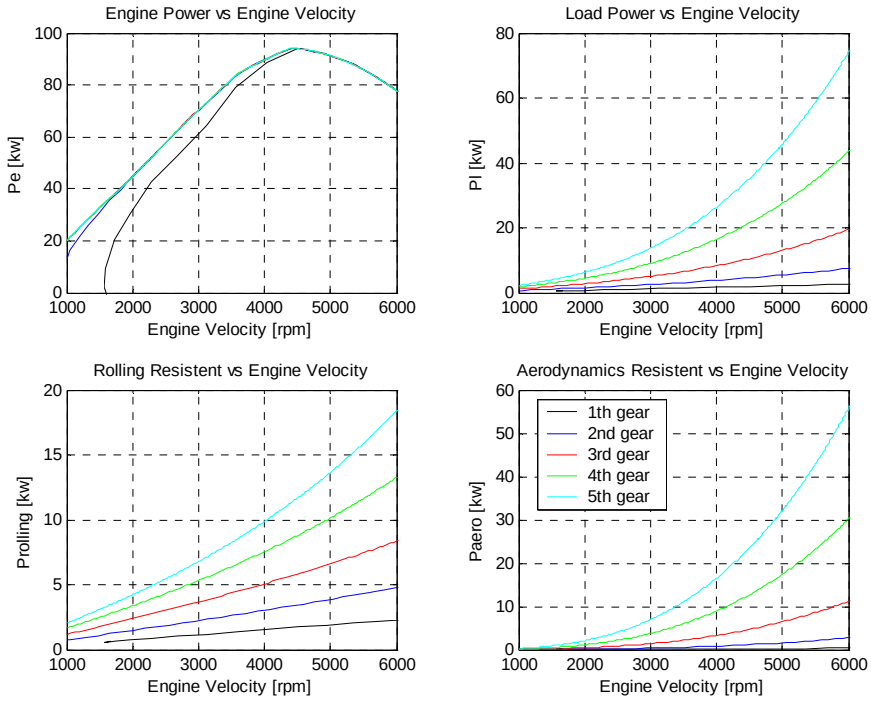

Figure 4.23: Power versus Engine Velocity.

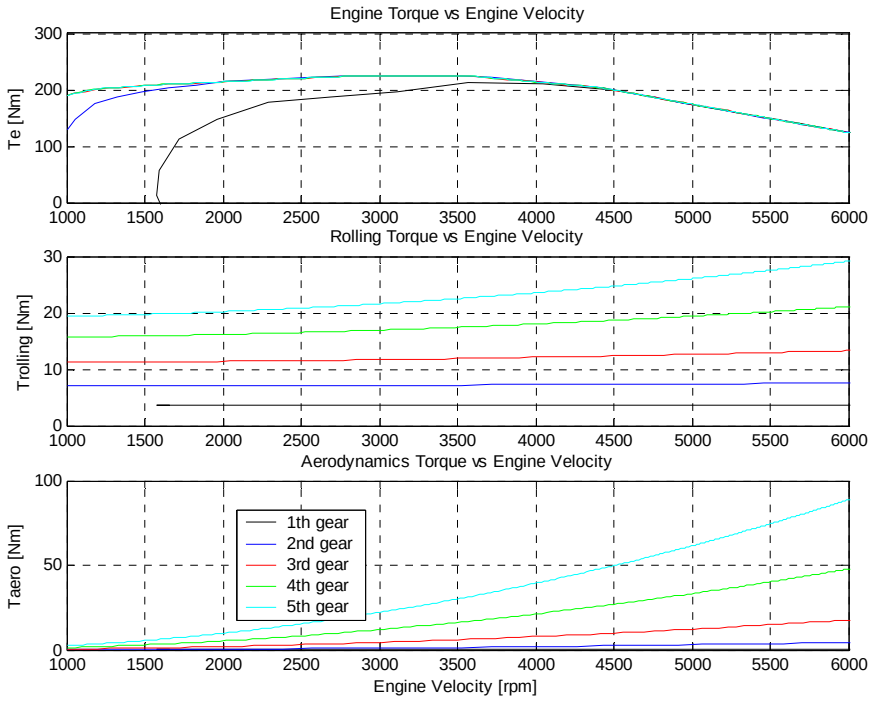

Figure 4.24: Torque versus Engine Velocity.

4.5 Simulation for longitudinal Model with Gearbox

4.5.1 Method of Vehicle-Simulation

The vehicle-following simulation is conducted to evaluate the dynamic performance of the vehicle in the longitudinal direction. The powertrain model with the gearbox is used in the simulation.

Throttle opening manoeuvres determine the developing of the low of motion of the vehicle, during the transient condition. In fact, varying this input signal, the engine torque produced changes completely. For this reason, the low of variation of the throttle opening during the time will be shown. Among many signals which can be chosen, the "ramp-signal" is taken into account; see Figure 4.25 for a accurate description. In other words, the driver increases the throttle opening from zero to full opening value, varying the throttle with linear way. The time required to obtain the full value is fixed at 2 seconds.

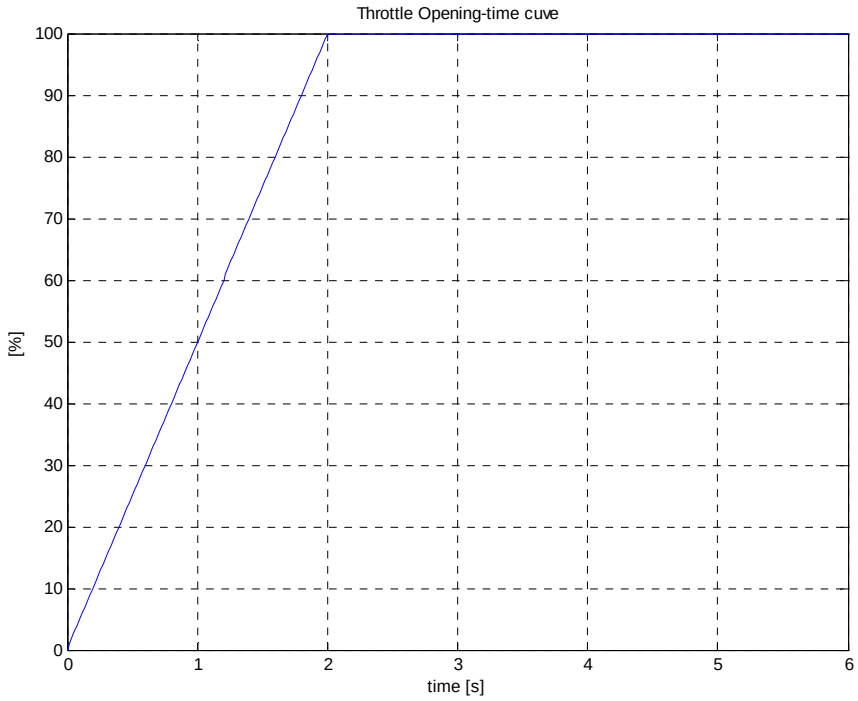

Figure 4.25: Throttle Opening Input

The temporal function of the vehicle can be obtained by integrating the equation of motion of the system. This latter cannot be integrated with an analytical method owing to the dependence of the engine torque by the angular velocity of the engine. Therefore, it is required a numerical method, such as Runge-Kutta Method 4th order.

4.5.2 Simulation Results

In order to conclude the longitudinal behaviour investigation, the numerical application about the previous sections, will be shown. In order to simulate the dynamic behaviour of the real vehicle, it was decided to use, like the test vehicle, Renault Mégane Coupé 16V 150 hp. This test-vehicle will be the same used for the validation of the complete model, explained in the 6th chapter; see Figure 4.26. In Appendix A are shown all the parameters used for the simulations.

Figure 4.26: Test Vehicle, Renault Mégane Coupé 16V 150 HP.

Simulation results are shown in Figures 4.27 to 4.32. During the initial vehicle manoeuvre, it is considered the former with a first gear in. It is assumed the gear change between n_{max}=5000 rpm and n_{min}=2000 rpm values. The gear change is also assumed with a simplified manoeuvre, without locked and unblocked clutch, but only considering the instantaneous ratios of transmission.

The Figures 4.27, 4.28 and 4.29 show the vehicle acceleration, velocity and displacement evolutions during six seconds simulated, respectively. One should note that the maximum acceleration touched is almost equal to 5 m/s^2 later than 2 s. Also, the velocity reached after the simulation time was about 23 m/s, equal to 82 km/h. A good result was obtained for according the displacement of the vehicle too an equal to 80 m later than 6s. Instead, the Figure 4.30 indicates the normal and tangential forces acting at front and rear tyres.

As it is possible to note, in corresponding to the maximum acceleration, with the full opening throttle, the tangential rear force assumes its maximum value, equal to 3300 N. At the same time, the normal load at the rear wheel reached is equal to 3200 N. So, in this way the rear wheels found themselves in a critical condition, defined in the chapter2.

In fact, Figure 4.30 (plot-bar) shows the correspondent value assumed by the traction parameter and the traction limit, equal to 1.08 for dry road. Finally, in the Figure 4.30 and 4.32 it is possible to note how the value assumed by the aerodynamic torque, applied at known distance from the centre of gravity, is smaller than the rolling one.

Obviously, being the velocity of the vehicle small during the first 5 seconds of the simulation, the aerodynamic torque is small because it is a function proportional to the square velocity.

The opposite case happens after this time and the aerodynamic torque, such as the aerodynamic power, is bigger than the rolling ones. As well, it is interesting to note the engine power released that, during the change gear is decreasing and immediately after it is increasing to tend to the constant steady-state value.

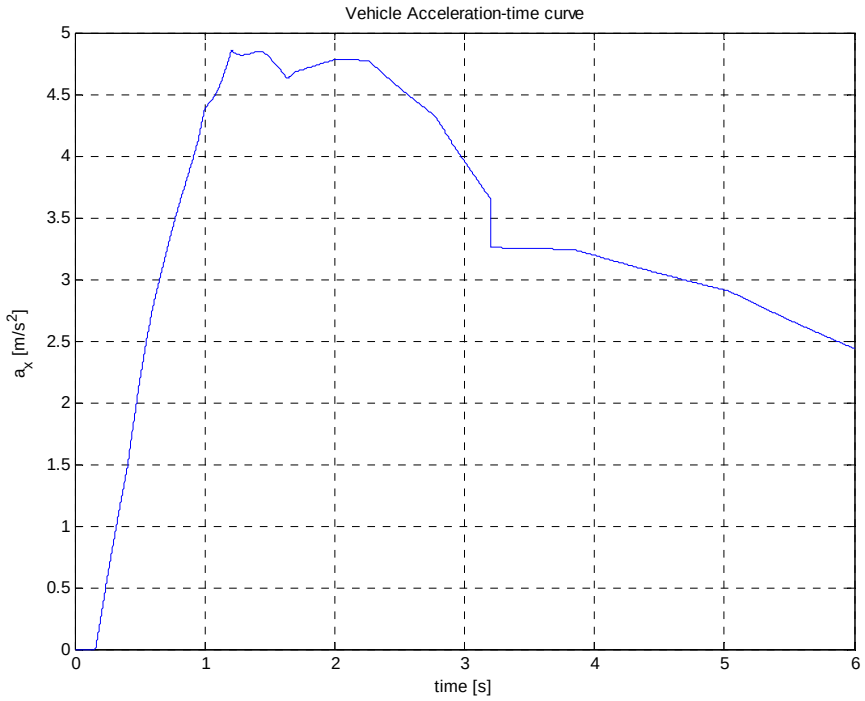

Figure 4.27: Acceleration-time curve.

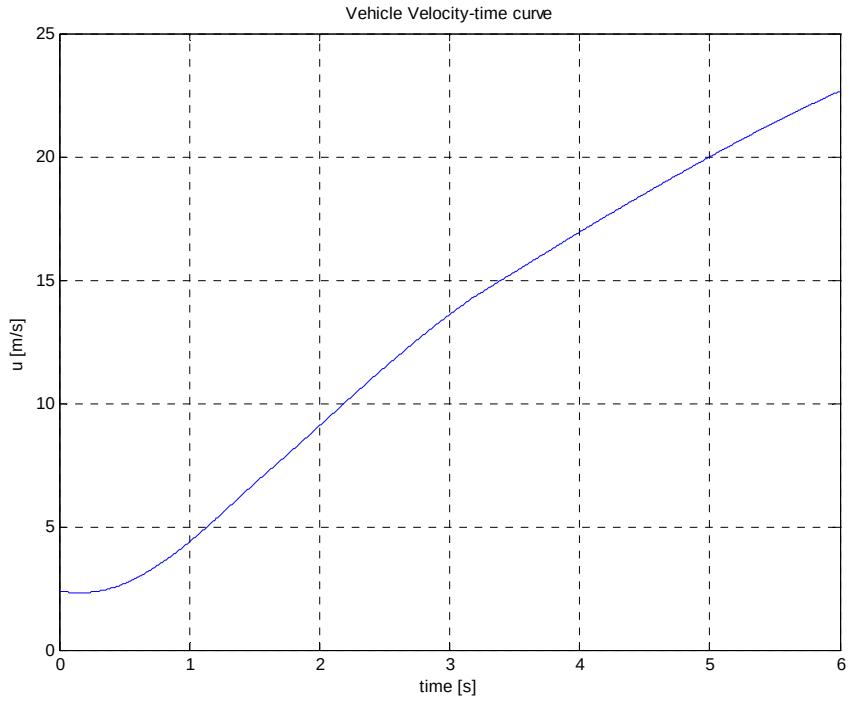

Figure 4.28: Velocity-time curve.

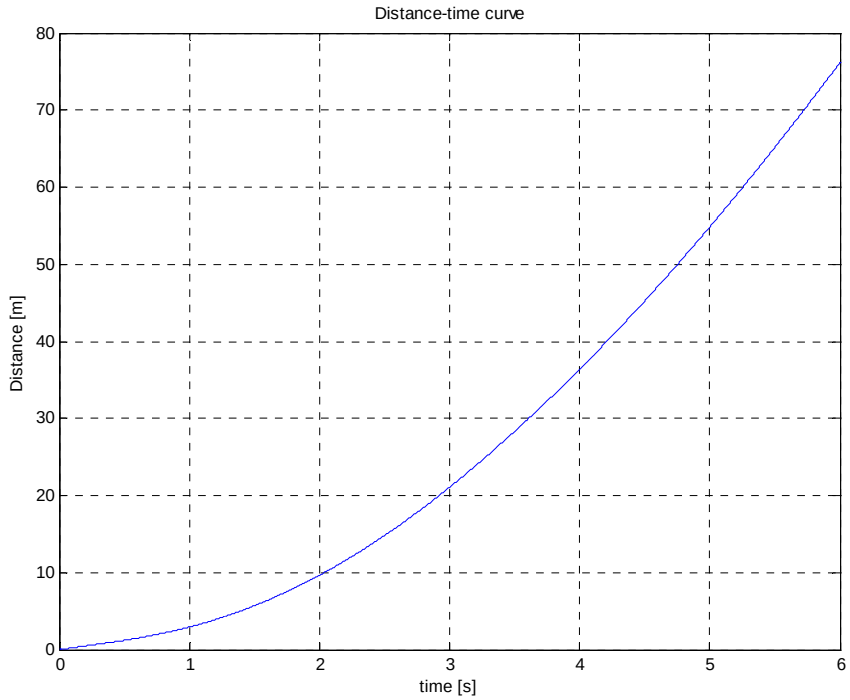

Figure 4.29: Displacement-time curve.

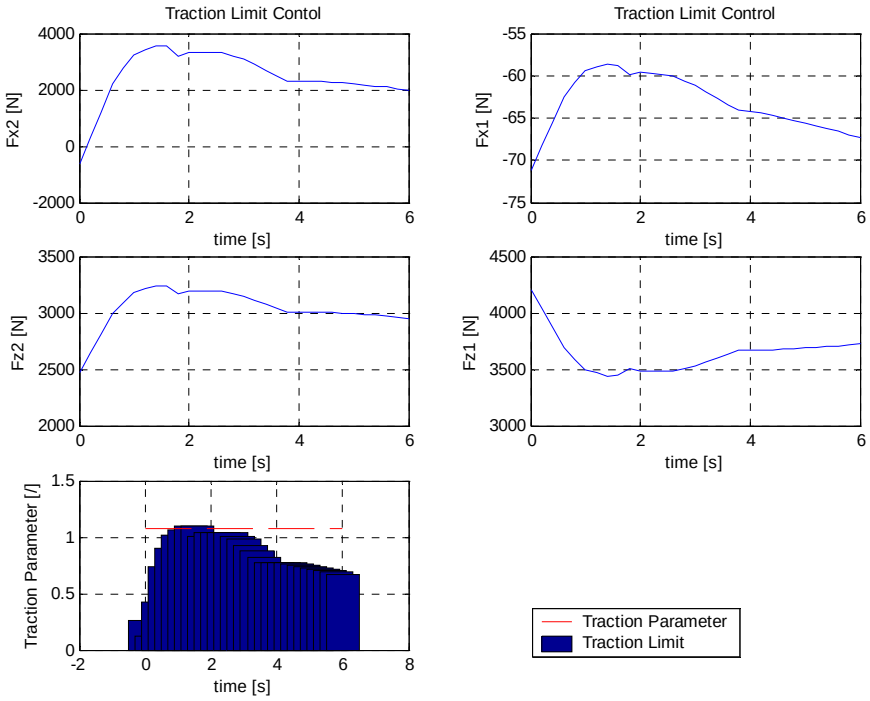

Figure 4.30: Traction Control curve.

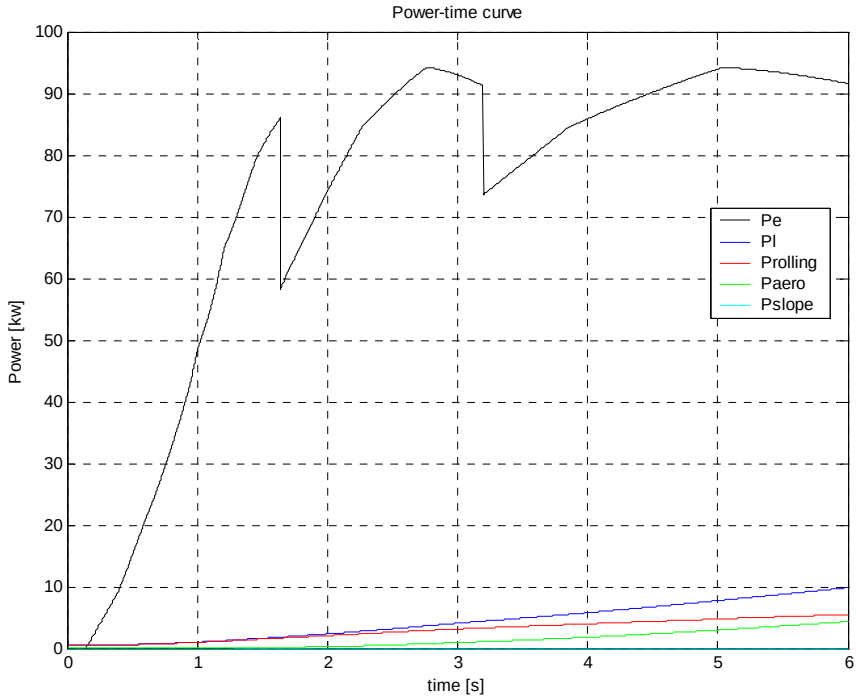

Figure 4.31: Power-time curve.

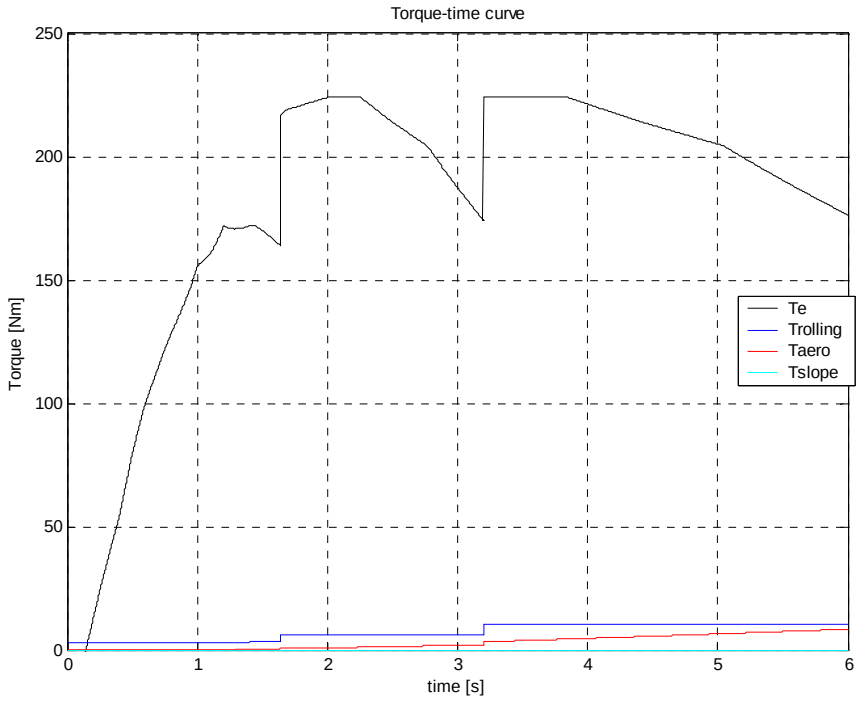

Figure 4.32: Torque-time curve.

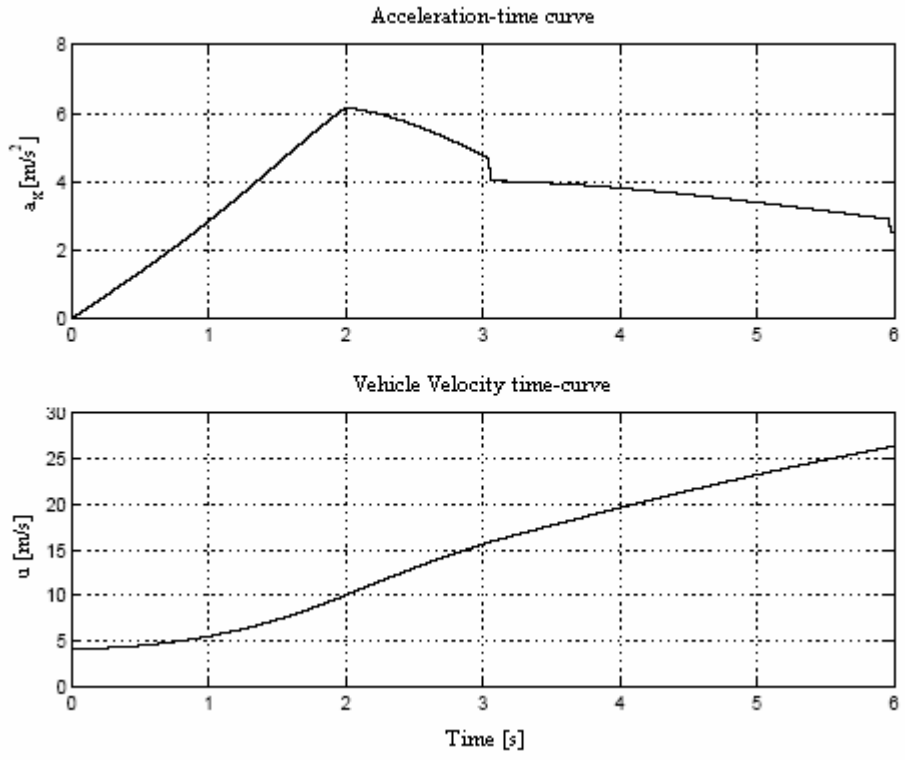

Figure 4.33: Reference Acceleration and Velocity of the Vehicle [25]

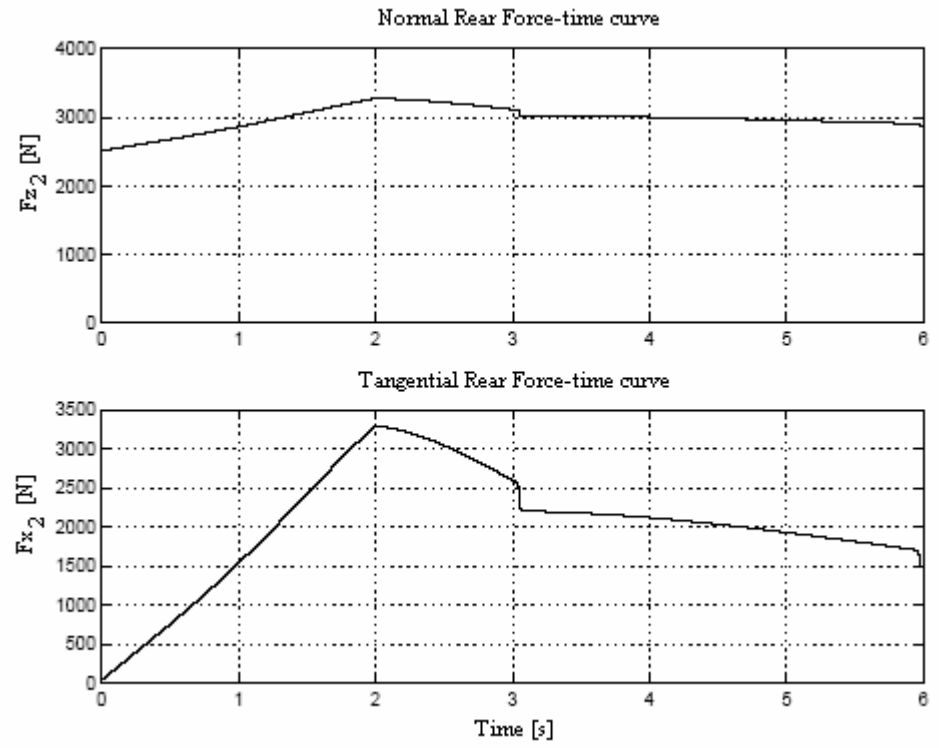

Figure 4.34: Reference Normal and Tangential Forces at Rear Tyre [25]

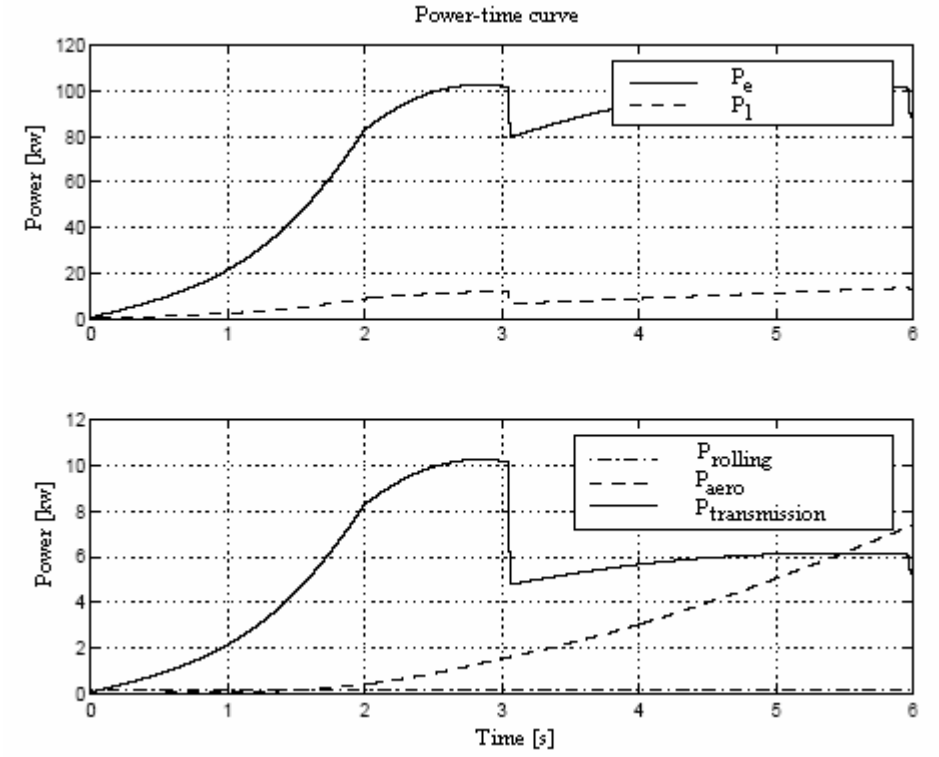

Figure 4.35: Reference Powers Transferred [25]

Chapter 5

5 Lateral Dynamics Model

There are numerous degrees of freedoms associated with vehicle dynamics. Obviously, the choice about how many variables to consider depends on aim study that it will make about. According to a brief research study of typical vehicle models, a linear two-degree-of-freedom (2D.O.F.s), a linear four-degree of freedom vehicle model (4D.O.F.s), and a non-linear four-degree-of-freedom (4D.O.F.s) will be used in this research in order to explain the principal characteristics about the transversal behaviour of the vehicle [20].

5.1 Working Hypotheses

To achieve an easy vehicle model but able to describe a lot of dynamics characteristics it is very interesting to fix all the working hypotheses which are the grounds of a good research.

The formulation of the following model takes into account these assumptions:

- the vehicle is a **rigid body**;
- the vehicle is moving on a **level road**, comparable as a geometrical plane;
- without **suspension system;**
- the longitudinal velocity is **steady-time**, only for this model;
- the trajectories have a **large radius of curvature**, without influences of the pitch and roll motion so that the variations of the camber angle can be neglected;

- the **steering angle is small**, in agreement with the previous hypothesis;
- the vehicle has a **rigid steering system**, so that the swerving wheels (*wheel angle*) is coupled directly by the steering angle;
- the weight of the wheels does not have an influence regarding the weight of the vehicle, so the position of the **centre of gravity does not change**;

The total effect of these considerations leads to construct a tow degree of freedom model (longitudinal motion constant), that is moving in plane motion.

5.2 Theoretical Model

According to foregoing statements, we can proceed to formulate the mathematical model. Consider the rigid body having mass *m* and centre of gravity *G*, as shown in Figure 5.1. Even though the vehicle is equipped by tow wheels steering, but their mass is supposed negligible.

As usual, it is fixed a coordinate system (*x, y, z; G)* behind the vehicle, so called *Body Axis*, with the origin situated in the centre of gravity and versors ***(i, j, k)***. As shown in Figure 5.1, *x*-axis is defined parallel to road and forward direct, *z*-axis is orthogonal to the road and *y*-axis is perpendicular to ones and left direct.

Generally, this coordinate system does not coincide with the inertia central coordinate.

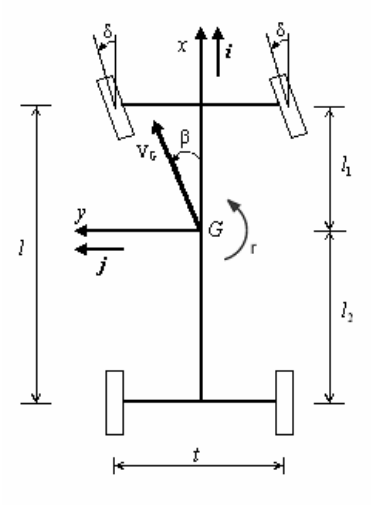

Figure 5.1: Vehicle Model.

However, for the longitudinal symmetry of vehicle in agreement with middle plane of symmetry, lying on *x* and *z* axis, the *y*-axis is a central inertia axis. In this way, the terms J_{xy} and J_{yz} are null but not the J_{zx} (for vehicle with order equal to ±200 *kg m^2*).
In any case, the terms J_x, J_y and J_z are always not null. As previously mentioned, the vehicle is a mechanical system, which is moving in "*Plane Motion*". It is defined with $\boldsymbol{\Omega}=r\,\boldsymbol{k}$ the yaw velocity (or *yawing rate* or *velocità di imbardata*), with $\boldsymbol{k}$ versor to the road and high direct. In according to fixed axis, for the "*Right Hand Low*" the yaw velocity is positive if it is anticlockwise. It is also defined with $\boldsymbol{V_G}$ the absolute centre of gravity speed. The geometrical position of the centre of gravity is supposed and so fixed through the lengths l_1 and l_2, called *semi step*. With $l = l_1 + l_2$ and *t* are called the *wheelbase* (or *passo*) and *track* (or *carreggiata*) of vehicle (always measured from the centre of the wheels) respectively. Simply, the front and rear track have the same length.
The "*kinematics steering"*(or *sterzatura cinematica*), defined how the steering with *slip angles* (or *drift angle* or *angolo di deriva*) null, is shown in Figure 5.2.
Note that the steering angle of internal wheel δ_i is bigger than the external one, δ_e. This observation leads to the sequent kinematical relation:

$$\frac{t}{l}=\frac{1}{\tan(\delta_e)}-\frac{1}{\tan(\delta_i)} \qquad \textbf{(5.1)}$$

and so, we have:

$$\delta_e=\delta_i-\frac{t}{l}\delta_i^2+O(\delta_i^3) \qquad \textbf{(5.2)}$$

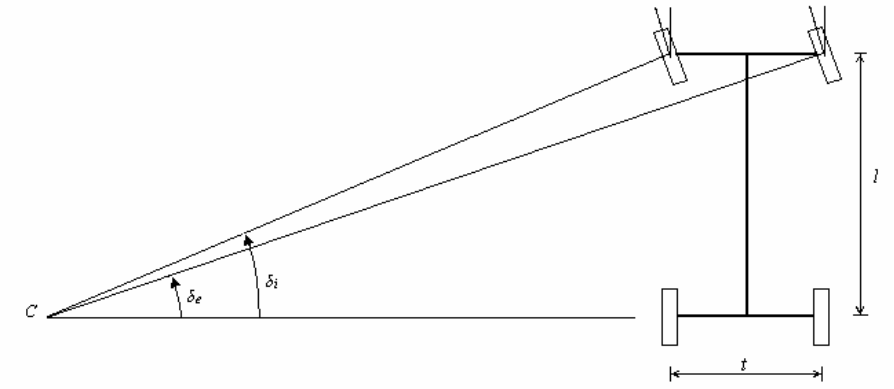

Figure 5.2: Kinematics Steering (slip angle null)

Therefore, in according to small steering angle, we have $\delta_l \sim \delta_e = \delta$, as shown in Figure 5.1. According to foregoing statements, we can proceed to formulate the mathematical model by three groups of equations:

- equations of congruence
- equations of equilibrium
- constitutive equations.

5.2.1 Equations of Congruence

As known, the side angle α individualizes the direction of the vector velocity of centre wheel as regards to the symmetric longitudinal plane of the same centre. This angle is assumed positive when clockwise. Since the vehicle is supposed rigid, the velocity of the centre of gravity $\boldsymbol{V_G}$ and the yaw velocity univocity characterize the slip angles α_{ij} of the four wheels (with $i=1,2$ and $j=1,2$).

Suitably, as represented in Figure 5.3, we express the absolute velocity $\boldsymbol{V_G}$ of the centre of gravity considering a coordinate system (*x, y, z; G)* behind the vehicle. Defined the versors ***i, j*** and ***k*** the vector velocity is described as:

$$V_G = u\mathrm{i} + v\mathrm{j} \qquad \textbf{(5.3)}$$

The longitudinal component of the vector velocity *u* is called "*feed velocity*" (or *velocità di avanzamento*) whereas the lateral component v is called "*lateral velocity*" (or *velocità laterale*). Since the centre of gravity does not move in regard to the coordinate system, before defined, the Equation 5.3 describes only the velocity components in two directions.

Mathematically, it is translated into the following equation:

$$\beta = \arctan\left(\frac{v}{u}\right) \qquad \textbf{(5.4)}$$

where *u* and *v* represent the longitudinal and lateral velocity, respectively.

It is defined, "*Sideslip angle*" β (or *vehicle attitude* or *body slip angle* or *angolo di assetto*) the angle between the longitudinal axis of vehicle and the direction of absolute velocity (in the centre of gravity).

5.2.1.1 Front and Rear Tyre Slip Angle Derivation

If we consider the absolute velocities of the centres wheel we can link the slip angle α_{ij} with the yaw velocity r and the translational components of velocity u and v.

As possible to note in Figure 5.4, 5.5, 5.6 and 5.7, the centres wheel have components of velocity in longitudinal and lateral directions.

From the lateral point of view the front centres wheel have a velocity equal to $v+r\ l_1$ and the rear ones equal to $v-r\ l_2$.

Instead in longitudinal direction the wheels on the left side (as regards to x-axis) have a velocity equal to $u-r(t/2)$ and these in right side a velocity equal to $u+r(t/2)$.

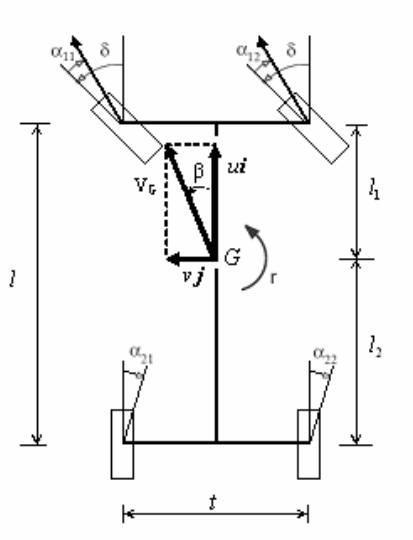

Figure 5.3: Definition of kinematics Quantities of the Vehicle

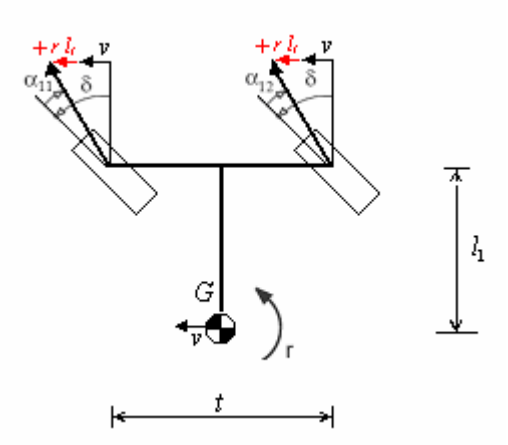

Figure 5.4: Lateral Components of Velocity at Front Tyres.

The slip angles are function of two basic motion variables, v (or β) and r. The relationships are developed below:

$$\begin{aligned}
\tan(\delta-\alpha_{11}) &= \frac{v+rl_1}{u-r(t/2)} \\
\tan(\delta-\alpha_{12}) &= \frac{v+rl_1}{u+r(t/2)} \\
\tan(\delta-\alpha_{21}) &= \frac{v-rl_2}{u-r(t/2)} \\
\tan(\delta-\alpha_{22}) &= \frac{v-rl_2}{u+r(t/2)}
\end{aligned} \qquad \textbf{(5.5)}$$

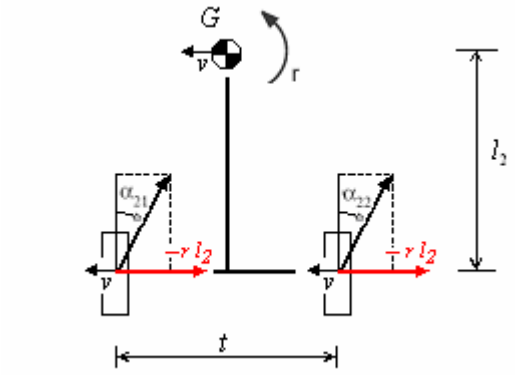

Figure 5.5: Lateral Components of Velocity at Rear Tyres

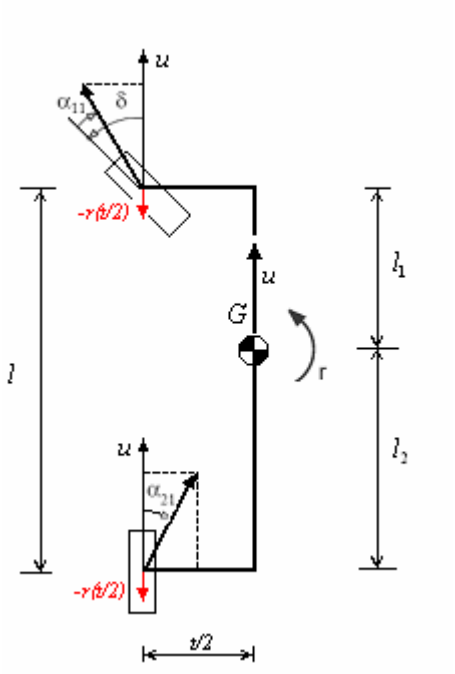

Figure 5.6: Longitudinal Components of Velocity at Left Tyres.

During normal conditions we can write:

$$u = |r|\frac{t}{2} \tag{5.6}$$

that means the wheels splined on the same axis have the same slip angles. For this reason, it is possible to denote with α_f the slip angle for either front wheels and with α_r the slip angle for the rear wheels.

According to this common hypothesis, the previous relationships become:

$$\begin{aligned} \tan\left(\delta - \alpha_f\right) &= \frac{v + rl_1}{u - r\left(t/2\right)} \\ \tan\left(-\alpha_r\right) &= \frac{v - rl_2}{u} \end{aligned} \tag{5.7}$$

Actually, during normal conditions the external slip angle as regards to the curve is slightly smaller than the internal one. This is only as geometrical consideration due by kinematics performance.

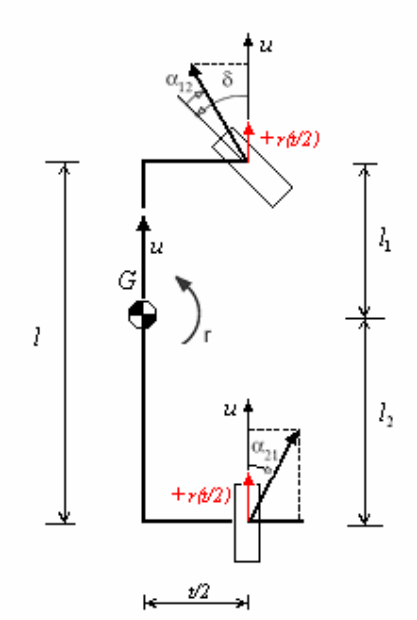

Figure 5.7: Longitudinal Components of Velocity at Right Tyres

As shown in the latterly figures, the position of the centre of rotation defines univocity all the slip angles.

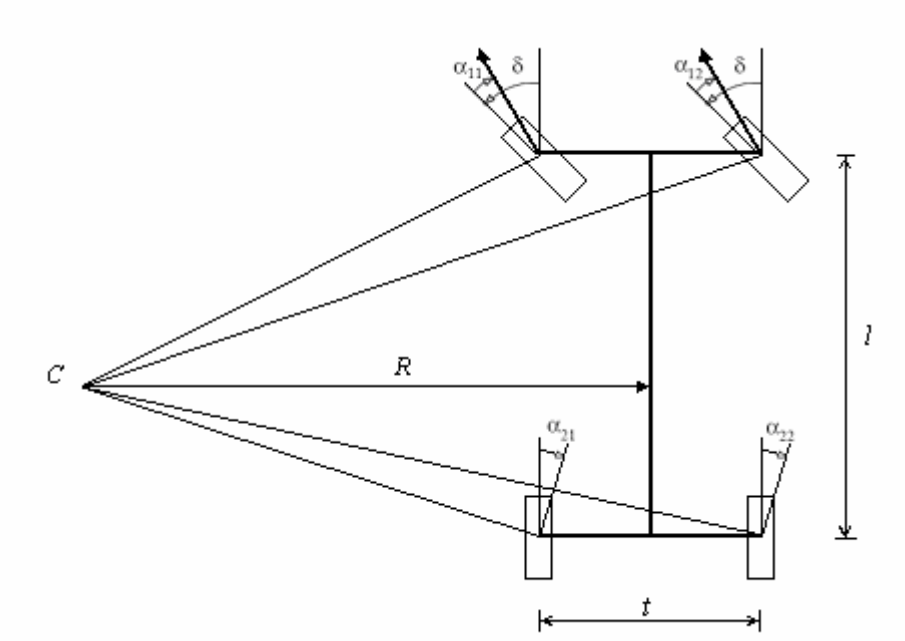

Figure 5.8: Relation between Slip Angles and Centre of Rotation Position

To simplify it, we can consider that the longitudinal velocity is always bigger than the lateral one and the other velocity caused by the yawing rate. Mathematically, we have:

$$u = |v + rl_1| \qquad u = |v - rl_2| \tag{5.8}$$

and so, we can approximately change the arc with its tangent (tangent with its argument):

$$\delta - \alpha_f = \frac{v + rl_1}{u} \qquad -\alpha_r = \frac{v - rl_2}{u} \tag{5.9}$$

Finally, we have the "*Linear Congruence Equations*":

$$\alpha_f = \delta - \frac{v + rl_1}{u} \qquad \alpha_r = -\frac{v - rl_2}{u} \tag{5.10}$$

where:

δ: steering angle;

l_1: centre of gravity location from vehicle front axle;

l_2: centre of gravity location from vehicle rear axle;

r: yaw velocity of vehicle;

v: lateral velocity of vehicle;

u: longitudinal velocity of vehicle.

5.2.1.2 Trajectory of the Vehicle

In order to investigate about the instantaneous position of the vehicle, the Figure 5.6 illustrates the vehicle motion as regards the fixed reference axis *(x_0, y_0, z_0; O_0)*, united with the road, namely "*ground axis*", as described in Chapter 3.

The rotational angle of the vehicle ψ at a generic instant of time $t=t'$ is available through the yaw rate integration, supposed now known.

$$\psi(t') - \psi(t) = \int_0^{t'} r(t)\, dt \qquad \textbf{(5.11)}$$

This particular angle is called "*yaw angle*", and it is able to show at any moment the angular position of the vehicle.

So, it also possible to know the coordinates of the centre of gravity of the vehicle, as regards to the same reference system. In fact, through the equation (5.11) we have absolute coordinates of the centre of the gravity, ${x_0}^G$ and ${y_0}^G$ during each instant $t=t'$

$$\begin{aligned} X_G &= {x_0}^G(t') - {x_0}^G(t) = \int_0^{t'} \dot{x}_0(t)\, dt = \int_0^{t'} \left[u(t)\cos\psi(t) - v(t)\sin\psi(t)\right] dt \\ Y_G &= {y_0}^G(t') - {y_0}^G(t) = \int_0^{t'} \dot{y}_0(t)\, dt = \int_0^{t'} \left[u(t)\sin\psi(t) + v(t)\cos\psi(t)\right] dt \end{aligned} \qquad \textbf{(5.12)}$$

Therefore, the position of the vehicle $Y_G=Y_G(X_G)$ will be obtained, being known the yaw rate as function of the time and the longitudinal and lateral velocity. It means that the equation of motion of the system should have to be written, and integrated successively.

5.2.2 Equations of Equilibrium

Substantially the equation of equilibrium can be written only after the computation of acceleration and the estimation of the forces and moments applied to the vehicle.

5.2.2.1 Valuation of the Accelerations

The expression of the acceleration of the centre of gravity, $\boldsymbol{a_G}$, can be immediately obtained deriving the velocity of the same point, $\boldsymbol{V_G}$, as function of the time t ; Equation 5.3.

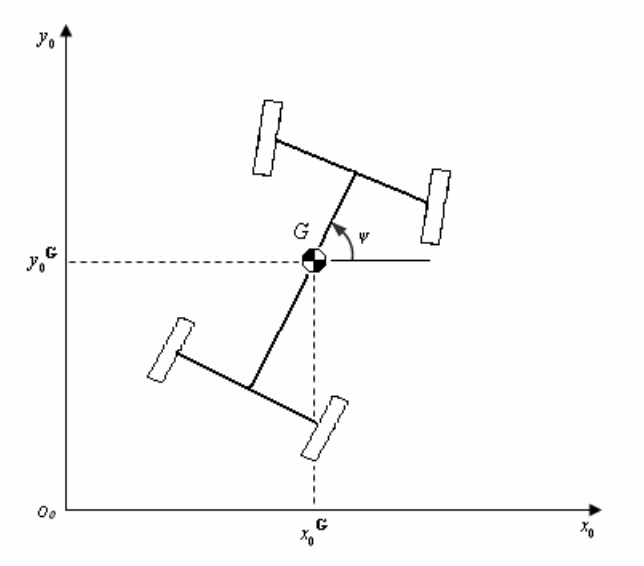

Figure 5.9: Trajectory of the Vehicle as regards to a Reference Coordinate System.

Obviously we must have into account that the versors i and j are changing direction while the vehicle is moving through particular relations[13]:

$$\begin{aligned} \mathrm{a_G} = \frac{d\mathrm{V_G}}{dt} &= \dot{u}\mathrm{i}+ur\mathrm{j}+\dot{v}\mathrm{j}-vr\mathrm{i} \\ &= \left(\dot{u}-vr\right)\mathrm{i}+\left(\dot{v}+ur\right)\mathrm{j} \\ &= a_x\mathrm{i}+a_y\mathrm{j} \end{aligned} \qquad \textbf{(5.13)}$$

Therefore, the acceleration of the centre of gravity has been broken up decomposed into longitudinal and lateral directions:

$$a_x = \dot{u}-vr \qquad \textbf{(5.14)}$$

and

$$a_y = \dot{v}+ur \qquad \textbf{(5.15)}$$

13 The versors are a function of the time and so the derivate are developed: $\frac{d\mathrm{i}}{dt} = r\mathrm{j}$ and $\frac{d\mathrm{j}}{dt} = -r\mathrm{i}$.

5.2.2.2 Forces and Moments

As known on a vehicle there are three kind of acting forces:

- force of gravity supposed acting in the centre of gravity;
- force of contact tyre-ground at four wheels;
- force of aerodynamics field due air resistent.

The external forces acting on the vehicle as a rigid body originate, at any moment, a resultant force acting in a variable direction. In according to our fixed coordinate system (*x, y, z; G)*, it is defined with (*X, Y, Z)*, the components of the resultant force totally acting on the vehicle and with (*L, M, N)*, its components of moments.

It is possible to write the equations of equilibrium, "*Newton's Laws*" about the rigid body which is moving in plane motion, having mass *m* and moment of inertia *J*, in *Z*-axis direction.

Synthetically, the equations are developed into the following relations:

$$\begin{aligned} ma_x &= X \\ ma_y &= Y \\ J\dot{r} &= Z \end{aligned} \qquad \textbf{(5.16)}$$

where *X*, *Y* and *Z* are the sum of longitudinal, transversal and rotational forces respectively.

The most important forces acting on the vehicle are the traction forces tyre-ground, shown in Figure 5.6. Strictly speaking, there are the aerodynamics resistent which is proportional to the square velocity and the lateral force (for example exercised as impulse by the wind).

In according to the conventions about the tyres, it is indicated with F_{xij} and F_{yij} the longitudinal and lateral components of traction forces[14] into point of contact tyre-ground. Formally, in these forces F_{xij} and F_{yij} the traction and rolling forces are included too.

14 The longitudinal and lateral forces F_{xij} and F_{yij} are denoted through the pedics *i* and *j* where the first describes the longitudinal or lateral direction and the second left or right wheels.

According to the working hypothesis about the steer angle, and particularly, for steer angle in order to 15 degrees, we can linearize the equilibrium relationships. With reference to Figure 5.10 the equilibrium equations are below shown:

$$\begin{aligned} m(\dot{u}-vr) &= (F_{x11}+F_{x12})-(F_{y11}+F_{y12})\delta+(F_{x21}+F_{x22})-F_{xaero} \\ m(\dot{v}+ur) &= (F_{x11}+F_{x12})\delta+(F_{y11}+F_{y12})+(F_{y21}+F_{y22}) \\ J\dot{r} &= \left[(F_{x11}+F_{x12})\delta+(F_{y11}+F_{y12})\right]l_1-(F_{y21}+F_{y22})l_2+ \\ &\quad -\left[(F_{x11}-F_{x12})\delta+(F_{x21}-F_{x22})-(F_{y11}+F_{y12})\delta\right]\frac{t}{2} \end{aligned} \qquad \textbf{(5.17)}$$

where F_{xaero} is the aerodynamics force[15] applied by the air resistent:

$$F_{xa}=\frac{1}{2}\rho S C_x u^2 \qquad \textbf{(5.18)}$$

For the symmetry of the vehicle, it is suited to sum the contributions of the same axle to have a compact notation, as shown into following relations:

$$\begin{aligned} F_{x1} &= F_{x11}+F_{x12} \\ F_{x2} &= F_{x21}+F_{x22} \\ F_{y1} &= F_{y11}+F_{y12} \\ F_{y2} &= F_{y21}+F_{y22} \end{aligned} \qquad \textbf{(5.19)}$$

If it is taken into account that the traction torque is shared among two wheels at the same axle by an ordinary differential (not auto-locked) it has another reduction in the equations:

$$\begin{aligned} F_{x11} &= F_{x12} \\ F_{x21} &= F_{x22} \end{aligned} \qquad \textbf{(5.20)}$$

Even though there was a reduction into last equation of equilibrium there was always the term $(F_{y11}- F_{y12})\delta(t/2)$, but it is neglected for simplify.

15 The aerodynamic forces in lateral and vertical direction, F_{yaero} and M_{zaero} was neglected.

The interesting observation made about these relationships is that even if the wheels at the same axle work with the same slip angle, the lateral forces at the same axle do not have the same value. For this reason it is $F_{y11} \neq F_{y12}$.

$$\begin{aligned} m(\dot{u} - vr) &= F_{x1} - F_{y1}\delta + F_{x2} - F_{xa} \\ m(\dot{v} + ur) &= F_{x1}\delta + F_{y1} + F_{y2} \\ J\dot{r} &= \left[F_{x1}\delta + F_{y1}\right] l_1 - F_{y2} l_2 \end{aligned} \qquad \textbf{(5.21)}$$

which denotes the "*Equation of Equilibrium*".

5.2.3 Constitutive Equations

To complete the vehicle dynamics modelling, we have to define the tyre behaviour at each wheel. From a general point of view, the lateral forces F_{yij} are a function of slip angle α, camber angle γ, longitudinal force F_{xij} and load transfer F_{zij}. Taking into account only the functional variation about the slip angle, we will formulate the tyre model able to integrate the equation of motion.

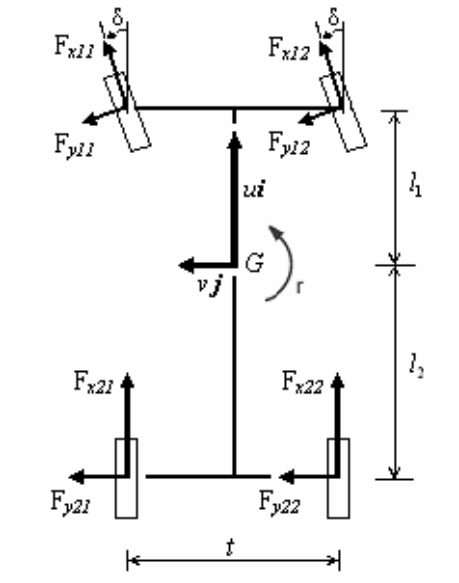

Figure 5.10: Forces Acting on the Vehicle

In the following section we again propose the linear tyre model. The most simplified tyre model is a linear function, representing between the lateral force (or *Cornering Force*) and the slip angle. This functional link is expressed into the following relation:

$$F_{y_{ij}} = C_{\alpha_{ij}} \alpha_{ij} \quad \textbf{(5.22)}$$

where, being $\alpha_{i1}=\alpha_{i2}$, we have:

$$F_{y_i} = C_{\alpha_i} \alpha_i \quad \textbf{(5.23)}$$

and C_i is the tyre cornering stiffness. The field working is characterized by small slip angle, which means the order of magnitude is equal to 15÷20 degrees on dry road.

5.3 Single-Track Model

The most simplified vehicle dynamic model is a two/four-degree-of-freedom bicycle model (or *single track model*), Figure 5.11, representing the lateral and yaw motions. The mean idea behind this model is that in first approximation to develop lateral theory it is not necessary or desirable to include the longitudinal direction, because we can consider it known. This model, which is easier to understand than the others, is often used in teaching purposes.

5.4 Two/Four-Degree-of-Freedom Vehicle Model Derivation

Capturing all the motions of a vehicle into analytical equations can be quite difficult. Although including more number of elements in the model may increase the model's accuracy, it substantially increases the computation time. This section describes the derivation of the two-degree-of-freedom bicycle model used in this study. It also includes the equations for the front and rear tyre slip angles.

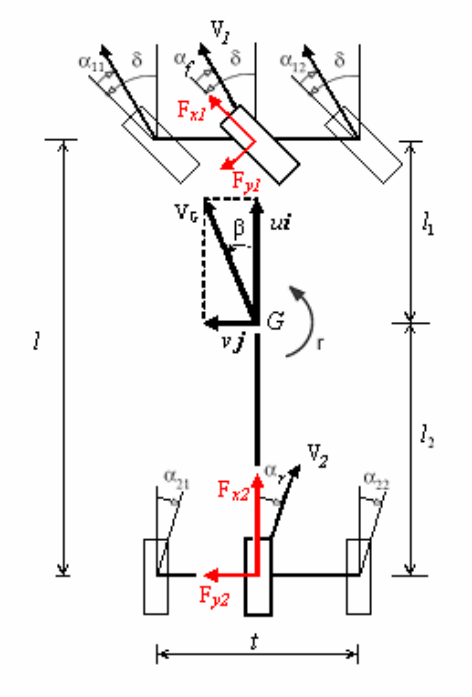

Figure 5.11: Reduction of Single Track Model.

5.5 Equations of Motion

Into the following section, the two degrees of freedom model considered for this study is shown. Referring to Figure 5.12, the lateral and yawing velocities of the vehicle with

respect to the fixed coordinate system, *XYZ* can be described as shown in Equation 5.17 by the "*equation of equilibrium*", below reported:

$$\begin{aligned} m(\dot{u} - vr) &= F_{x1} + F_{x2} - F_{y1}\delta - F_{xa} \\ m(\dot{v} + ur) &= F_{x1}\delta + F_{y1} + F_{y2} \\ J\dot{r} &= \left[F_{x1}\delta + F_{y1}\right] l_1 - F_{y2} l_2 \end{aligned} \qquad \textbf{(5.24)}$$

and (5.10), "*equations of congruence"*:

$$\begin{aligned}\alpha_f &= \delta - \frac{v + rl_1}{u} \\ \alpha_r &= -\frac{v - rl_2}{u}\end{aligned} \tag{5.25}$$

which includes the "*constitutive equations*", referring to the tyre model, described through one of these Equations 3.32, 3.34, and 3.43:

$$\begin{aligned}F_{y_i} &= C_{\alpha_i}\alpha_i \\ \frac{d}{u}\dot{F}_{yi} + F_{yi} &= C_{\alpha_i}\alpha_i = Y_p(\alpha) \\ \frac{d}{u}\dot{F}_{yi} + F_{yi} &= \mu F_z\left(1 - \exp\left(-\frac{C_\alpha \alpha}{\mu F_z}\right)\right)\end{aligned} \tag{5.26}$$

where the subscript is $i=f,r$.

5.5.1 Rear Traction Model (RWD)

Further simplification about these equilibrium equations can be shown if we consider the longitudinal velocity constant and the rear traction. In this case, the equations are uncoupled and the first equation is algebraic one.

However, the mathematical problem is uncoupled only when the steer and traction have been at different axis, but in this work it happens only in rear traction case. Also, the longitudinal front force, F_{xi}, which includes only the rolling and the slope resistent, could be neglected ($F_{x1}=0$).

To note that the longitudinal force, F_{x2}, does not appear into the equilibrium equations even if it is the traction force applied by the tyre during the vehicle motion.

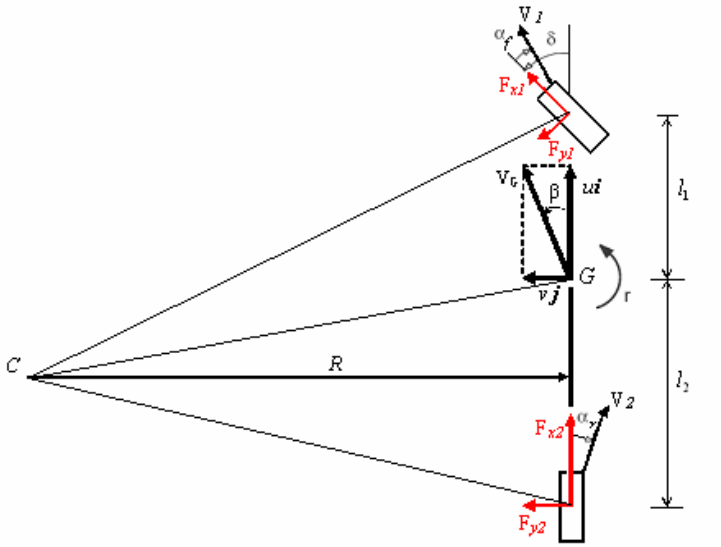

Figure 5.12: Single Track Model

5.5.1.1 Linear Tyre Model

Finally, the lateral dynamics system, 2 D.O.F. is described with only two differential equations into variables *v(t)* and *r(t)*.

$$\begin{aligned}\dot{v} &= -\left(\frac{C_{\alpha 1}+C_{\alpha 2}}{mu}\right)v-\left(\frac{C_{\alpha 1}l_1+C_{\alpha 2}l_2}{mu}+u\right)r+\frac{C_{\alpha 1}+F_{x1}}{m}\delta \\ \dot{r} &= -\left(\frac{C_{\alpha 1}l_1-C_{\alpha 2}l_2}{Ju}\right)v-\left(\frac{C_{\alpha 1}l_1^{\,2}+C_{\alpha 2}l_2^{\,2}}{Ju}\right)r+\frac{C_{\alpha 1}+F_{x1}}{J}l_1\delta\end{aligned} \qquad \textbf{(5.27)}$$

These differential relations can be solved into analytical form too. During the following paragraph we will show this kind of solution in comparison with the numerical form, obtained by Matlab/Simulink software. Simply, the influence on the longitudinal force F_{xi} can be neglected into the lateral problem, so the final equation of motion in rear traction is:

$$\begin{aligned}\dot{v} &= -\left(\frac{C_{\alpha 1}+C_{\alpha 2}}{mu}\right)v-\left(\frac{C_{\alpha 1}l_1+C_{\alpha 2}l_2}{mu}+u\right)r+\frac{C_{\alpha 1}}{m}\delta \\ \dot{r} &= -\left(\frac{C_{\alpha 1}l_1-C_{\alpha 2}l_2}{Ju}\right)v-\left(\frac{C_{\alpha 1}l_1^{\,2}+C_{\alpha 2}l_2^{\,2}}{Ju}\right)r+\frac{C_{\alpha 1}}{J}l_1\delta\end{aligned} \qquad \textbf{(5.28)}$$

5.5.1.1.1 Analytical Solution with Linear Tyre Model

To research the analytical solution, we had better have the state space representation of the dynamic equations in (5.28) which is,

$$\underline{\dot{w}}=\underline{\underline{A}}\,\underline{w}+\underline{b} \qquad \textbf{(5.29)}$$

where, $\underline{w}(t)=(v(t),r(t))$ is the state variables vector and the known term is given by $\underline{b}(t)=(C_{\alpha 1}/m,\ C_{\alpha 1}l_1/J)\delta(t)$ and the matrix $\underline{\underline{A}}$ is:

$$\underline{\underline{A}}=\begin{bmatrix} \dfrac{C_{\alpha 1}+C_{\alpha 2}}{mu} & \dfrac{C_{\alpha 1}l_1+C_{\alpha 2}l_2}{mu}+u \\ \dfrac{C_{\alpha 1}l_1-C_{\alpha 2}l_2}{Ju} & \dfrac{C_{\alpha 1}l_1^{\,2}+C_{\alpha 2}l_2^{\,2}}{Ju} \end{bmatrix} \qquad \textbf{(5.30)}$$

One must note that the matrix $\underline{\underline{A}}$ is a function of longitudinal velocity but not a steer angle. The opposite case is vector $\underline{b}$, which is a function of steering angle but not of a longitudinal velocity.

The general solution of the equations of motion is a sum of a solution of associate homogeneous problem and the solution of particular problem:

$$\underline{w}(t)=\underline{w}_h(t)+\underline{w}_p(t) \qquad \textbf{(5.31)}$$

As known, the homogenous solution represents the transient history of the system, instead the particular one the steady-state condition. Because the matrix $\underline{\underline{A}}$ is not a function of steer angle we can calculate the homogenous solution without fixed test of simulation. In fact the first solution does not depend by the test simulation but the second one can be valuated fixing the test of vehicle (for example "*Steering Pad*" and "*Lateral Impulse*").

The homogenous solution can be investigated imposing the known term vector as zero, below shown:

$$\dot{\underline{w}}_h = \underline{\underline{A}}\,\underline{w}_h \qquad \textbf{(5.32)}$$

As known, the solution of differential equation of the first order is hypothesized as an exponential form:

$$\underline{w}_h(t) = \left(v_h(t), r_h(t)\right) = \underline{x}\exp(\lambda t) \qquad \textbf{(5.33)}$$

end so, calculating its derivate:

$$\dot{\underline{w}}_h(t) = \lambda \underline{x}\exp(\lambda t) \qquad \textbf{(5.34)}$$

Replacing and simplifying the exponential operator, we immediately have the eigenvalues and eigenvectors problem.
The eigenvalues are obtained from the characteristic equation:

$$\det\left(\underline{\underline{A}} - \lambda \underline{\underline{I}}\right) = 0 \qquad \textbf{(5.35)}$$

in this case the matrix $\underline{\underline{A}}$ has size 2×2 so we have:

$$\lambda^2 - tr\left(\underline{\underline{A}}\right)\lambda + \det\left(\underline{\underline{A}}\right) = 0 \qquad \textbf{(5.36)}$$

resolving the eigenvalues are:

$$\lambda_{1,2} = \frac{tr\left(\underline{\underline{A}}\right) \pm \sqrt{tr\left(\underline{\underline{A}}\right)^2 - 4\det\left(\underline{\underline{A}}\right)}}{2} \qquad \textbf{(5.37)}$$

If the determinant of the matrix is negative, that is:

$$\mathrm{tr}\left(\underline{\underline{A}}\right)^2 < 4\det(\underline{\underline{A}}) \qquad \textbf{(5.38)}$$

the eigenvalues are complex and conjugate.

In this case, developing both terms:

$$\mathrm{tr}\left(\underline{\underline{A}}\right) = -\frac{1}{u}\left[\frac{C_{\alpha 1}+C_{\alpha 2}}{m}+\frac{C_{\alpha 1}l_1^{\,2}+C_{\alpha 2}l_2^{\,2}}{J}\right] < 0 \qquad \textbf{(5.39)}$$

and

$$\det\left(\underline{\underline{A}}\right) = \frac{1}{u^2 mJ}\left[C_{\alpha 1}C_{\alpha 2}\left(l_1+l_2\right)^2 - mu^2\left(C_{\alpha 1}l_1 - C_{\alpha 2}l_2\right)\right] \qquad \textbf{(5.40)}$$

These two quantities are very important concerning the eigenvalues:

$$\begin{aligned} tr\left(\underline{\underline{A}}\right) &= \lambda_1+\lambda_2 \\ \det\left(\underline{\underline{A}}\right) &= \lambda_1\lambda_2 \end{aligned} \qquad \textbf{(5.41)}$$

Obtained from the characteristic equation:

$$\left(\lambda-\lambda_1\right)\left(\lambda-\lambda_2\right) = 0 \qquad \textbf{(5.42)}$$

Once known the eigenvalues, the eigenvectors are known too, through:

$$\left(\underline{\underline{A}}-\lambda_i\underline{\underline{I}}\right)\underline{x}_i = \underline{0} \qquad \textbf{(5.43)}$$

where *i=1,2*.

The particular solution of the dynamics system can be obtained fixing the test of vehicle.

Assuming a "*Steering pad*" test (or "*prova di colpo di sterzo*"), [30, 31, 32, 33, 34, 35, 36], the particular solution is calculated from the system of equations:

$$-\underline{\underline{A}}\underline{w}_p = \underline{b} \qquad \textbf{(5.44)}$$

and so:

$$v_p = \frac{\left(C_{\alpha 2} l_2 I - m l_1 u^2\right) C_{\alpha 1} u}{m J u^2 \det\left(\underline{\underline{A}}\right)} \delta = \frac{\left(C_{\alpha 2} l_2 I - m l_1 u^2\right) C_{\alpha 1} u}{C_{\alpha 1} C_{\alpha 2} l^2 - m u^2 \left(C_{\alpha 1} l_1 - C_{\alpha 2} l_2\right)} \delta$$
$$r_p = \frac{C_{\alpha 1} C_{\alpha 2} l u}{m J u^2 \det\left(\underline{\underline{A}}\right)} \delta = \frac{C_{\alpha 1} C_{\alpha 2} l u}{C_{\alpha 1} C_{\alpha 2} l^2 - m u^2 \left(C_{\alpha 1} l_1 - C_{\alpha 2} l_2\right)} \delta \quad \textbf{(5.45)}$$

Once known v_p and r_p, lateral velocity and yaw rate in steady-state condition, it is possible to calculate the "*bend radius*", defined through the following relationship:

$$R_p = \frac{u}{r_p} = \frac{1}{\delta}\left[l - \left(\frac{C_{\alpha 1} l_1 - C_{\alpha 2} l_2}{C_{\alpha 1} C_{\alpha 2}} \right) \frac{m_v u^2}{l} \right] \quad \textbf{(5.46)}$$

where the value of r_p was substituted. Using the definition of the slip angle at front and rear wheels we have:

$$\alpha_{1p} = \delta - \frac{v_p + r_p l_1}{u}$$
$$\alpha_{1p} = -\frac{v_p - r_p l_2}{u} \quad \textbf{(5.47)}$$

and, immediately, the value of a characteristic velocity[16] u_t, which is illustrated for completeness:

$$u_t = \sqrt{\frac{\left[J\left(C_{\alpha 1} + C_{\alpha 2}\right) + m_v J\left(C_{\alpha 1} l_1^2 - C_{\alpha 2} l_2^2\right) \right]^2 - 4 m_v J C_{\alpha 1} C_{\alpha 2} \left(l_1 + l_2\right)^2}{4 m_v^2 J \left(C_{\alpha 1} l_1 - C_{\alpha 2} l_2\right)}} \quad \textbf{(5.48)}$$

Once known these variables, eigenvalues and eigenvectors are known and the solution, consequently. In Appendix C, the Matlab m-file is illustrated.

5.5.1.1.2 Comparison between Analytical and Numerical Solution

In the following section the results concerning the analytical and numerical solution are presented. The Runge-Kutta numerical method was used for the integration, with an

16 This velocity is defined as a particular velocity which defines a limited for the eigenvalue, changing from real and negative values to complex and conjugate.

integration step of 0.02 s and a simulation time of 1 s. Same set-up characteristics were chosen for the other simulations, such as linear and non-linear model for the FWD models. Step must be small enough, particularly, for the non-linear models.

In table 2 the principal symbols used in the equation of motion notation are illustrated.

A steering pad test was performed with a steering angle of 40 deg, as illustrated in Figure 5.13; it means that the value assumed by the steering wheel angle[17] was equal to 2 deg(about 0.035 rad).

Term	**Symbol**	**Units**	**Sign**
CG location	l1,l2	m	always +
Wheelbase	l	m	always +
Weight of vehicle	W	N	always +
Gravitational acceleration	G	m/s2	always +
Mass of vehicle (W/g)	mv	Kg	always +
Yawing moment of inertia	Iz	Kg m2	always +
Lateral force	Fy	N	+ to right
Longitudinal force	Fx	N	+ for backward
Lateral acceleration	ay	m/s2	+ for forward
Lateral coefficient (ay/g)	Ay	/	+ for forward
Vehicle absolute velocity	V	m/s	+ for forward
Yawing velocity	r	rad/s	+ for anticlockwise
Lateral velocity	v	m/s	+ for left direction
Longitudinal velocity	u	m/s	+ for forward
Steer angle front wheels	δ	Rad	+ for anticlockwise
Slip angles	αf,αr	Rad	+ for clockwise
Vehicle slip angle	β	Rad	+ for slip to left
Cornering stiffness	Cα	N/rad	always +

Table 5.1: Terminology used in Equation of Motion.

17 As known, the steering angle is different by the steering wheel angle in reason of a transmission ratio steer of value equal to 16÷20.

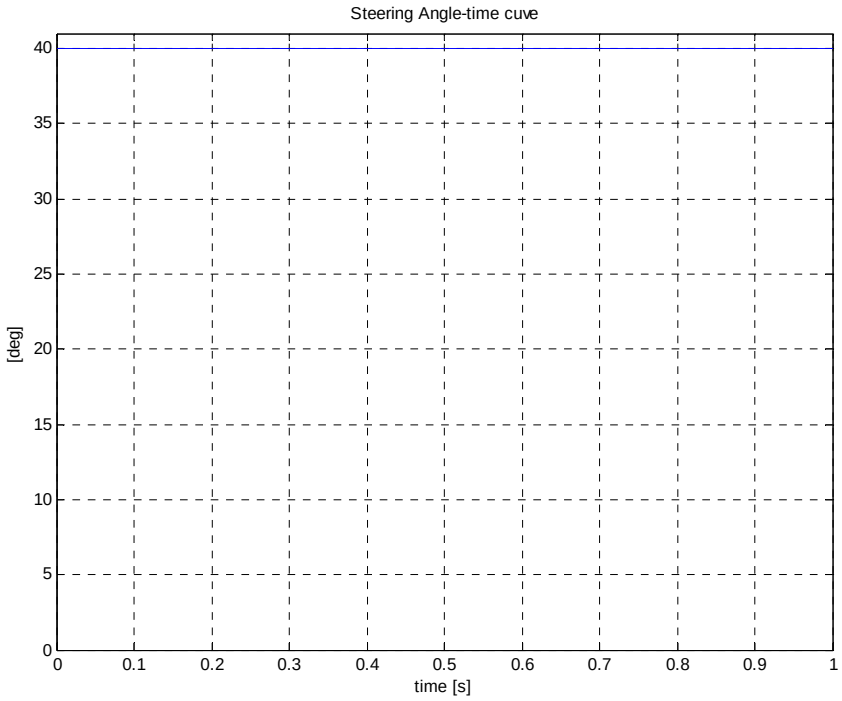

Figure 5.13: Steering Angle-time curve.

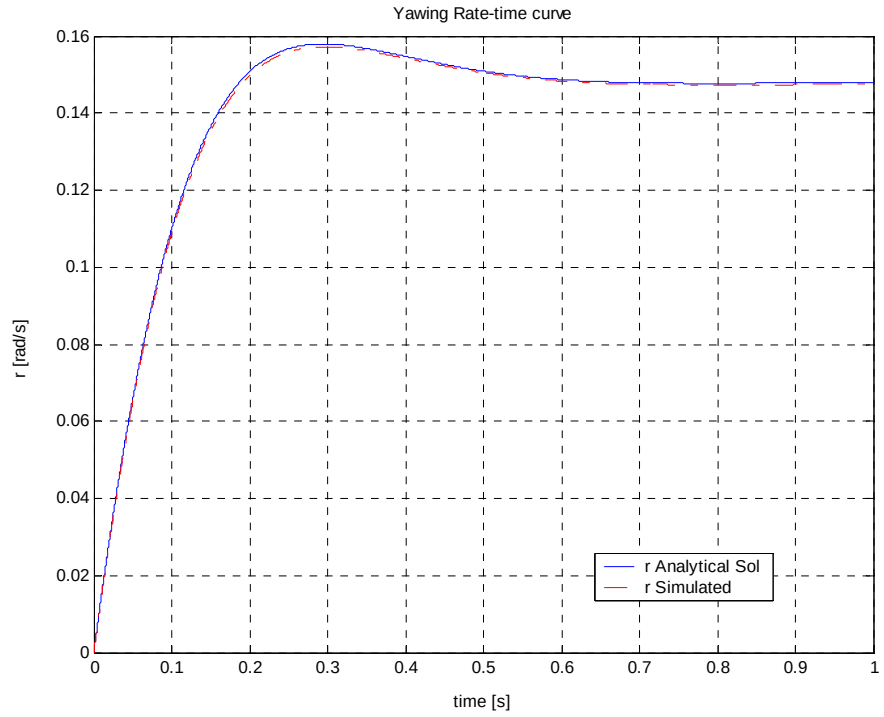

Figure 5.14: Yaw Rate-time curve.

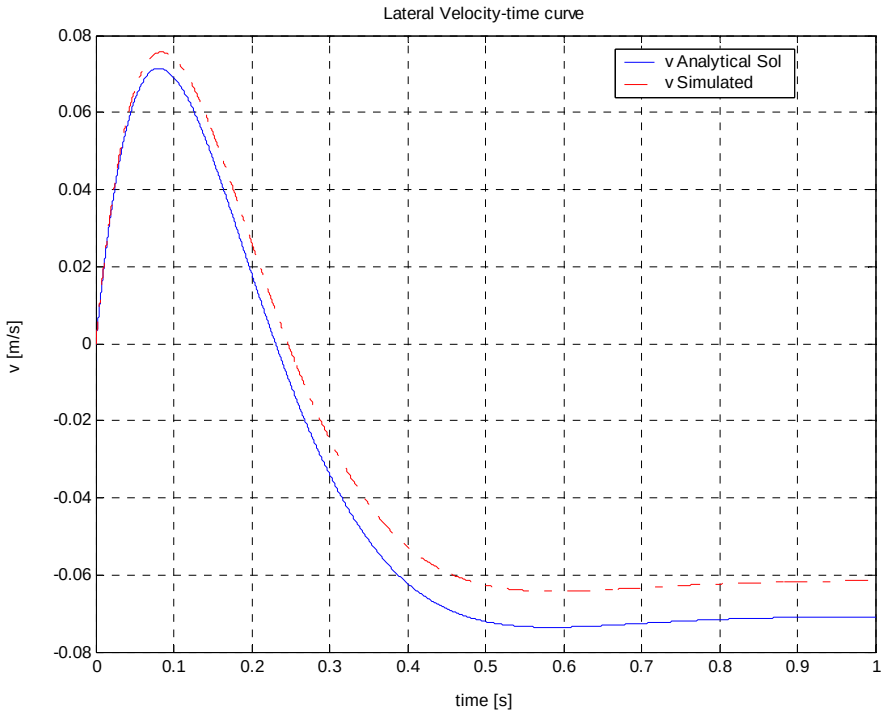

Figure 5.15: Lateral Velocity-time curve.

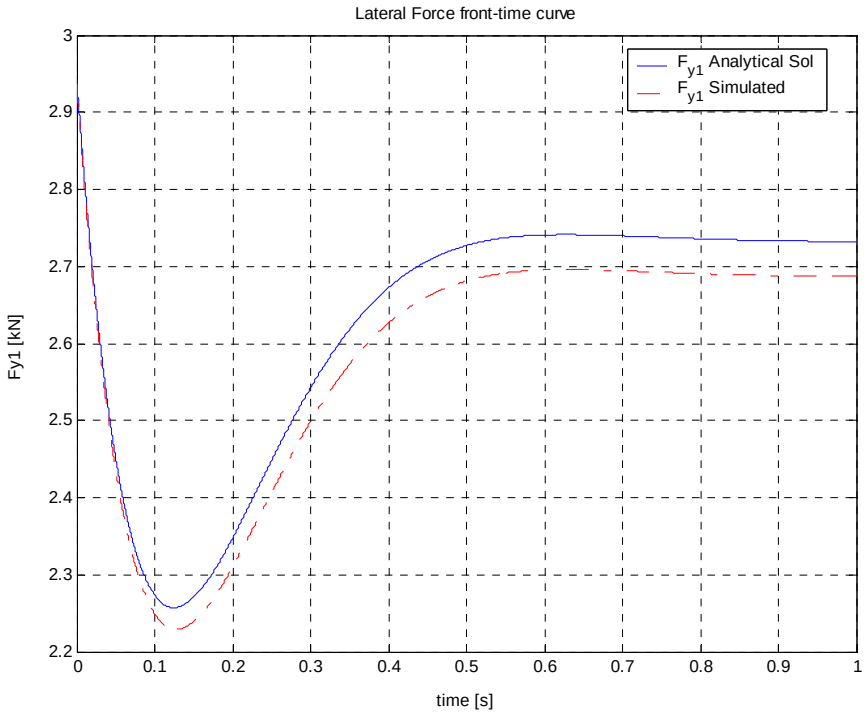

Figure 5.16: Lateral Force Front-time

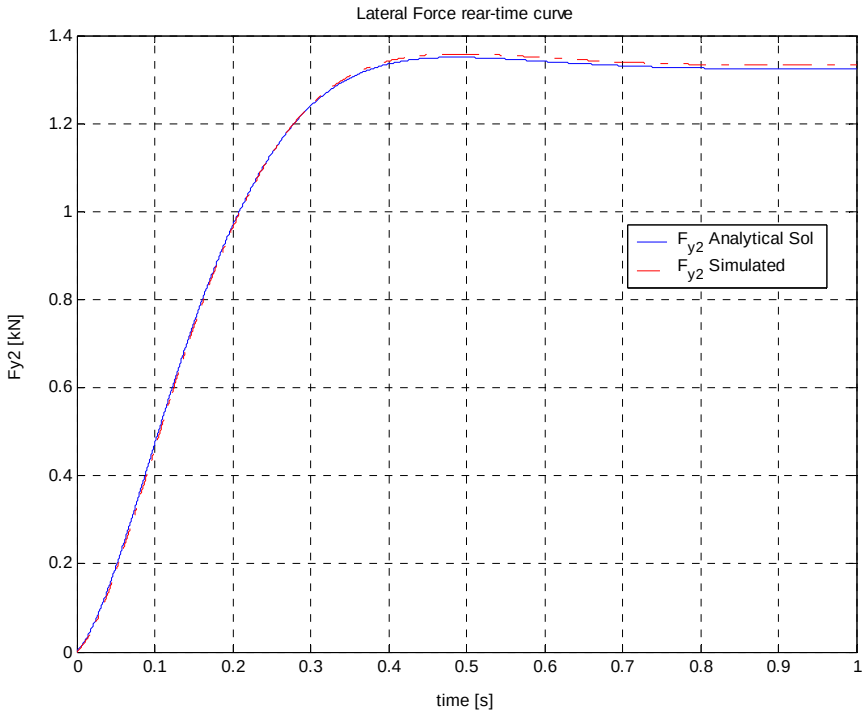

Figure 5.17: Lateral Force Rear-time curve.

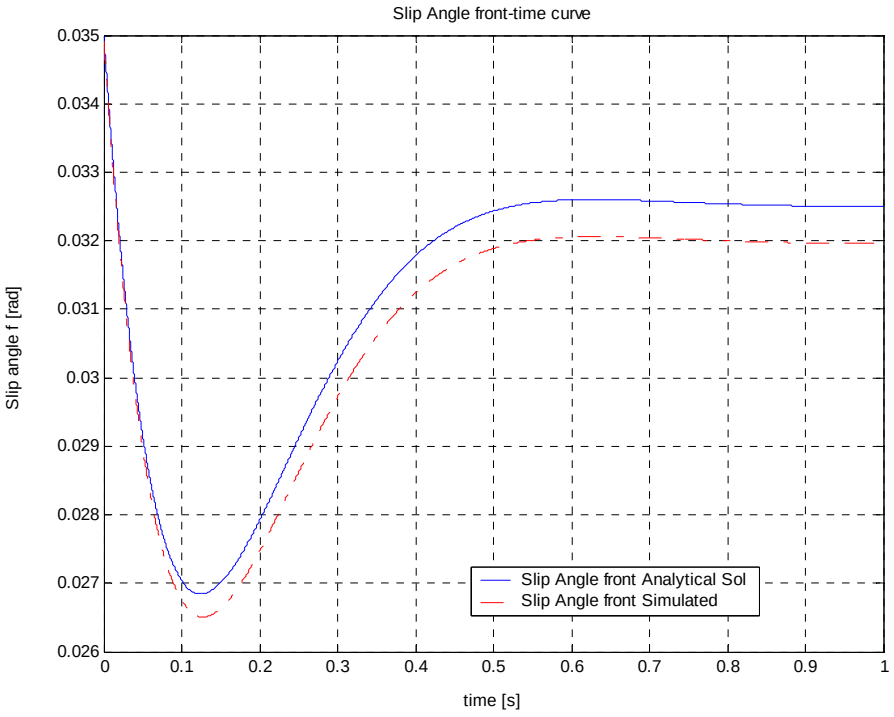

Figure 5.18: Slip Angle Front-time curve.

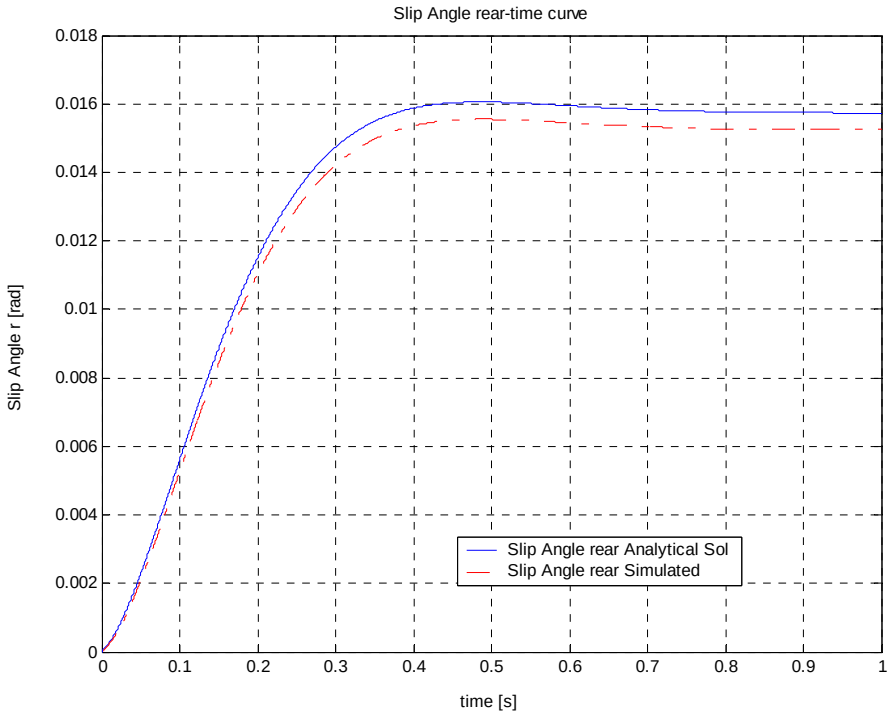

Figure 5.19: Slip Angle rear-time curve.

5.5.1.2 Linear Tyre Model with Relaxation Length

In the following treatment the equations for a single track model with linear tyre model and relaxation length will be shown. One should note that in this case the degree of freedom number of the system is changed. In fact, considering a linear tyre, the system is a 2 D.O.F.s model, but taking into account a tyre model, traduced through a differential equation, the new system will be defined as a 4 D.O.F.s model. In order to develop this model completely, the equations (5.49) will be presented.

$$\begin{aligned} m\left(\dot{v}+ur\right) &= F_{y1}+F_{y2} \\ J\dot{r} &= F_{y1}l_1 - F_{y2}l_2 \\ \frac{d}{u}\dot{F}_{y1}+F_{y1} &= C_{\alpha_f}\left(\delta-\frac{v+rl_1}{u}\right) \\ \frac{d}{u}\dot{F}_{y2}+F_{y2} &= C_{\alpha_r}\left(\frac{rl_2-v}{u}\right) \end{aligned} \qquad \textbf{(5.49)}$$

5.5.1.3 Non-Linear Tyre Model with Relaxation Length

In analogy, it will be necessary to illustrate the equation of motion using the non-linear tyre model. Likewise the former case, the model is a 4 D.O.F., too. The value of the constants required for the integration are included as Appendix B.

$$
\begin{aligned}
m\left(\dot{v}+ur\right) &= F_{y1}+F_{y2} \\
J\dot{r} &= F_{y1}l_1 - F_{y2}l_2 \\
\frac{d}{u}\dot{F}_{y1}+F_{y1} &= \mu F_{z1}\left(1-\exp\left(-\frac{C_{\alpha f}}{\mu F_{z1}}\left(\delta-\frac{v+rl_1}{u}\right)\right)\right) \\
\frac{d}{u}\dot{F}_{y2}+F_{y2} &= \mu F_{z2}\left(1-\exp\left(\frac{C_{\alpha r}}{\mu F_{z2}}\left(\frac{v-rl_2}{u}\right)\right)\right)
\end{aligned}
\qquad \textbf{(5.50)}
$$

5.5.1.3.1 Simulation Results

Simulation results for the first time are illustrated in Figures 5.20 to 5.25. Later than this observation time all the working variables assume already a steady-state condition. Moreover, the yaw rate is a increasing monotonic function and the lateral velocity acquires a relative maximum in corresponding of 0.1 second and than it reaches the steady-state condition.

Through the congruence equations, it is not hard to obtain the slip angles response. However, it is possible to note the lateral forces at the front and rear wheels tendency. In fact, owing to the steep steer angle, the front force in lateral direction assumes a discontinuity about zero value. On the basis of that, the lateral front force does not start from the zero value but from beginning it assumes a constant value, approximately equal to the steady-state value.

This happens only for the linear tyre model without relaxation length, and Actually, for this reason it is not able to describe the dynamic behaviour of the vehicle.

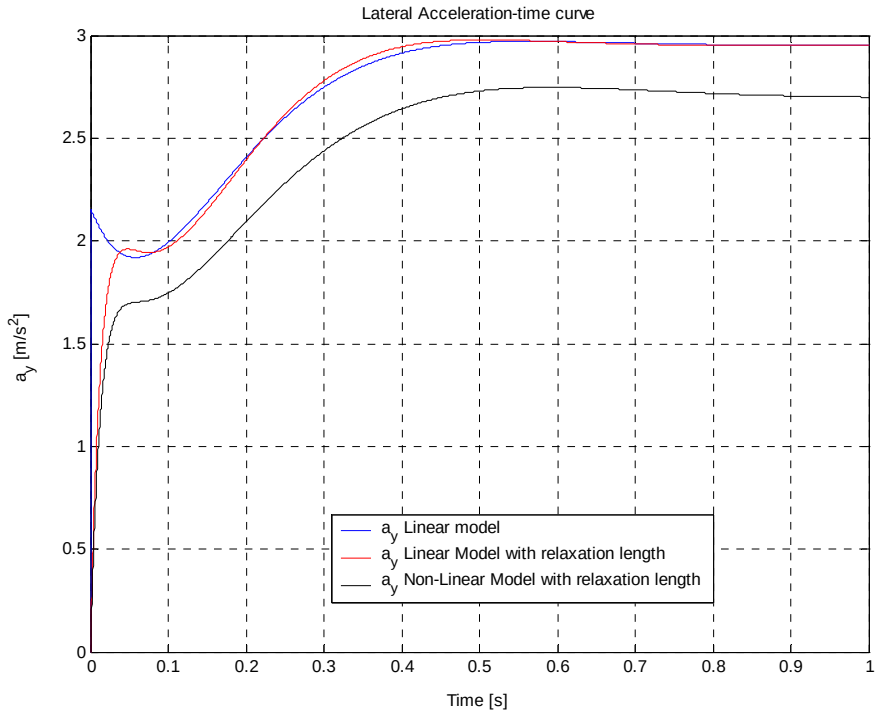

Figure 5.20: Lateral Acceleration-time curve.

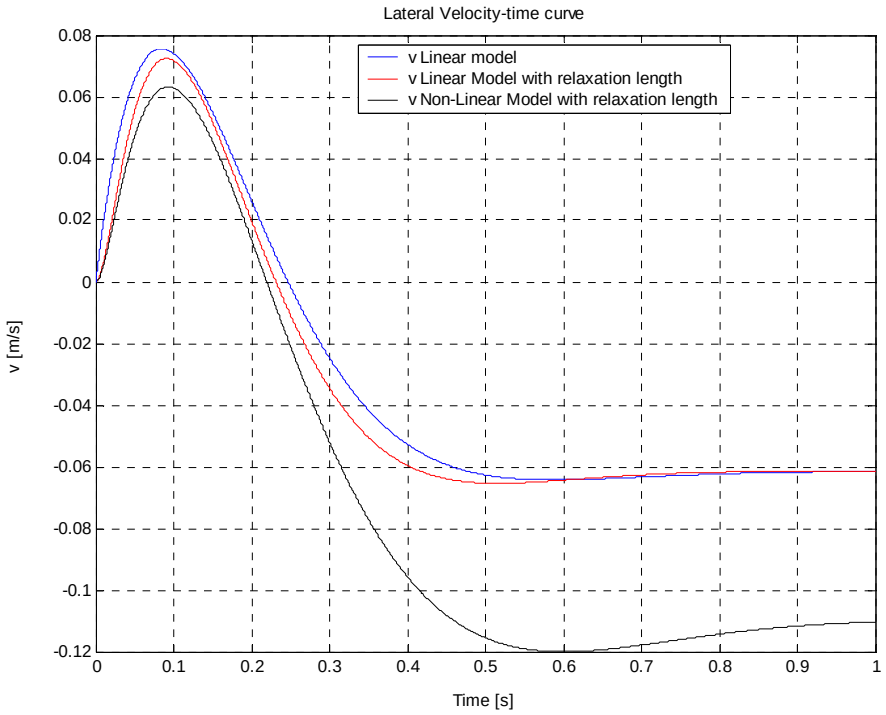

Figure 5.21: Lateral Velocity-time curve.

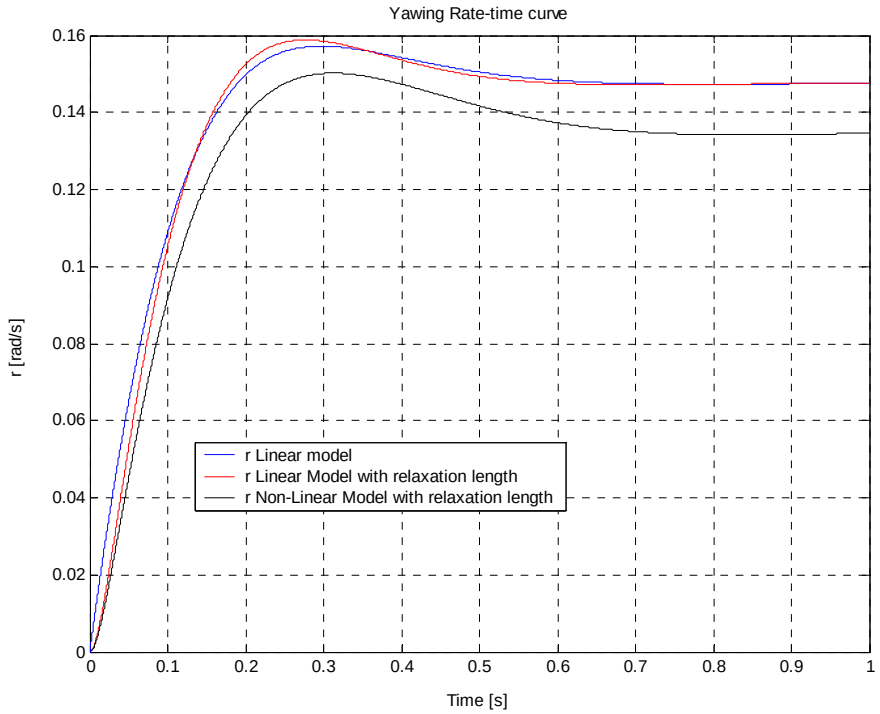

Figure 5.22: Yaw Rate-time curve.

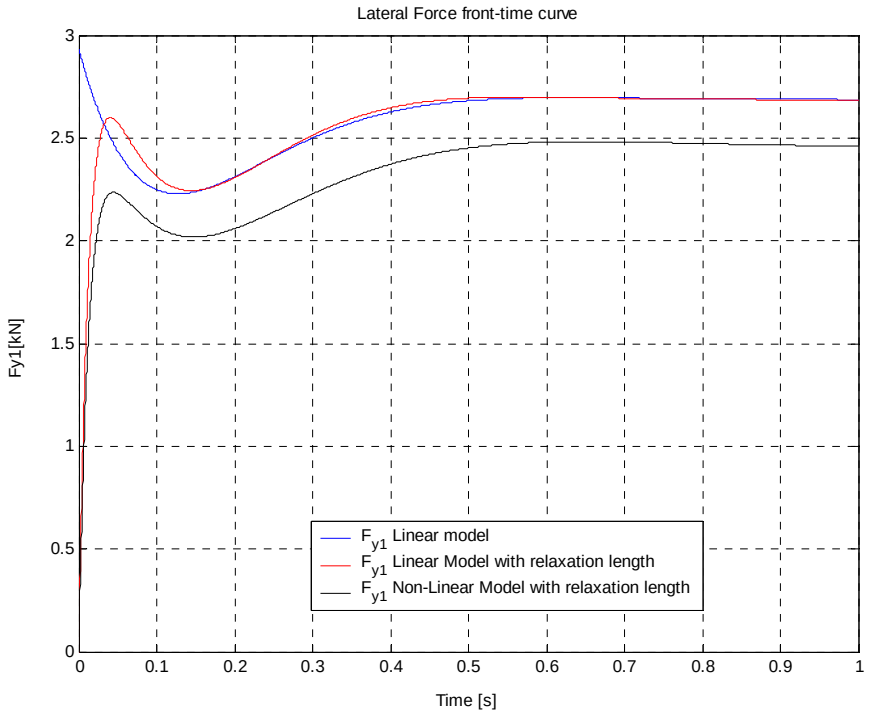

Figure 5.23: Lateral Force Front-time curve.

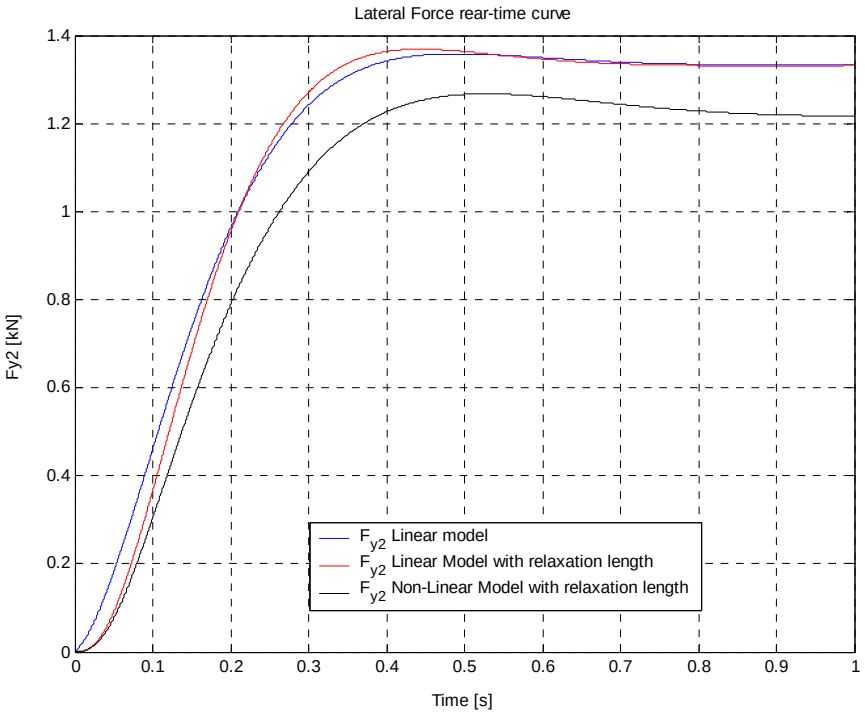

Figure 5.24: Lateral Force Rear-time curve.

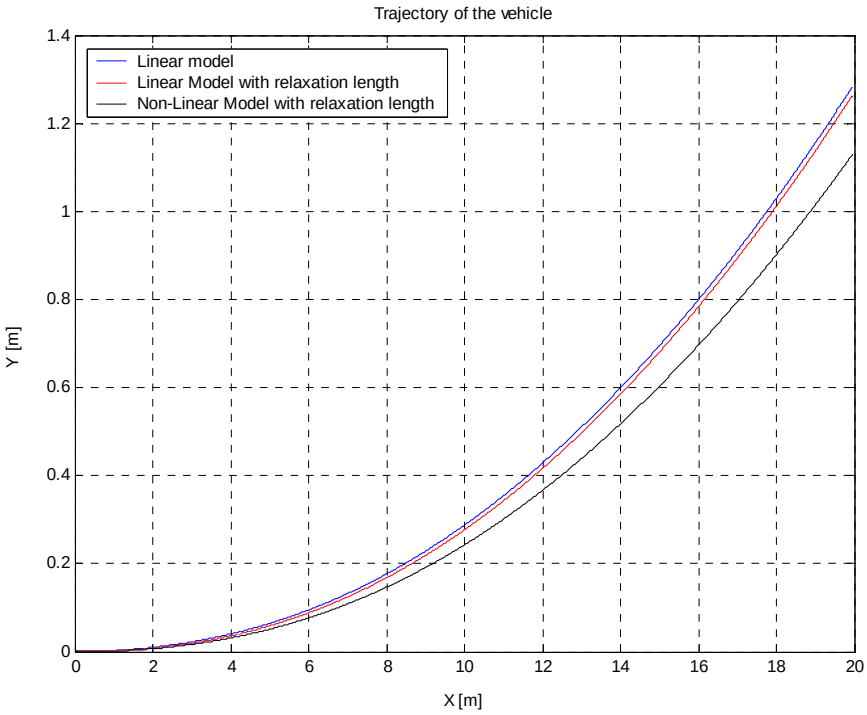

Figure 5.25: Trajectory of the Vehicle.

5.5.2 Front Traction Model (FWD)

When the traction is assumed to be at the front wheels, namely front wheel drive, the analytical solution is not possible, even if a linear tyre model could be used. In this case, the solution does not exist and these equations can be solved only with numerical methods. This mathematical difference approach is caused by a *non-linearity* due to the product between the independent variables and the aerodynamic term. This does not happen if a rear wheel drive is considered.

One should note that in the following equations the tractive rear force cannot be considered equal to zero owing to the front wheel drive definition, and it will be deduced using the equilibrium in the longitudinal direction.

Contrarily, the longitudinal rear force can be consider as null ($F_{x2}=0$) in order to simplify the equations required to investigate about the vehicle behaviour.

5.5.2.1 Linear Tyre Model

The equation of motion of the lateral vehicle dynamics for a front wheel drive, equipped with a linear tyre model, characterized through a 3 D.O.F. model, are shown in the following section.

$$\begin{aligned}\dot{v} &= -\left(\frac{C_{\alpha 1}+C_{\alpha 2}}{mu}\right)v - vr\delta - \left(\frac{C_{\alpha 1}l_1 - C_{\alpha 2}l_2}{mu} - u\right)r + \left(\frac{C_{\alpha 1}}{m} + \dot{u} + \frac{F_{x1}}{m}\right)\delta \\ \dot{r} &= -\left(\frac{C_{V1}l_1 - C_{\alpha 2}l_2}{Ju}\right)v - \frac{ml_1}{J}vr\delta - \left(\frac{C_{\alpha 1}l_1^{\,2} + C_{\alpha 2}l_2^{\,2}}{Ju}\right)r + \left(\frac{C_1 + F_{x1}}{J}l_1\right)\delta\end{aligned} \qquad \textbf{(5.51)}$$

where the longitudinal force at front wheel has been described by the following relationship:

$$F_{x1} = m\left(\dot{u} - vr\right) + F_{y1}\delta + F_{xa} \qquad \textbf{(5.52)}$$

5.5.2.2 Linear Tyre Model with Relaxation Length

According to the corresponding model for the rear wheel drive, in this section it will be illustrated the equations of motion for a 5 D.O.F.s model with front traction.

$$\begin{aligned} m\left(\dot{v}+ur\right) &= F_{y1}+F_{y2}+F_{x1}\delta \\ J\dot{r} &= F_{y1}l_1-F_{y2}l_2+F_{x1}l_1\delta \\ \frac{d}{u}\dot{F}_{y1}+F_{y1} &= C_{\alpha_f}\left(\delta-\frac{v+rl_1}{u}\right) \\ \frac{d}{u}\dot{F}_{y2}+F_{y2} &= C_{\alpha_r}\left(\frac{rl_2-v}{u}\right) \end{aligned} \qquad \textbf{(5.53)}$$

With the tractive front force F_{x1} is expressed by the following relation, deduced by the equilibrium in longitudinal direction; deduced by the longitudinal direction:

$$F_{x1}=m\left(\dot{u}+vr\right)+F_{y1}\delta+F_{xa} \qquad \textbf{(5.54)}$$

To note that in all equations concerning the FWD (each time the 1th of 5.24 was used), the longitudinal acceleration was not simplified because the final purpose is to couple the longitudinal and lateral models considering the variability longitudinal velocity. Obviously, for fixed feed velocity, the value corresponding to the acceleration is null.
In the complete vehicle model, except the vertical dynamics, the tractive force will be formed by more contributions, that during this section did not be consider, such as, the rolling resistent which cannot simplified owing to the longitudinal velocity variability.

5.5.2.3 Non-Linear Tyre Model with Relaxation Length

In analogy to the former section, the front wheel drive model, 5 D.O.F. is traduced through the following set of equations:

$$
\begin{aligned}
m\left(\dot{v}+ur\right) &= F_{y1}+F_{y2}+F_{x1}\delta \\
J\dot{r} &= F_{y1}l_1-F_{y2}l_2+F_{x1}l_1\delta \\
\frac{d}{u}\dot{F}_{y1}+F_{y1} &= \mu F_{z1}\left(1-\exp\left(-\frac{C_{\alpha f}}{\mu F_{z1}}\left(\delta-\frac{v+rl_1}{u}\right)\right)\right) \\
\frac{d}{u}\dot{F}_{y2}+F_{y2} &= \mu F_{z2}\left(1-\exp\left(\frac{C_{\alpha r}}{\mu F_{z2}}\left(\frac{v-rl_2}{u}\right)\right)\right)
\end{aligned}
\qquad \textbf{(5.55)}
$$

where F_{x1} assumes the same form used in the linear front model with the relaxation length, Eqs. (5.45).According to the former treatment about the simulations shown, the front wheel drive model response will be proposed, with three different tyre models, before analyzed, Figures 5.26 to 5.31.

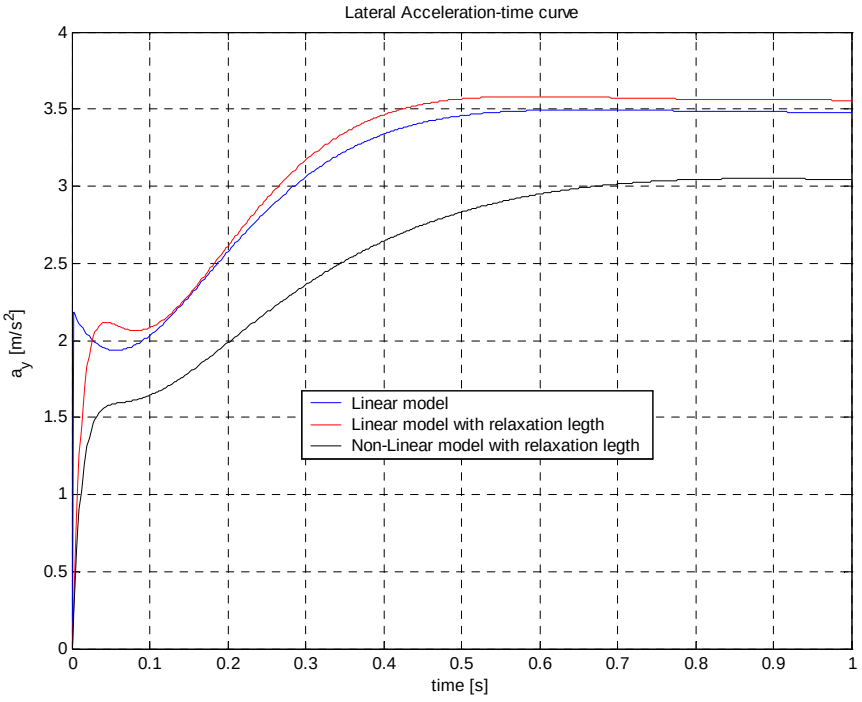

Figure 5.26: Lateral Acceleration-time curve.

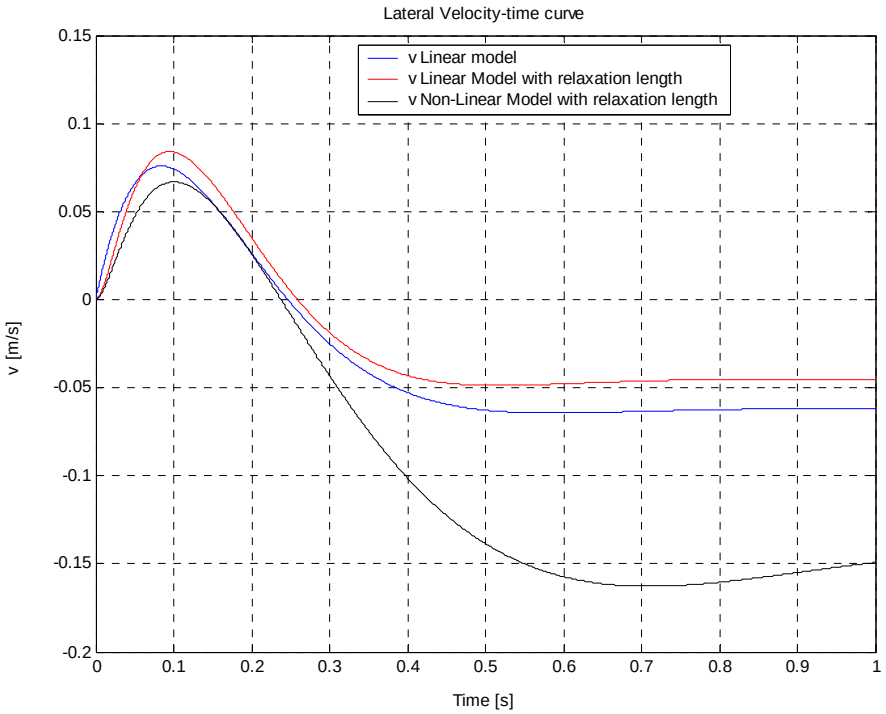

Figure 5.27: Lateral Velocity-time curve.

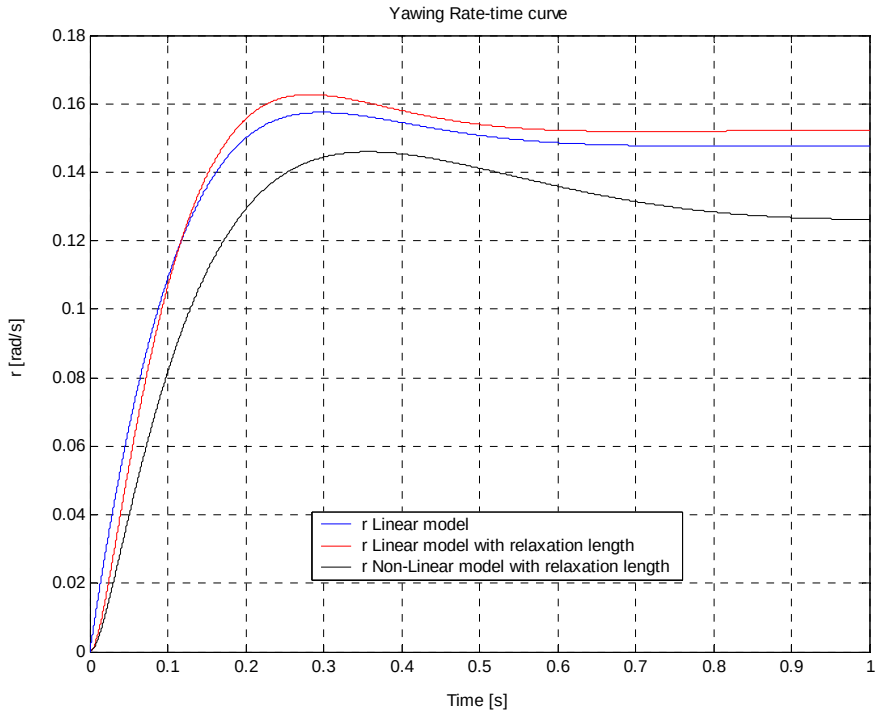

Figure 5.28: Yaw Rate-time curve.

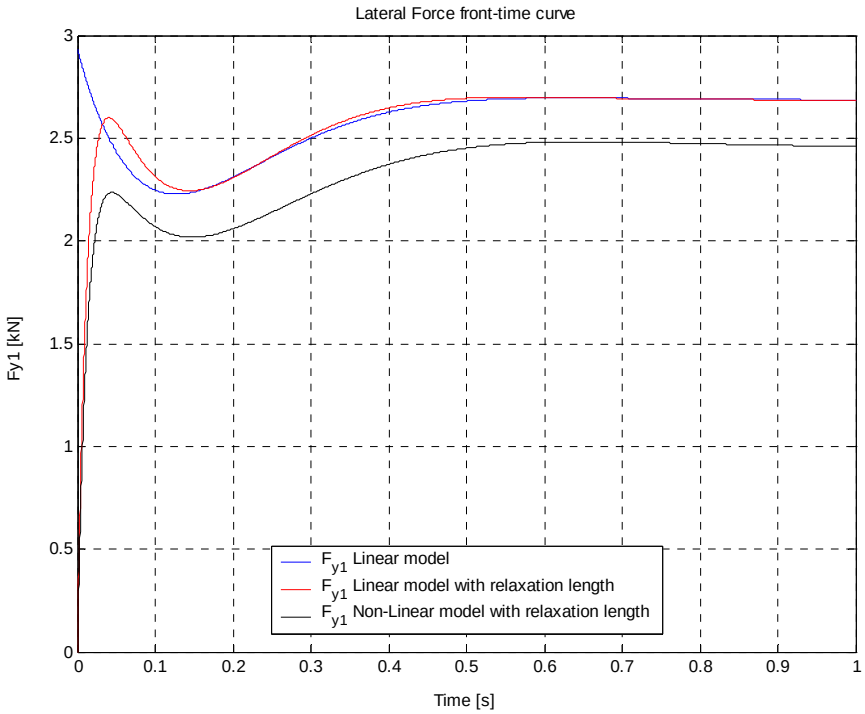

Figure 5.29: Lateral Force Front-time curve.

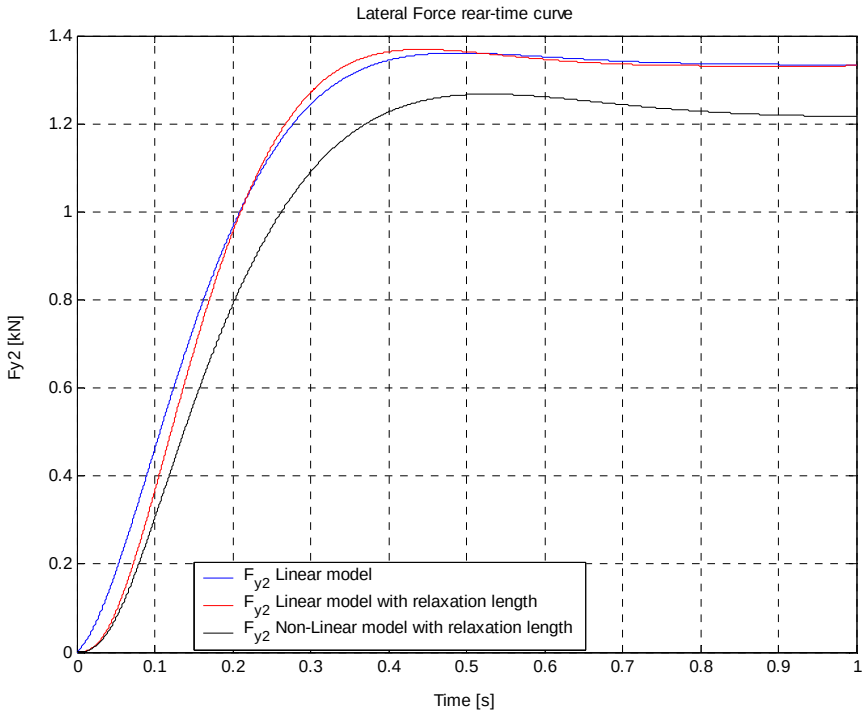

Figure 5.30: Lateral Force Rear-time curve.

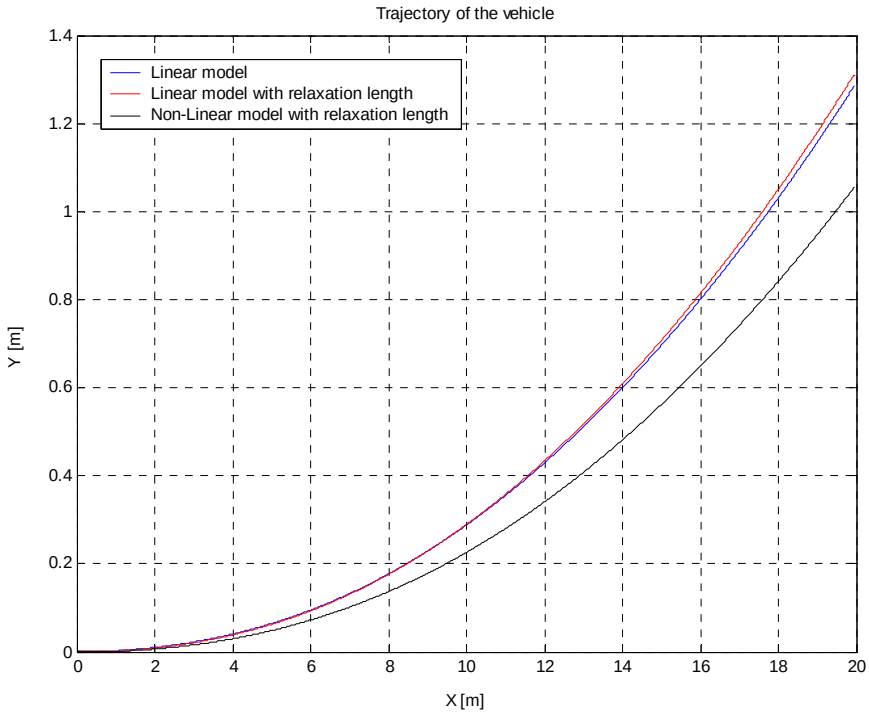

Figure 5.31: Trajectory of the Vehicle.

5.5.3 Conclusions

Schematically, the models developed in this section can be summarized in a single table; see Table 5.2.

	Degrees of Freedom	Tyre Model
RWD	2	L
	4	L with R-L
	4	N-L with R-l
FWD	3	L
	5	L with R-L
	5	N-L with R-l

Table 5.2: Degrees of Freedom Corresponding to each Lateral Model

The mean of the symbols is reported in the following sentences:

- L: Linear tyre model without relaxation length;
- L with R-L: Linear tyre model with relaxation length
- N-L with R-L: Non-Linear tyre model with relaxation length
- RWD: Rear wheel drive;
- FWD: Front wheel drive.

To note that, for the vehicle complete model, so with the interaction between the longitudinal and lateral variables, each model will acquire one degree of freedom considering a linear tyre model with/without relaxation length and three degrees fo freedom considering the non-linear tyre model. Schematically these concepts are illustrated in the following table:

	Longitudinal Model (D.O.F.s)	**Lateral Model (D.O.F.s)**	**Degree of Freedom**
RWD	1	2	3
	1	4	5
	3	4	7
FWD	1	3	4
	1	5	6
	3	5	8

Table 5.3: Degrees of Freedom Corresponding to each Complete Model

Chapter 6

6 Simulink Environment Model

As described into the former chapters, numerous equations are required to develop a complete vehicle model and study the principal characteristics about vehicle dynamics. Obviously, the decision about how to go into details rests entyrely on the discretion of the research worker. In fact, it always happens that the choice about the details is imposed due to the final goal of the research, and for this reason, one does not need to model the complete physical system, only part of it. In this section we will introduce the simple model, previously discussed, in order to give a complete vision about the principal characteristics of longitudinal and transversal behaviour of the vehicle. Thus, the general characteristics of vehicle, will be implemented in Simulink/Matlab environment.

6.1 Simulink Modelling

In order to analyze the dynamic characteristics of the vehicle and to study its performance, a computer simulation model of the vehicle system, using the Matlab/Simulink computer software, has been developed.

In fact, this section describes the Matlab/Simulink model that was implemented. Simulink is a software package for modelling, simulating, and analyzing dynamical systems in general.

The software, implemented runs under Matlab, a mathematical workshop. Simulink and Matlab are available from the *MathWorks*, Inc. Simulink provides a graphical user interface for building models as block diagrams.

The graphical interface is popular for developing dynamical models for many fields, such as electronics, hydraulics, chemistry, and many others.

Simulink is not particularly useful for building equation sets for complex mechanical 3D systems. However, it includes S-functions (system functions) to augment and extend the building blocks in SIMULINK to include arbitrary complex systems.

The S-function appears in a SIMULINK model as a block in the block diagram. The mathematical behaviour of S-functions can be defined either as a MATLAB M-file, or as an executable piece of object code in the form of a DLL (dynamic link library) obtained by compiling C or FORTRAN source code. Such "executable" functions are called MEX files (where the EX stands for executable). The S-functions can be loaded and run by SIMULINK. The simulations can be run from within SIMULINK, using the SIMULINK integrators and the SIMULINK environment for setting control inputs to the vehicle model.

6.2 Simulating a Complete Vehicle

The simulation model, illustrated in Figure 6.1, includes many sub-models, some of that will simulate the powertrain, other the lateral motion of the vehicle, and others the tyre behaviour.

The green and yellow blocks on the right, named "*Vehicle Dynamics*" and "*Tyre Model*" represent the final part of the vehicle modelling: the dynamics behaviour of the chassis, vehicle inertia, the wheels, and their coupling to the road.

All the other subsystems in the model represent input that control the former or outputs that measure its behaviour.

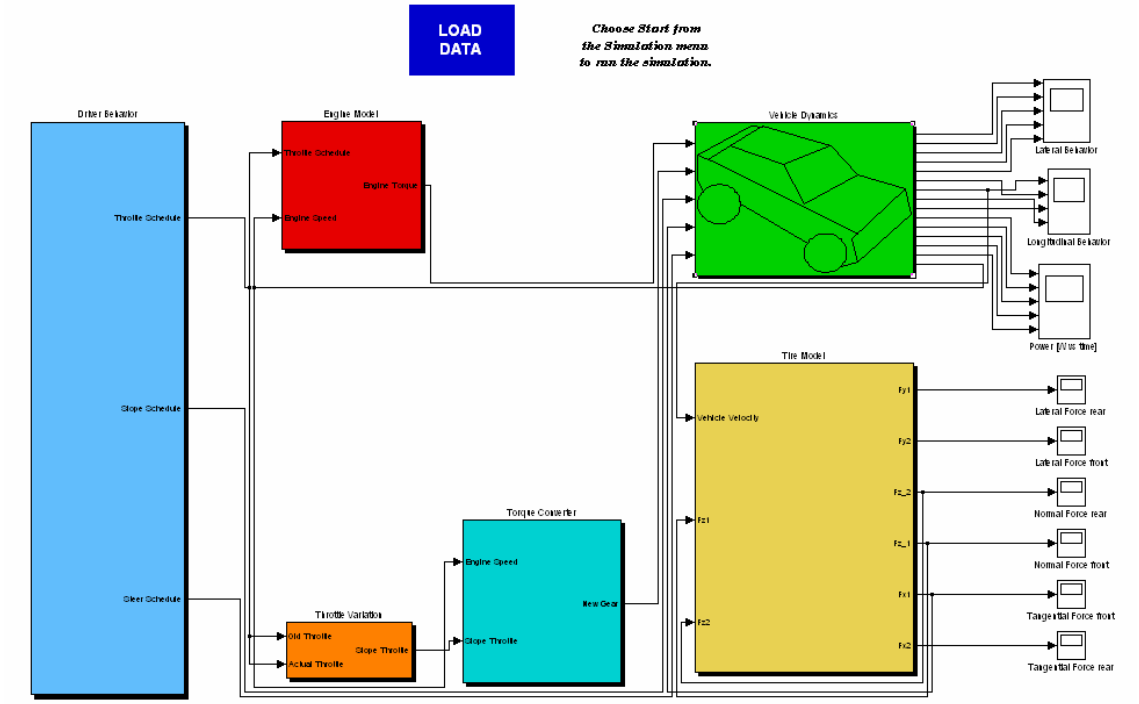

Figure 6.1: Complete Vehicle Model.

The main subsystems are:

- Driver Behaviour
- Engine Model
- Throttle Variation
- Torque Converter
- Vehicle Dynamics
- Tyre Model

The following sections explain these subsystems in greater details, recalling each time the corresponding name of the block.

6.2.1 Driver Behaviour

The easy driver model, presented in Figure 6.2, is a package for simulating and analyzing how the vehicle responds dynamically to inputs from the driver and the environment (road and wind but for us under driver control us an user). It provides the same types of output that might be measured with physical test involving instrumented

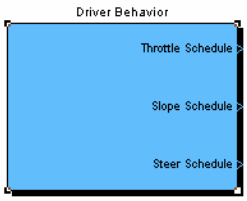

Figure 6.2: Driver Behaviour Block

vehicles (as will be the case for the validation test). The aim of this section is to provide information on the technical aspects of the simulations.

6.2.2 Powertrain Modelling

As cited into Chapter 4, modelling the powertrain requires good knowledge of the involved components and their physic. It is remembered the division modelling into three parts, *Engine Model* and *Throttle Variation Model* and *Torque Converter Model*, including torque converter model.

6.2.2.1 Engine Model

The characteristic curve of an internal combustion engine defines the torque supplied as function of engine speed n_e and throttle opening α. The former is regulated by the driver behaviour model, assuming values between zero and one.

The Simulink block "Engine Model", first element of the complete vehicle model is shown in Figure 6.3. It should be noted that this block is called MISO (*Multi-Input-Single-Output*) because, during the simulation, for a fixed value of the engine speed and throttle opening, it gives the value of the corresponding engine torque.

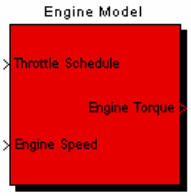

Figure 6.3: Engine Model.

From this, we obtain the subsystem shown in Figure 6.4. In this former block a "*Look up table 2D*" was used. It gives the interpolation points in the engine map; so, Tables 6.1, and 6.2 show the functional description of this block.

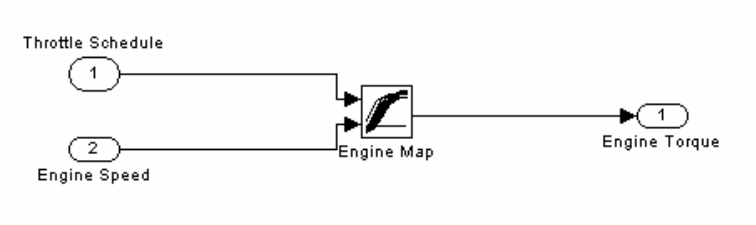

Figure 6.4: Subsystem Corresponding to the Engine Model.

Input	***Description***	***Size***	***Units***
Throttle Schedule	Matrix value assumed by the driver	*tout× 1*	%
Engine Speed	Instantaneous value assumed by the engine speed	*tout× 1*	rpm

Table 6.1: Input of the Engine Model.

Output	***Description***	***Size***
Engine Torque	Engine torque value of needed to integrate the state equation	*tout× 1*

Table 6.2: Output of the Engine Model.

6.2.2.2 Throttle Variation Model

The next subsystem in the powertrain is the driveline, in this case an automated manual transmission, driveshaft, wheels and chassis. Actually, the transmission has three working states: engaged, disengaged and during engagement/disengagement.

When the transmission is engaged the engine power is transferred to the wheels via a fixed gear ratio. On the other hand, when the transmission is de-coupled the rotational parts in engine run without transferring tractive effort to the wheels.

In this work, we have designed a simple Torque Converter model to simulate the gear change, as shown in Table 6.3:

Acceleration	Deceleration
1-2	5-4
2-3	4-3
3-4	3-2
4-5	2-1
Steady speed	*Arrest*

Table 6.3: Gear Change during Acceleration and Deceleration Manoeuvreing.

Before describing this subsystem accurately, we have to understand which manoeuvreing we are using. To do this, we need a special block, called "*Throttle Variation*", shown in Figure 6.5.

In following Tables 6.4, 6.5, and 6.6 we have the functional description, with reference to the Function *Fcn(u)*, *Derivate Computation*, where *tout* assumes values depending on the simulation time.

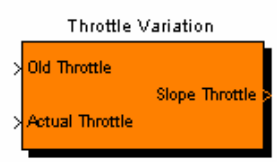

Figure 6.5: Throttle Variation Model.

Also, we will illustrate the corresponding subsystem of this model, as shown in Figure 6.5.

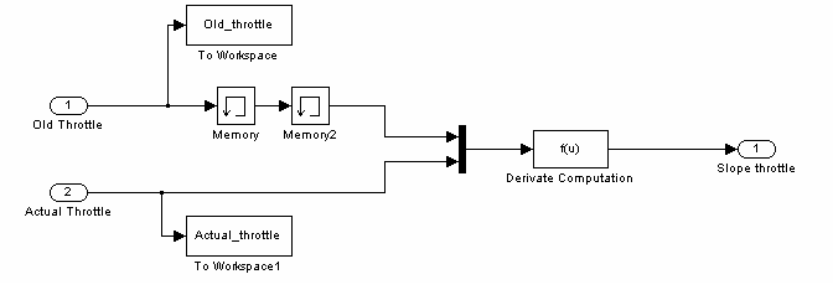

Figure 6.6: Subsystem corresponding to the Throttle Variation Model.

Input	*Description*	*Size*	*Units*
Old Throttle	Old Value assumed by Throttle	*tout×1*	/
Actual Throttle	Actual Value assumed by Throttle	*tout×1*	/

Table 6.4: Input of the Throttle Variation Model

Function	*Description*	*Size*
F(u)	Evaluate the numerical derivate between Actual and Old Throttle	/

Table 6.5: Fcn-Function of the Throttle Variation Model

Output	*Description*	*Size*
Slope Throttle	Variable needed to simulate the gear-change manoeuvreing	*tout× 1*

Table 6.6: Output of the Throttle Variation Model

Depending on the value assumed by Slope Throttle, it should have the corresponding gear change. This logic disposition is dictated from the S-Function, "*gear_box_change*", included in Torque Converter model, explained into section.

6.2.2.3 Torque Converter Model

As mentioned previously, the power-torque-speed characteristics of the internal combustion engine are not suited for direct vehicle propulsion. Transmission, therefore, is required to provide the vehicle with tractive effort speed characteristics that will satisfy the load demands under various operating conditions.

The term "transmission" includes all the systems or subsystems used for transmitting the engine power to the driven wheels or sprockets. There are two common types of transmission with a torque converter: the manual gear transmission, and the automatic transmission with a torque converter. Other types of transmission such as the continuous variable transmission (CVT) and the hydrostatic transmission are also used.

In this project, an automatic transmission is simulated, according to two limit values of engine speed. These two limits are imposed arbitrarily setting a range between maximum and minimum number of revolutions. In this case, the higher limit to change-up gear (acceleration) is 5000 rpm and the lower one to change-down gear (deceleration) is 2000 rpm.

The "Torque Converter" model, shown in Figure 6.7, works according to an S-Function, called "gear_box_change", and are included in Appendix B.

In the following Tables 6.7, 6.8, and 6.9 a description functionally was shown. Therefore, the corresponding subsystem of this model is illustrated in Figure 6.8.

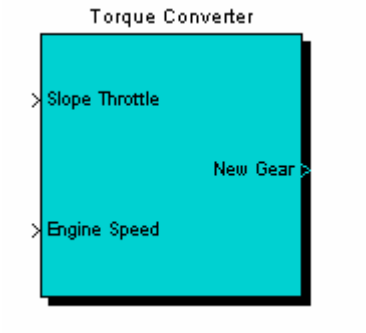

Figure 6.7: Torque Converter Model

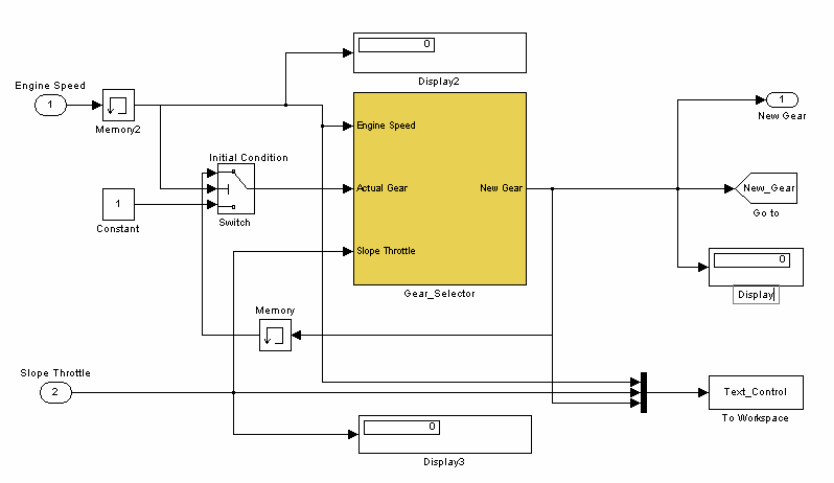

Figure 6.8: Subsystem Corresponding to the Torque Converter Model

However, as shown in the previous subsystem, we have two main parts: the *Switch* block and *Gear Selector* block. The first one is indispensable to give the initial condition corresponding to start in 1_{st} gear. On the other hand, the other block recalls the S-Function, as shown in Figure 6.8.

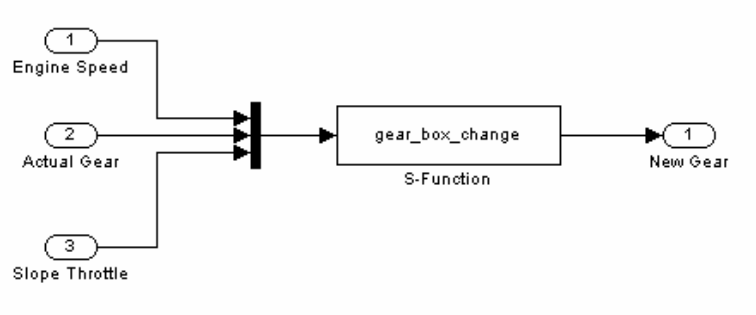

Figure 6.9: Subsystem Corresponding to the Gear Selector Block

Input	***Description***	***Size***	***Units***
Slope Throttle	Slope Value assumed by Throttle	*tout×1*	/
Engine Speed	Instantaneous value assumed by Engine Speed	*tout×1*	/

Table 6.7: Input of the Torque Converter Model

Function	***Description***	***Size***
F(u)	Valuate the new gear number	/

Table 6.8: S-Function of the Torque Converter Model

Output	***Description***	***Size***
New Gear	Value of new gear number	*tout×1*

Table 6.9: Output of the Torque Converter Model

6.2.3 Vehicle Dynamics

The Vehicle Dynamics model, Figure 6.10, is divided into two parts:

- Driveline Model;
- Lateral Model.

In the following sections, all the subsystems will be illustrated.

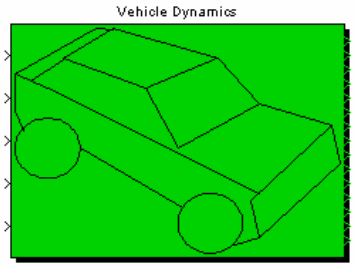

Figure 6.10: Vehicle Dynamics.

6.2.3.1 Driveline Model

This easy model can be considered as the latter link of the chain, namely *Longitudinal Vehicle Dynamics*.

The equation of motion is a function of time-varying quantities that characteristic curve of an internal combustion engine defines the torque supplied as function of engine speed n_e and throttle opening α that is as function of a parameter able to show how much the throttle should be opened. In fact, as known, the throttle opening is proportional to the mass flow rate of air.

The throttle opening assumes included values between 0, section completely closed and 1 (or percentage value) for fully opening.

Particularly attention may be given to the *Memory* block, Figure 6.22, which contains the condition concerning the velocity of the wheels constant during the gear-change manoeuvreing. In fact, during an unitary step of simulation, when the gear has engaged the simulation is stopped artificially and the rotational velocity of the wheels is imposed to be constant. All these manoeuvreings are controlled by the variable "*trigger*", which

gives the null value, when the gear number is constant, and unitary value during the change-gear. To have the graphical visualization see Figure 6.17.

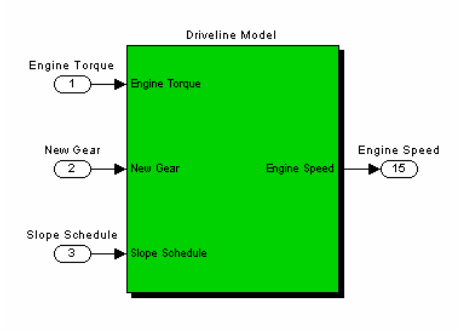

Figure 6.11: Driveline Model.

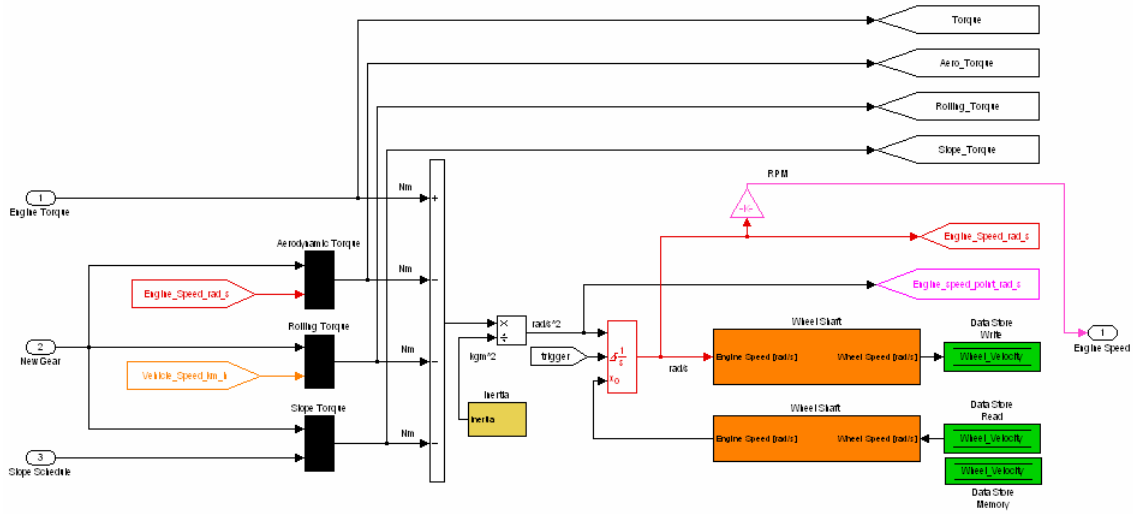

Figure 6.12: Driveline Subsystem.

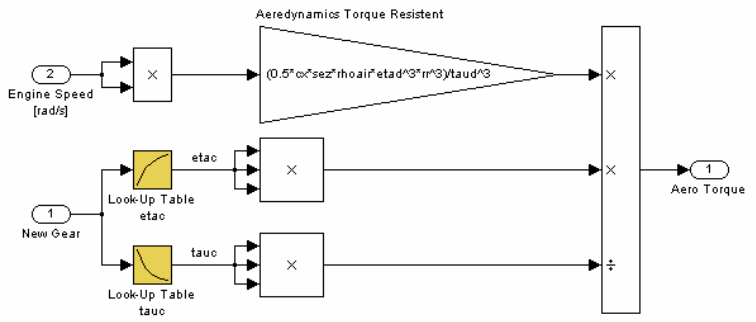

Figure 6.13: Aerodynamic Block.

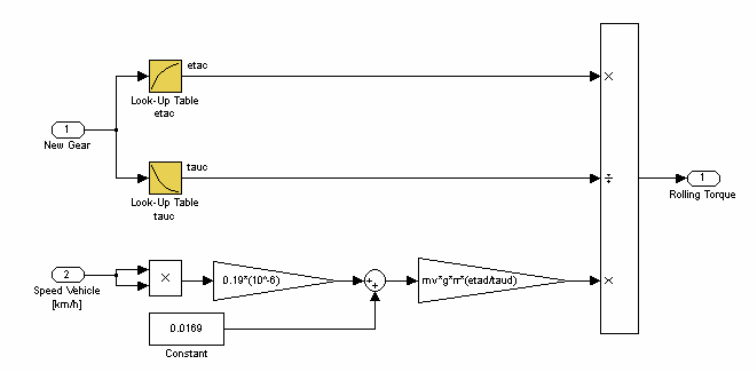

Figure 6.14: Rolling Torque Block.

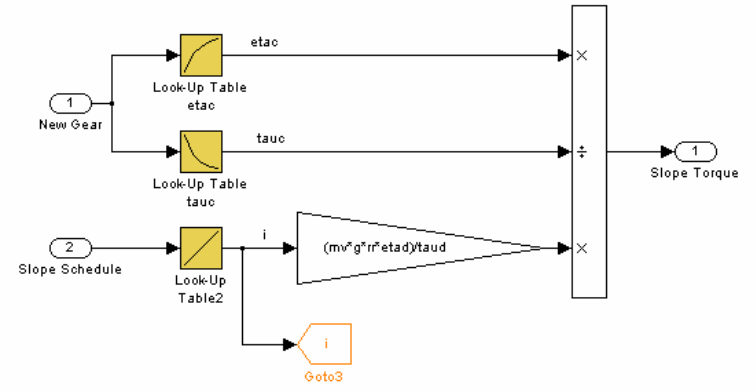

Figure 6.15: Grade Torque Block.

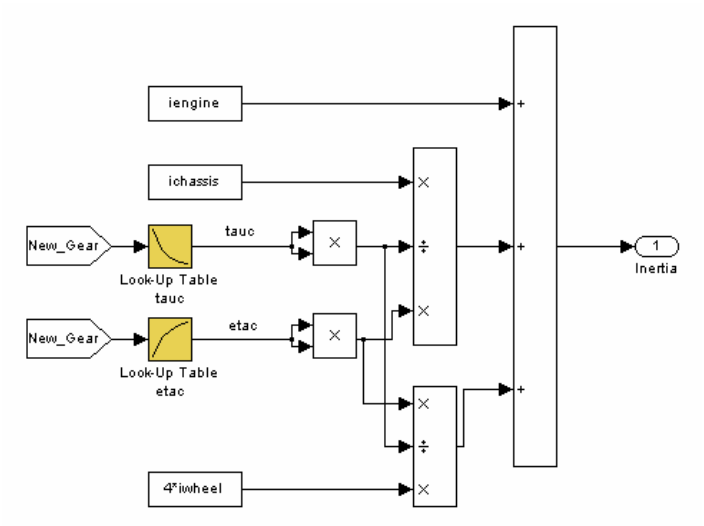

Figure 6.16: Inertia Evaluation Block.

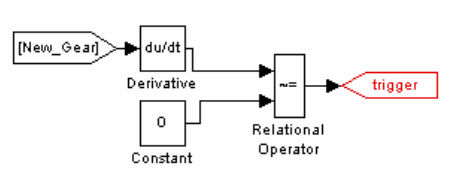

Figure 6.17: Trigger Block.

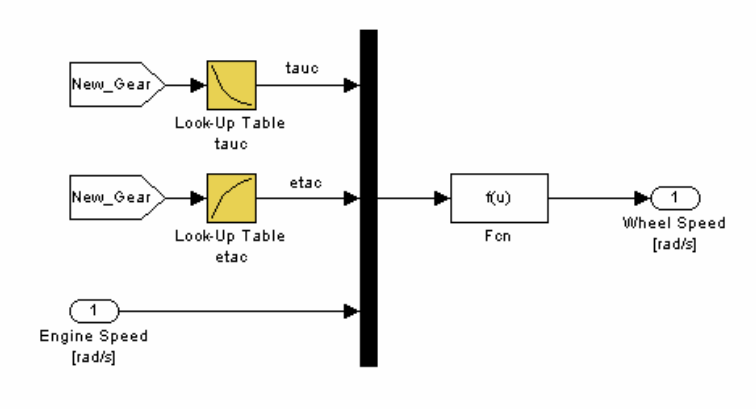

Figure 6.18: Wheel Shaft Block 1

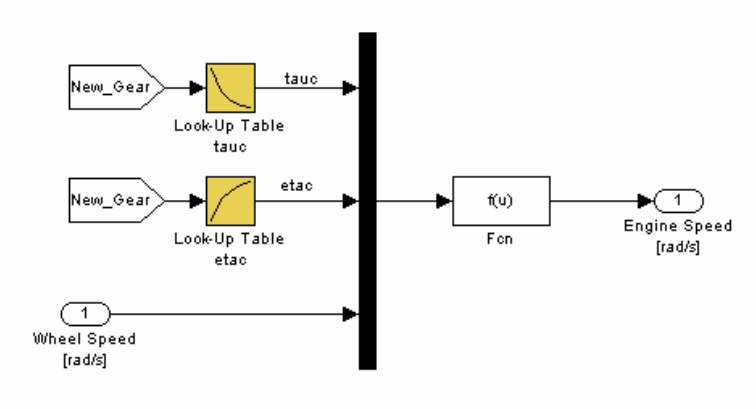

Figure 6.19: Wheel Shaft Block 2

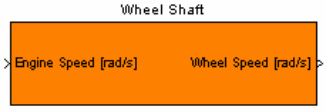

Figure 6.20: Wheel Shaft Subsystem 1

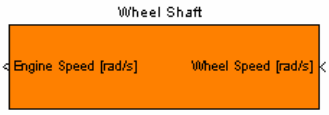

Figure 6.21: Wheel Shaft Subsystem 2

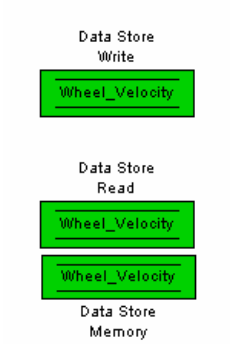

Figure 6.22: Memory Block

6.2.3.2 Lateral Model

In following section the lateral dynamics system (only FWD one) in Matlab/Simulink environment will be illustrated.

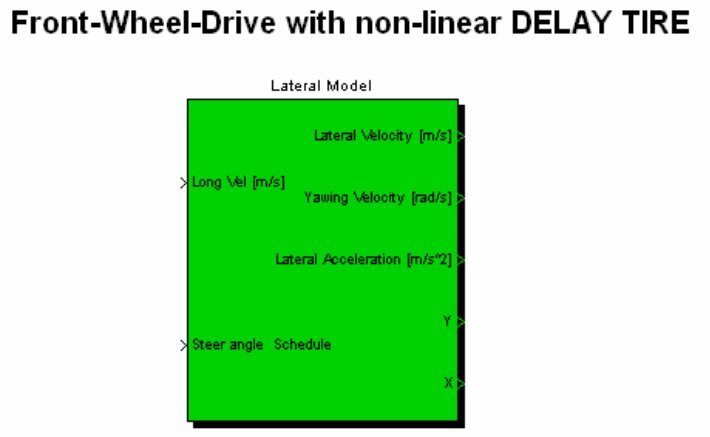

Figure 6.23: FWD Lateral Model Block

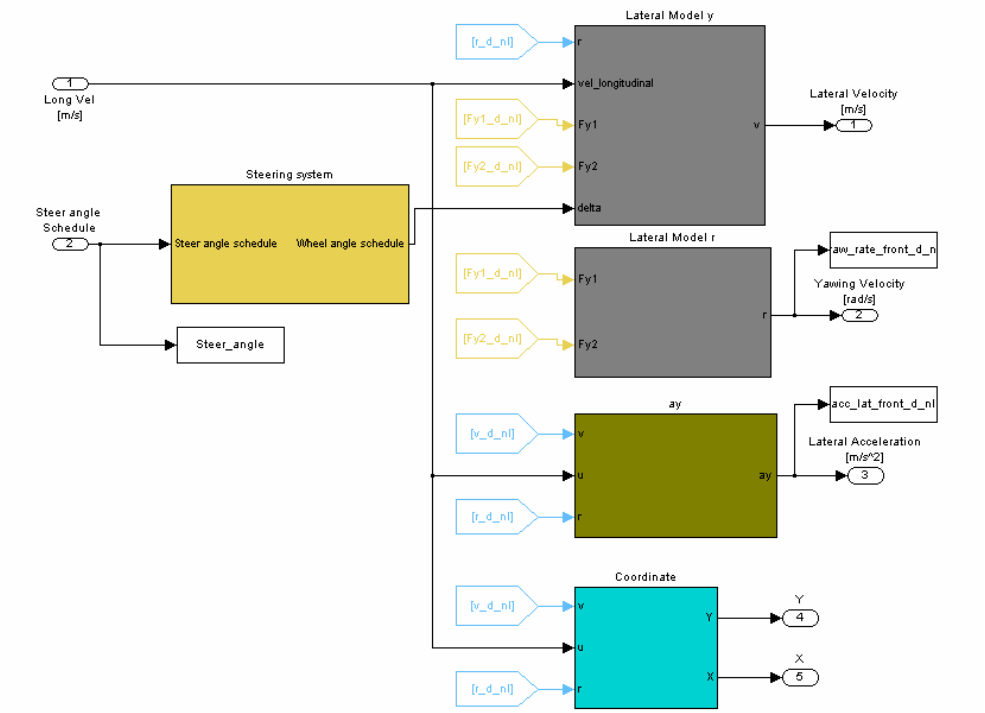

Figure 6.24: FWD Lateral Model Subsystem Block

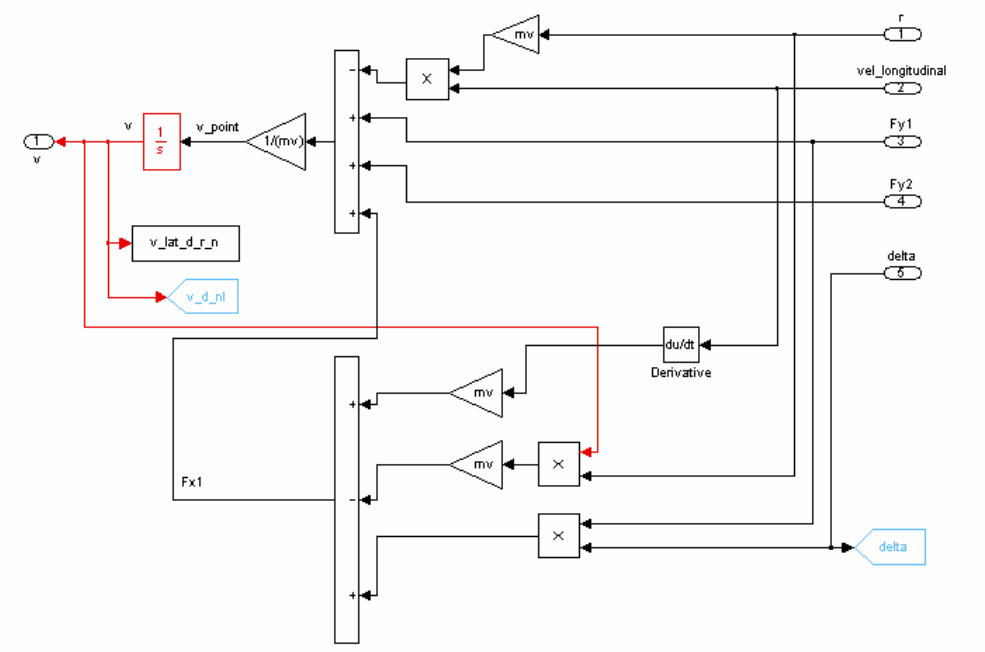

Figure 6.25: Lateral Model y Subsystem Block

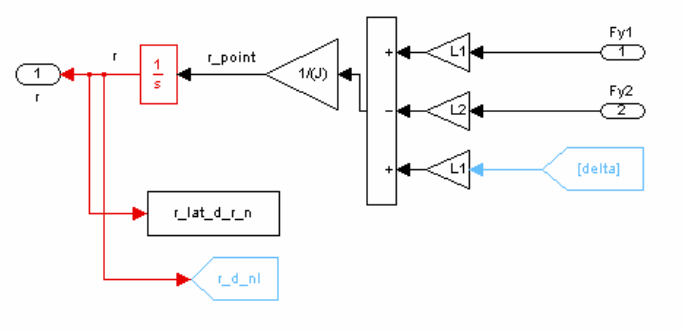

Figure 6.26: Lateral Model r Subsystem Block

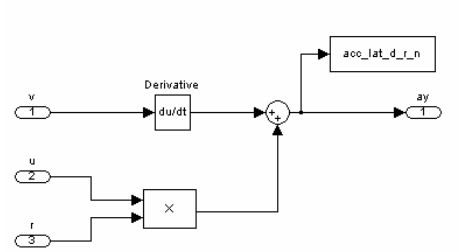

Figure 6.27: Lateral Acceleration Subsystem Block

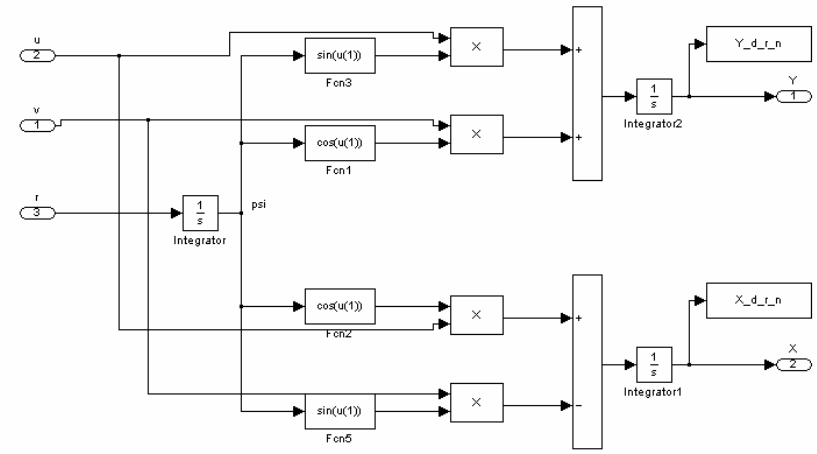

Figure 6.28: Trajectory Subsystem Block

6.2.4 Tyre Model

In order to have more simplicity the tyre model is subdivided into two parts:

- Longitudinal and normal behaviour;
- Lateral behaviour.

Therefore, the blocks are shown separately, dividend the normal and longitudinal forces at the wheels and the lateral ones. One can note that changing the tyre model concerning the lateral behaviour, the longitudinal and normal behaviour does not change.

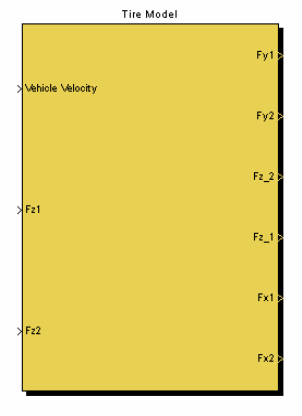

Figure 6.29: Tyre Model.

6.2.4.1 Normal and Longitudinal Behaviour

In the following section, the former one is illustrated; see Figures 6.30, 6.31, 6.32, 6.322, 6.34, and 6.35.

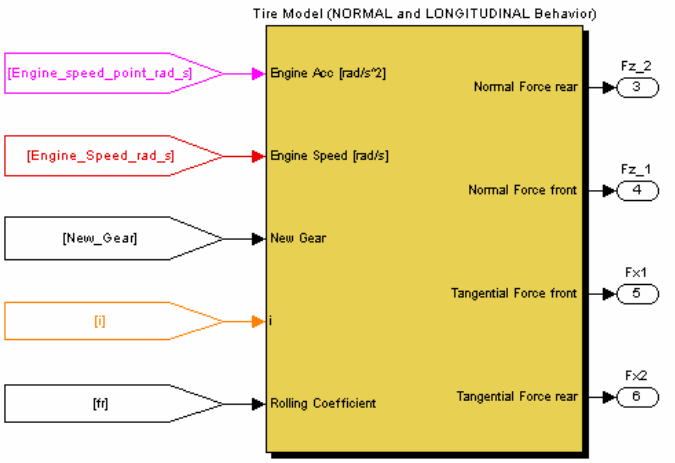

Figure 6.30: Normal and Longitudinal Behaviour (Tyre Model).

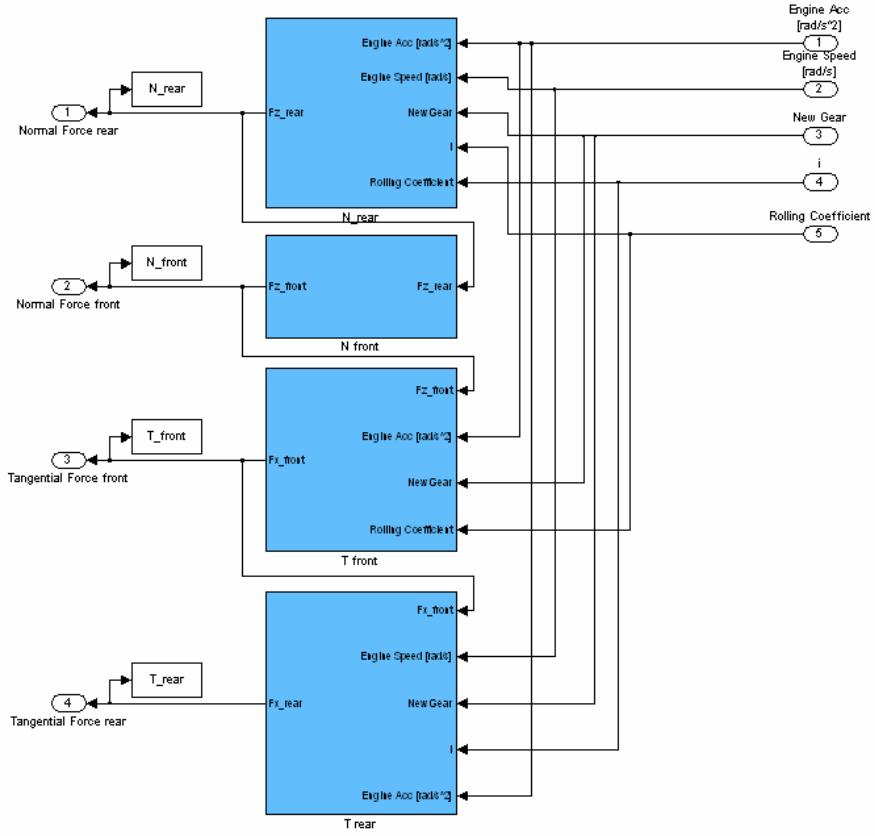

Figure 6.31: Normal and Longitudinal Behaviour Subsystem.

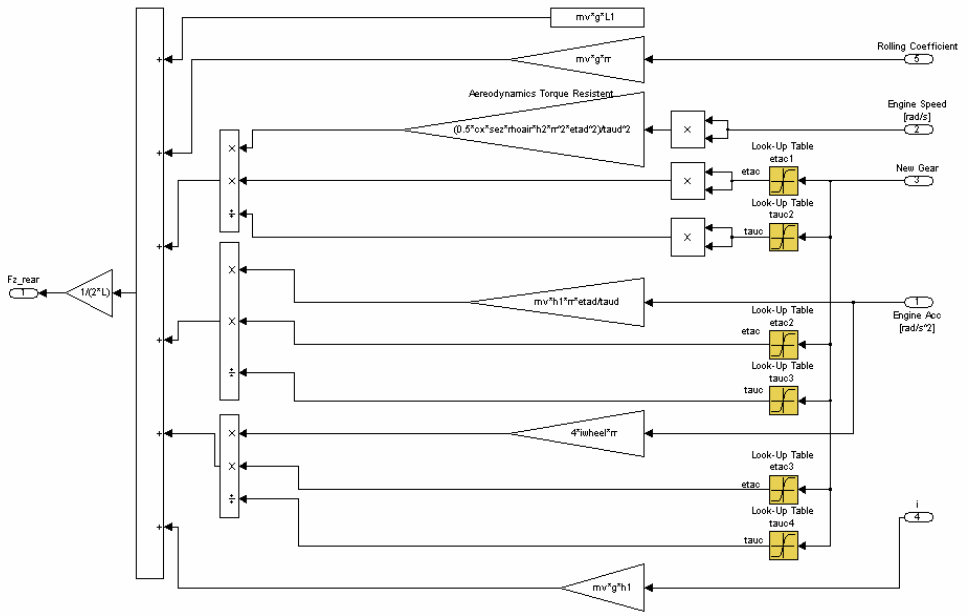

Figure 6.32: Normal rear Force Sub-Model (Tyre Model).

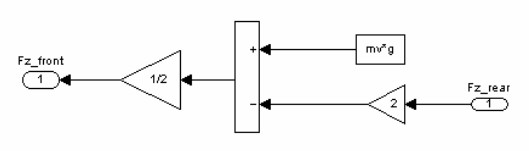

Figure 6.33: Normal front Force Sub-Model (Tyre Model).

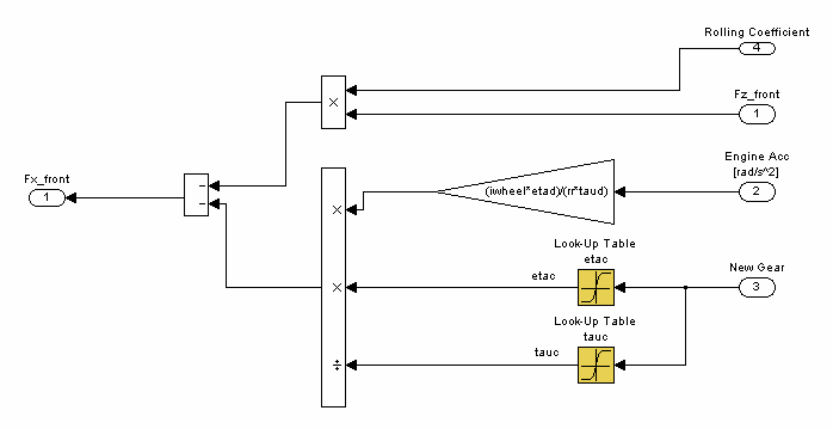

Figure 6.34: Longitudinal front Force Sub-Model (Tyre Model).

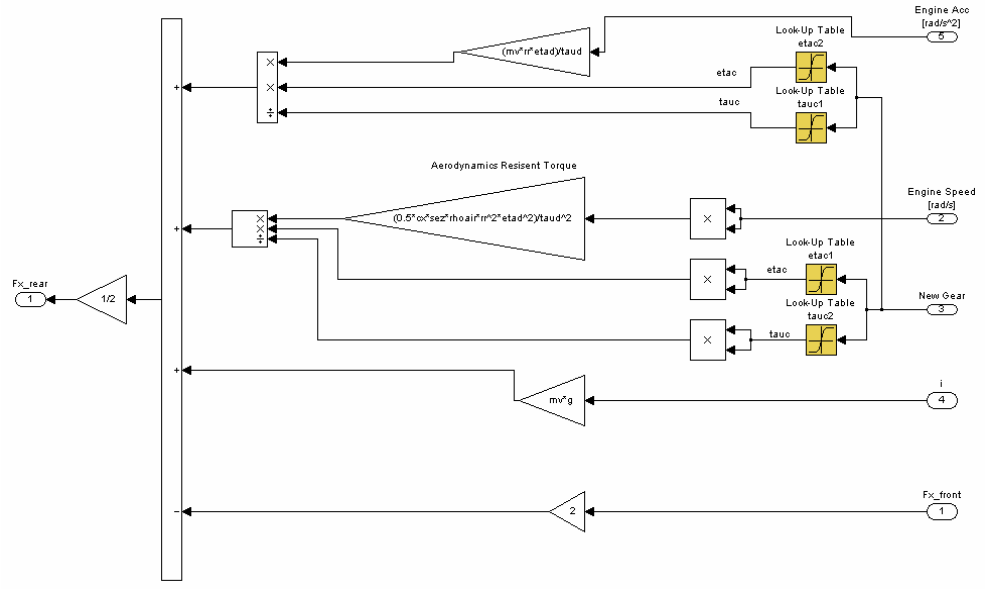

Figure 6.35: Longitudinal rear Force sub-Model (Tyre Model).

6.2.4.2 Lateral Behaviour

In analogy the lateral behaviour is configured as shown in Figures 6.36 and 6.37.

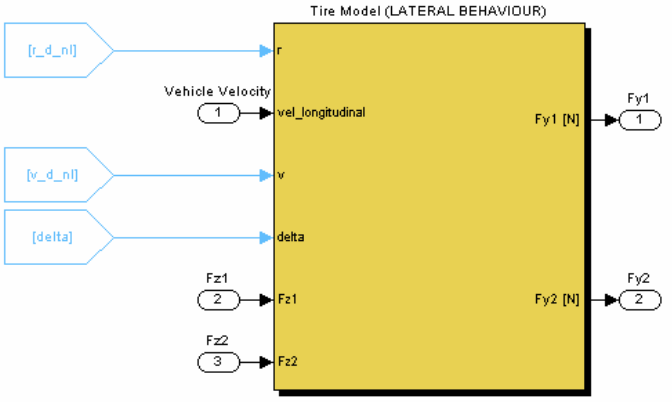

Figure 6.36: Lateral Behaviour (Tyre Model).

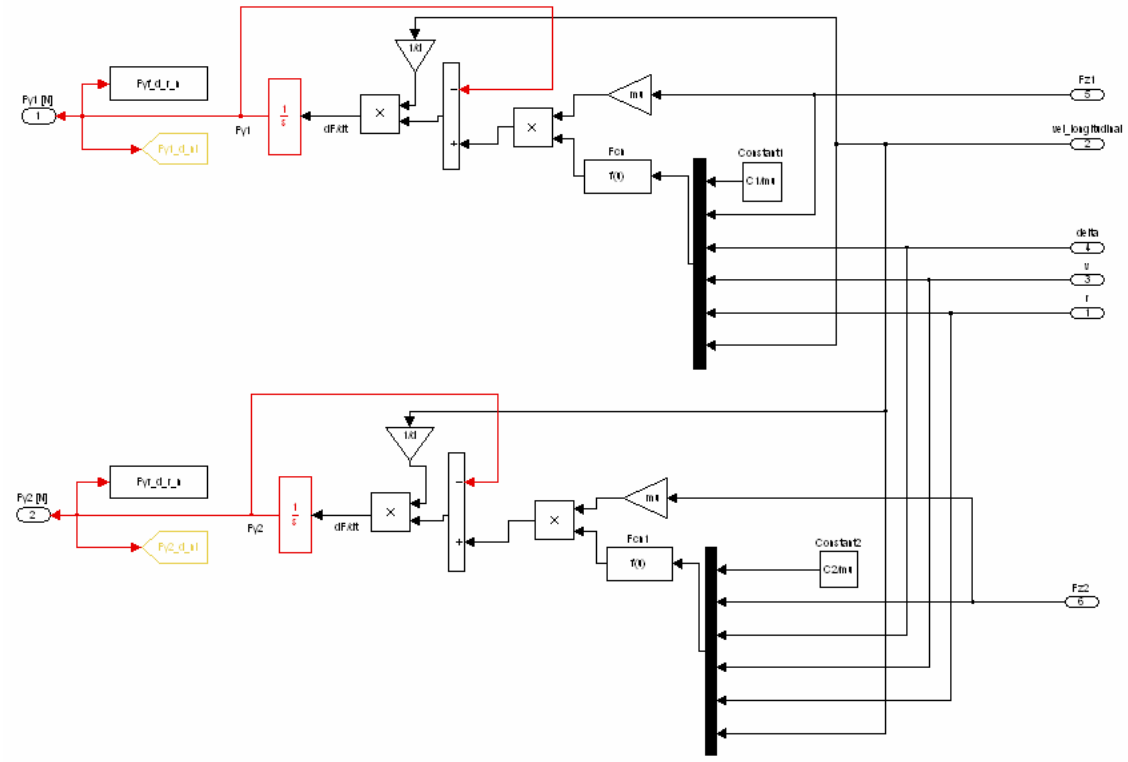

Figure 6.37: Lateral Front and Rear Forces subsystem (Tyre Model).

6.2.5 Real time Simulator Block

The Vehicle Driving Simulator is a simple sub-model implemented in the Driver-Block. It is only an "physical" interface between the human driver and the vehicle complete model.

From now on the VDS block was running on a 1.39 GHz AMD Atlon-based computer while the driving scene was presented on a 15-inch monitor. A more powerful computer could be useful in order to simulate the behaviour of the model not in “real time”, without delays due to the complete integration of the mathematical equations.
The physical configuration of the simulator consist of:

- Seat
- Steer system
- Monitor
- Accelerator and brake pedal (the latter is not used)

The whole elements, shown in Figure 6.37, such as the steer and accelerator pedal have been added to the PC to reproduced with startling realism the physical environment of a typical vehicle.
The VDS simulator software is configured to represent the control/response characteristics typical of a real vehicle. In fact, step for step the differential equations of motion were integrating.
Obviously, the graphical aspect was take into account. The vehicle was represented by a single point and the trajectory was just a single line.
Even so the model represents with good approximation the real system, according to the whole hypothesis made.

Figure 6.38: Elements of the Vehicle Simulator

The bock used to link the human driver to the Simulink/Matlab model is a Virtual Reality Toolbox, as shown in Figure 6.38.

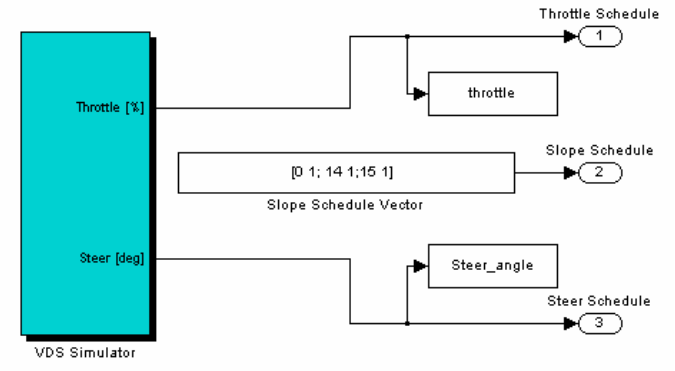

Figure 6.39: VDS Simulator block

Chapter 7

7 Validation of the Vehicle Model

Once the model is constructed it must be verified with as much information from the real system as possible. This process is known as "*validation*". The most common method to evaluate the reaction of the model to measured data and compare it with actual values. For this reason, this chapter begins with our approach to the validation of the model and all connected problems concerning the measure errors. In the foregoing chapters, we used a simplified mathematical model of the complete vehicle to develop some basic concepts, and then we conclude with test results on real vehicles.

7.1 The Simulation of the Systems

The simulation is a method used to verify a model which represents the behaviour of a physical system. Therefore, a validation phase is required, during which the results of the model will come compared with the experimental data.

As described into Chapter 2, the simulators are much utilized in all industrial fields such as aero spatial, aeronautic, motor and many others, in order to understand the physical behaviour of a system. In some applications user is constrained to work with a simulator model, because there is no other way to study the phenomenon, such as the evolution of the universe, the meteorological and seismic ones.

The results obtained by the simulations, such as the tendency of the variables, can be visualized graphically, by animation software (2D or 3D), in order to represents the evolution of the system during the time.

7.2 Validation Procedure

The construction of a model often involves many simplifications through which the outputs of the model deviate to a greater or lesser extent from the real values. Before proceeding to the real validation, some responses could be interesting, to understand completely the following development:

- Do the model outputs correspond well enough to the measured data?
- Is the model suitable for the purpose for which it was constructed?

The more data are available from the real system, the better the above questions can be responded. A model can in general be considered validated when, following evaluation with suitable validation data, it satisfies the requirements for which it was constructed.
Before the validation, one must clearly know which purpose the model is to be put to, which outputs must be precisely modeled, and where certain errors can be accepted. Once the model will result “true” we will be arrived to the last stage of the modelling. Opposite a cut-off stage for the model will be required.
Generally, the principle of validation of the model consists to compare the output variables of the model with the estimations measured experimentally. Initially, to do this, it is necessary to fix rich input variables and so to realize a test protocol. The principal aim of the test execution is the acquisition of the data, which will come used to validate the model.
Some sensors will have to fix on the working system in order to measure the physical variables. These variables will be subject to measurement errors and, for this reason, it will be necessary an arrangement stage.

7.2.1 Definition of a Test Protocol

To realize the validation of a model, the choice about the working signal is very important. It is necessary that these signals should have much information in order to

investigate on a large functioning field of the vehicle. For this reason, the working signal must be continuous. Generally, the ideal signal to validate all the models is the *white noise*.

Unluckily, this kind of signal often is not available. The binary signal which has similar characteristics to the white noise is available. This kind of signal is a deterministic one with a rich frequency band.

The different signals used will have to allow the validation of the model in all working regimes, transient or steady-state. The choice about the working signals influence the tests made. The definition of the test protocol is very important to validate the mathematical model. It allows realizing the suitable tests that we have to analyze.

In the literature many norms (ISO), [30, 31, 32, 33, 34, 35, 36] are available for different applications. In the section 7.2.5, the discussion about the tests used for our application will be shown.

The description of the norms ISO presents a particular structure constituted by different specifications:

- Application data;
- Instrumentation (standard or special);
- Installation of the sensors;
- Tests conditions;
- Analysis and presentation of the tests.

All this information will have to be planned during the time, in order to understand what we have to do before, during and after the tests. The basis notions, which have to be respectful, are described in the theory about the experience plane [37, 38].

7.2.2 Data Acquisition. Measures

Before making all the tests, one should question oneself about the variables to be measured for the current application. Obviously, the choice about the measure variables influences the typology of the mechanical sensors, but the latter are only a link of the complete measure chain, as shown in Figure 7.1.

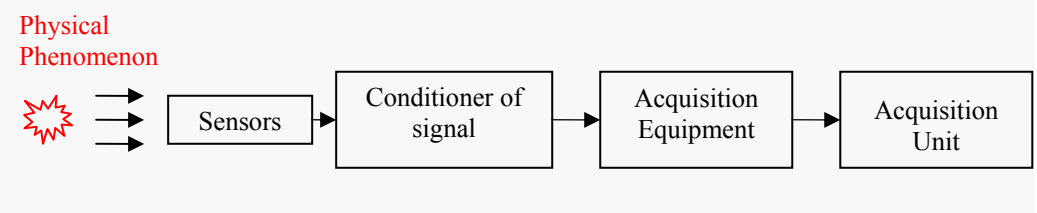

Figure 7.1: Measure Chain.

According to the section 7.2.8, all the measures will have some errors. These will be a different nature: typical errors of the measure chain, errors links with the noises, and many others.

7.2.3 Elements of the Measure Chain

The *sensors* are the first link of the measure chain. The principal role of a sensor is to translate a physical quantity into another one, generally electrical, and directly proportional to the quantity measured.

Currently, many sensors exist according to various industrial applications [39, 40, 41, 42]. We will relate in the sections 7.2.4 and 7.2.5 to the sensors required for our application. Principally, this application will regard the acceleration sensor, linear velocity, angular velocity (girometers), and the angular displacement.

Continuing along the acquisition chain we find an electronic instrument, called *Conditioner of signal*. This instrument is always present each time we have a sensor and for each one. They will serve us as a linkage between the sensor block and the next block. Among many functions which this instrument has, the most important is the amplification of the signal, the linearization of the sensor into its functioning field, the isolation of the sensor away from the measure chain, the filtering signal, and the alimentation of the sensors eventually.

Actually, the measure chains most used, and those used in our application, is numerical type. These work on acquisition unit, equipped with schedules able to measure all the electrical quantities. These particular schedules guarantee the amplification of the signal, the arrangement about the input and output quantity, the sampling, and the conversion analogical/numeric of the measure.

The *acquisition unit* serves to manipulate all the measure chain from a PC in order to store the acquired data on a memory support. Finally, the software is able to pilot the acquisition chain according with specified rules. The last element of the measure chain is the connection between the different elements with the cables. This aspect is very important because it could verify same disturbances on account of interferences.
Today the multiplication technique is used frequently. This kind of connection is able to link many blocks with only one common cable. Particularly, for this application the CAN control Area Network has been used. In this way the wiring is reduced to the minimum.

7.2.4 Tests and Measurements

To validate a mathematical model, an experimental stage is required in order to evaluate all variables. Therefore, these will have to be compared with the estimates of our model. In our case, some tests on a track have been performed with a suitably-equipped test vehicle.
Previously, we needed to decide the necessary instruments, such as the sensors, the acquisition system and all the components for the measure chain.First, for a good validation of our models, we need to choose correct practice signals to supply the large functioning of the vehicle. Therefore, we are required to define a *test protocol* which explains the dynamic manoeuvreing in terms of external conditions and other factors. Finally, the results obtained will be manipulated to develop their own meaning.

7.2.5 Instrumentation of Vehicle

To study the dynamics problems, shown in previous chapters, it was decided to use, like the test vehicle, Renault Mégane Coupé 16V 150 hp equipped with different sensors and an acquisition system AUTOBOX; see Figure 7.2.
To validate the mathematical model, tests on a track have been performed with a suitably-equipped test vehicle. Thus, prior to this study, the necessary instrumentation as well as the acquisition system had to be defined. A particular study on the excitation

signals was carried out to allow them to excite a very wide frequency band of the vehicle (including critical driving situations).

Figure 7.2: Instrumentation of the Test Vehicle

Distant from the centre of gravity there are two "accelerometers" which are able to measure the longitudinal and transversal acceleration. This kind of sensor works with "piezoresistivity" propriety. The rotational speed about the vertical spin axis of the vehicle, *z*-axis (yaw rate), Figure 7.3 (a), was measured with a "gyrometer". The steering angle is measured by a "potentiometer"; see Figure 7.3 (b).

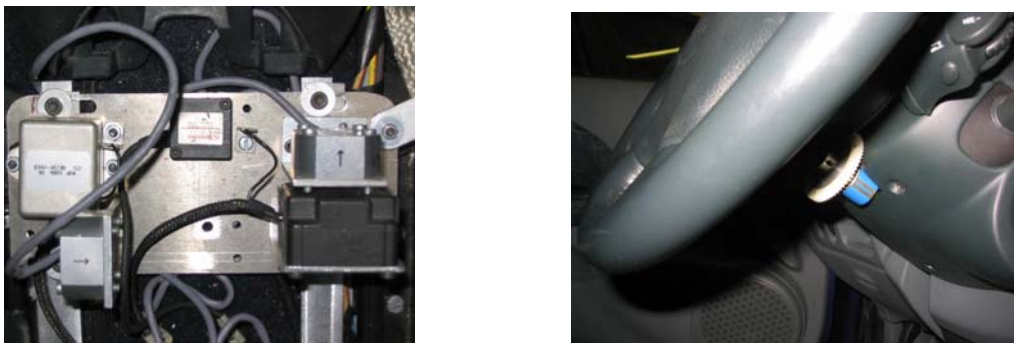

(a) **(b)**

Figure 7.3: Instrumentation of the Test Vehicle

The longitudinal and transversal speeds are measured by an optical intermediate sensor DATRON; see again Figure 7.2. This last instrument is very expensive, costing just under ten thousand euros for one. An interesting alternative instrument for using this model [42] is based on artificial intelligence techniques working through Fuzzy Logic.

7.2.6 Definition of Tests

In order to carry out validation, test drives were carried out with an experimental vehicle, and the following variables recorded:

Model input variables		**Model output variables**	
α	Throttle opening	u	longitudinal velocity
δ	Steering angle	a_x	acceleration in x-direction
		a_y	acceleration in y-direction
		r	yaw rate

Table 7.1: Inputs and Outputs of the Validation Model

The validation model calculates, from the inputs α and δ, the outputs u, a_x, a_y, and r, so that a direct comparison can be carried out between the model and experimental data. Thus, in order to describe the functioning of the vehicle, two tests have been executed. These tests include the principal driving characteristics which could show the mean critical conditions.

In normal driving conditions, it is possible to take in account the easier tyre model known, linear one. There are many tests which are able to investigate the behaviour of the vehicle, [30, 31, 32, 33, 34, 35, 36]. For example, the braking test is able to study the longitudinal behaviour.

Instead, the manoeuvres about angular dynamics can show the principal characteristic of the transversal behaviour, the braking test in band will be able to study the lateral behaviour in transient conditions. Last, the sinusoidal test can be able to study the response for frequency of the vehicle model.

7.2.7 Circuit Test

According to Figure 7.3, two kind of experimental tests have been performed. Precisely, these tests regard the bands 3 and 7. Referring to the track, clockwise sense, the second

curve had run with higher velocity in owing to its radius of curvature which was smaller. Opposite means for the 7th band, that its excessive bend limits the fast manoeuvreing. As well, the faster is characterized by an high deceleration.

7.2.8 Handling of Data

The acquisition data which comes from the experimental tests can not be utilized directly. In fact, it is necessary to choose the frequency of measures sampling, in this case it is 50 Hz. This frequency corresponds to the same one utilized by the acquisition system which works on the test vehicle (Dspace/RT-LAB). In this way, the frequencies of the system can be held.

Every acquisition system has tabulation in order to store the data. Once known these latter we need to traduce this information in order to utilize it in our ambient work (Matlab/Simulink). However, all the measurements are suffering from a lot of noises, such as vibrations due to the motion of the vehicle, and noises due to mechanical origin (rigid parts moving), and finally electrical noises which disturb the acquisition field.

For all these reasons a specific filter can be used. A good arrangement to improve the ratio signal/noises can be obtained with a filtering of 10 Hz by a third order Low-Pass filter.

Opposite, another kind of noise could be a malfunctioning of the instruments, of the acquisition system, such as slip and setting.

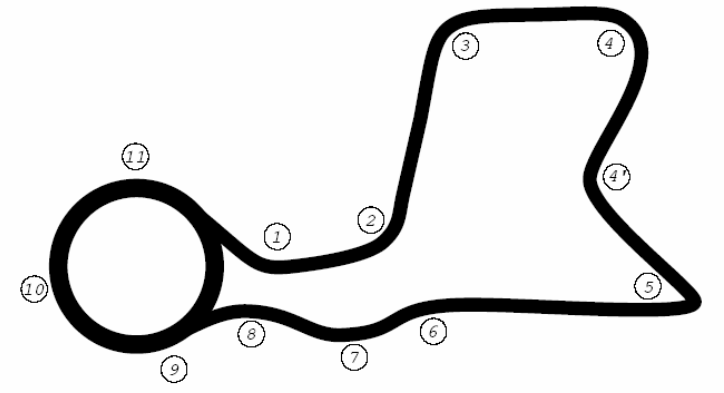

Figure 7.4: Track used to Perform the Experimental Tests

Finally, all the measure chain can be exposed to many perturbations. Meanly, these perturbations can be summarized in the following factors:

- No accuracy during the assembly and balancing of the sensors;
- DATRON sensor can be equipped in wrong way because its specifications do not give exactly the working limit, such as the time response and many other factors.

During the validation tests, some measurement problems have been presented, such as problem af estimation for the velocity sensor (DATRON) and problem to initialize the files while the acquisition system was beginning.

Some checks can be made to set completely all the sensor. For example, for the accelerometer varying around ±90° and so verifying that the measure corresponds with the acceleration of gravity. For the sensor to be able to measure the steering angle, it is possible to make a completely round about its spin axis in order to verify if the measure is equal to 2π rad.

The next step, before comparing the experimental data and the simulation results, is to rearrange the values assumed by the variable. Two filter-values for the throttle opening have been made. First, according to the values bigger than full opening and the second about values smaller than zero.

Into the following sentences it will be reported the cycles (Matlab/Simulink) used to clean the final vectors before the validation graphs, where the letter *T* means throttle opening [%].

Filter 1	Filter 2
`% Control about values bigger than 100%`	`% Control about values negative.`

`for x=1:length(T_tot),`
`  if T_tot(x)>100`
`  disp('Filter 1')`
`  T_tot(x)=100;`
`  end`
`end`
	`for x=1:length(T_tot),`
	`  if T_tot(x)<0`
	`  disp('Filter 2')`
	`  T_tot(x)=0;`
	`  end`
	`end`

Table 2: Filters for the Handling Data

7.2.9 Analysis of the Results

In the following section, many graphs, Figure 7.5 to 7.24, will illustrate the comparison of the experimental data and the simulation data. That means all the following diagrams will show some differences between the data measured by the sensors and the results of the mathematical model. The latter includes the front and rear wheel drive (FWD-RWD). One may note that the FWD model presents lots resolution difficulty that the rear one. Particularly, as illustrated FWD with non-linear tyre model is 8 D.O.F. because the lateral forces depend by the load transfer, so to obtain the dynamic solution it is required solving all the blocks model. The front traction has more interaction with the longitudinal model than the rear model, which contains only the velocity longitudinal as linkage.

Therefore, the simulated with FWD model in the 3^{th} and 7^{th} turn is illustrated, Figures 7.5, 7.6, 7.7, 7.8, 7.9, and 7.10.

First, the simulations carried out in the 3^{th} curve are characterized by discordance in terms of velocity. In fact, this comes from a transient problem. During the first part of the throttle opening curve, it is possible to note a physical discordance between the throttle opening and the longitudinal velocity. In fact, the velocity signal measured by the sensor was different from that simulated; physically, this happens because the vehicle had its velocity, due to the inertia forces. The theoretical model cannot reproduce this phenomenon; therefore, in corresponding to a throttle opening null, there is a velocity smaller than that measured. The incongruence could be annulled operating a set up on the velocity of vehicle that means to begin to store data from a steady state of the speed and so operate the tests manoeuvres.

The second difference could come from an oscillating measure of the longitudinal acceleration which is, obviously, particularly stable in the model. In fact, in the model the vibration noises are neglected.

Moreover, some differences, concerning the evaluation of inertia in the lateral model, can be visualized. It is very clear for the non-linear tyre model because it is not able to reproduce very well the real behaviour of the automobile. For this reason more concordance could be obtained with the Pacejka model.

In 7th curve, according to the problem concerning the transient problem, shown in the former sentence, the corresponding between the experimental data and simulation results is sufficiently good. Only one problem is discovered, concerning the lateral behaviour. In fact, while the steering angle presents a decreasing trend, in corresponding of the time step 148, 232 and 403 seconds, the yaw rate and the lateral acceleration do not have the same behaviour. Physically, this incongruence could come from imperfect measurements. Taking care to the simulations 2, 3 and 5, there is not a good accordance of the yawing rate for the fixed steering angle. In fact, there is a simple delay in terms of the response. Probably, because the flexibility of the body is always present in realty. Opposite in the model, hypnotizing the vehicle as a rigid body, the response in transversal terms is instantaneous.

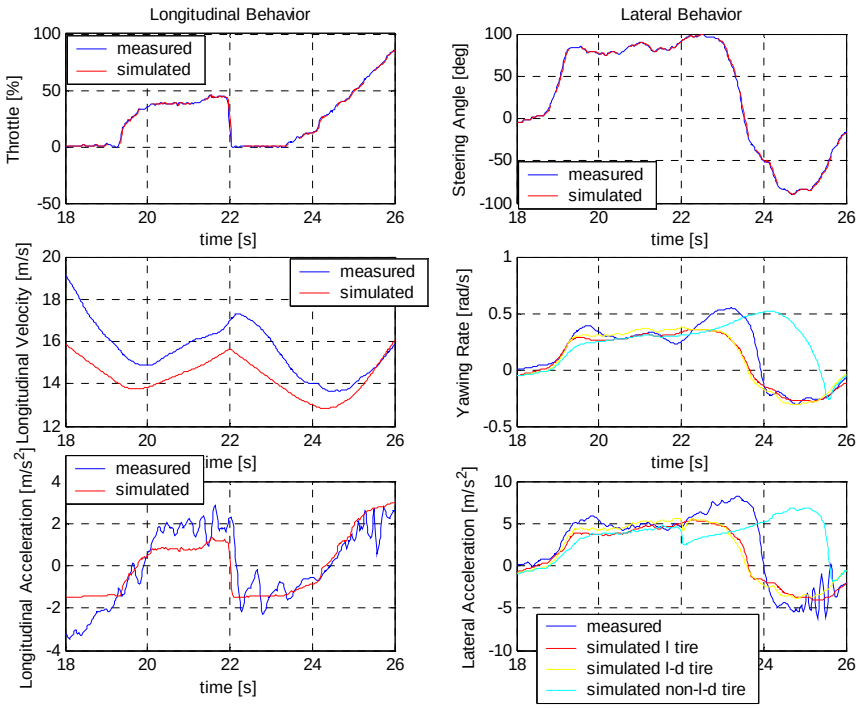

Figure 7.5: Experimental Test-Curve 3 Sim1, Simulated FWD.

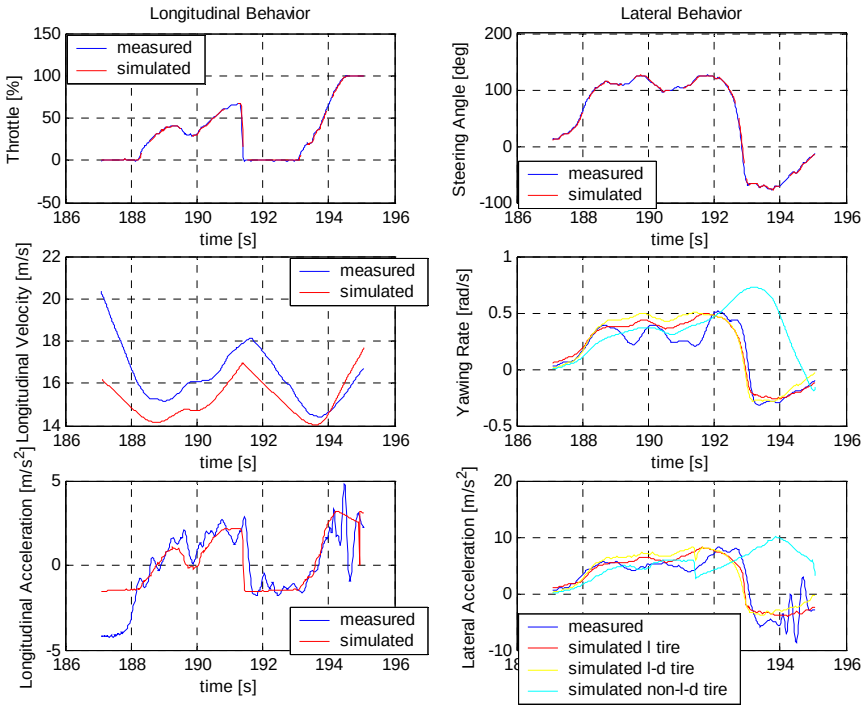

Figure 7.6: Experimental Test-Curve 3 Sim2, Simulated FWD.

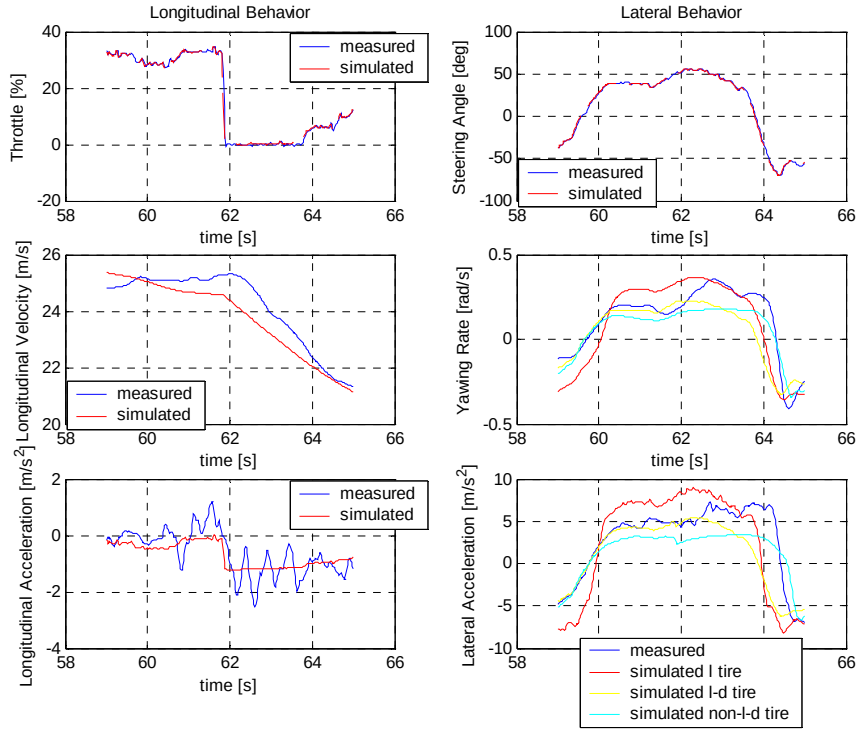

Figure 7.7: Experimental Test-Curve 7 Sim1, Simulated FWD.

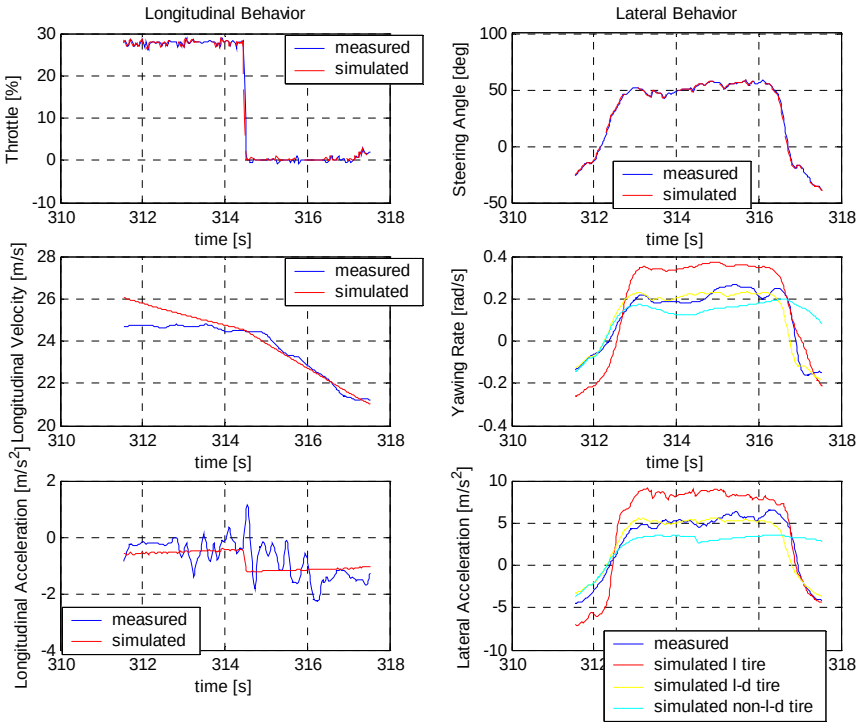

Figure 7.8: Experimental Test-Curve 7 Sim2, Simulated FWD.

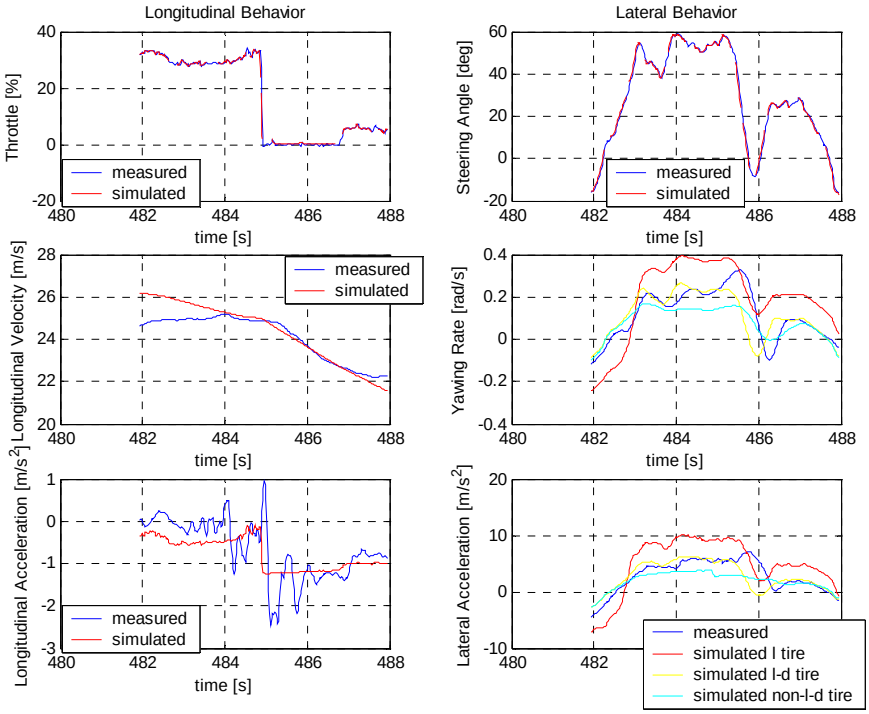

Figure 7.9: Experimental Test-Curve 7 Sim3, Simulated FWD.

In the following section the simulation with RWD model is carried out. One has to note that the longitudinal behaviour is always independent by the lateral one. Opposite is not right. For this reason, even though the lateral model could not reproduce very well the real data, the longitudinal model could have a good accordance.

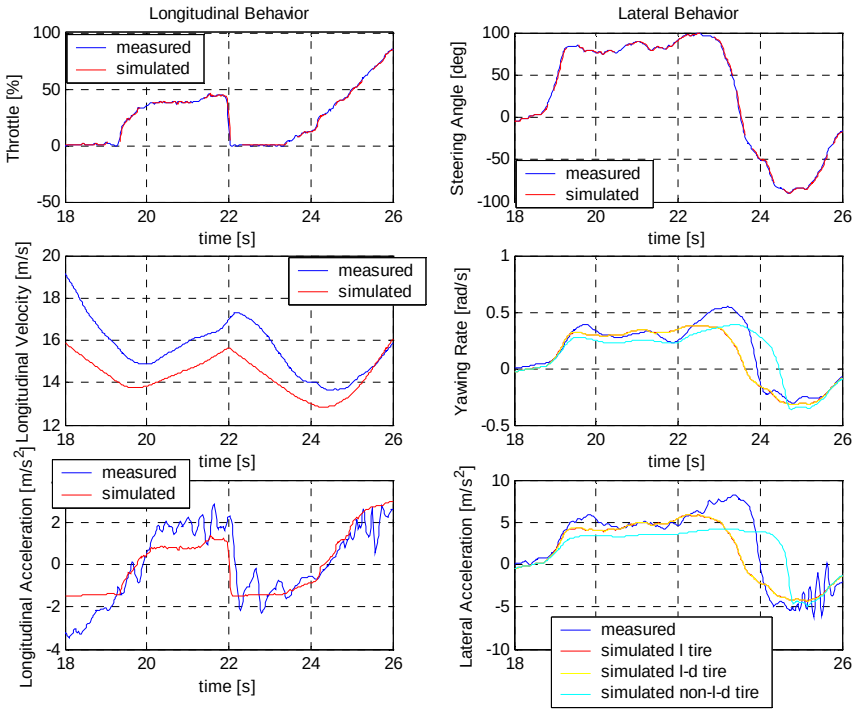

Figure 7.10: Experimental Test-Curve 3 Sim1, Simulated RWD.

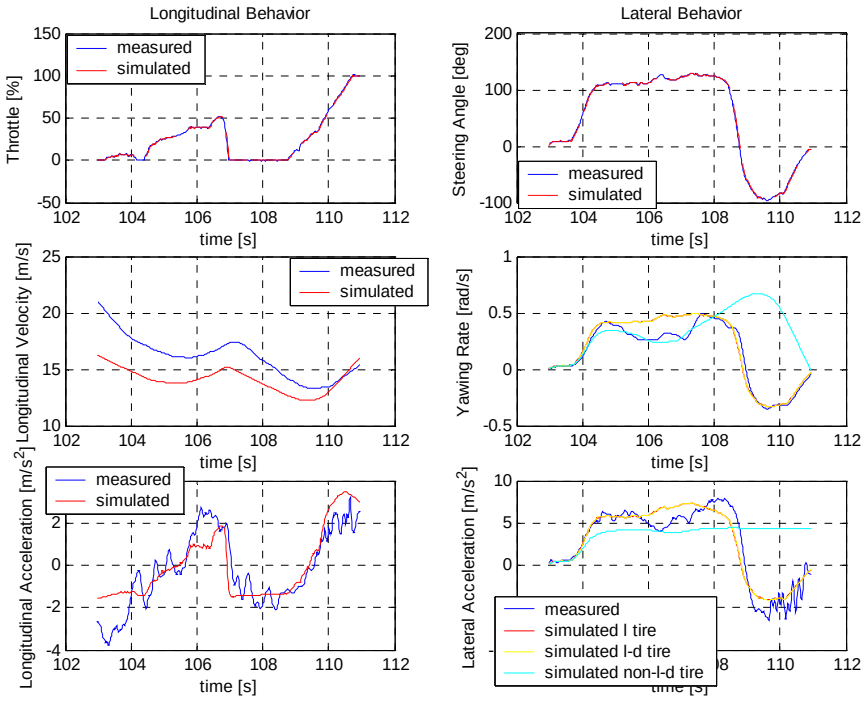

Figure 7.11: Experimental Test-Curve 3 Sim2, Simulated RWD.

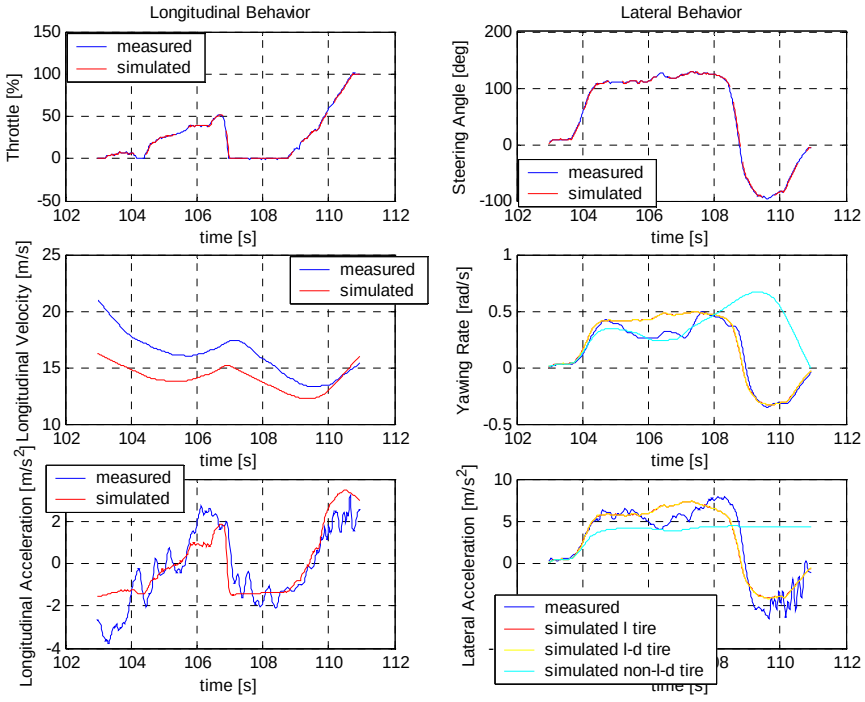

Figure 7.12: Experimental Test-Curve 3 Sim2, Simulated RWD.

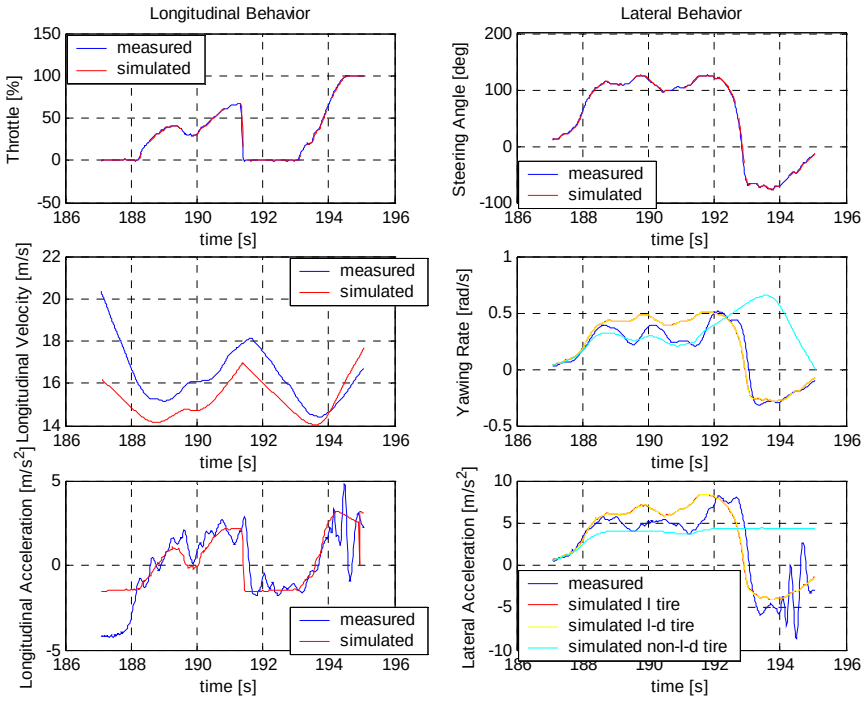

Figure 7.13: Experimental Test-Curve 3 Sim3, Simulated RWD.

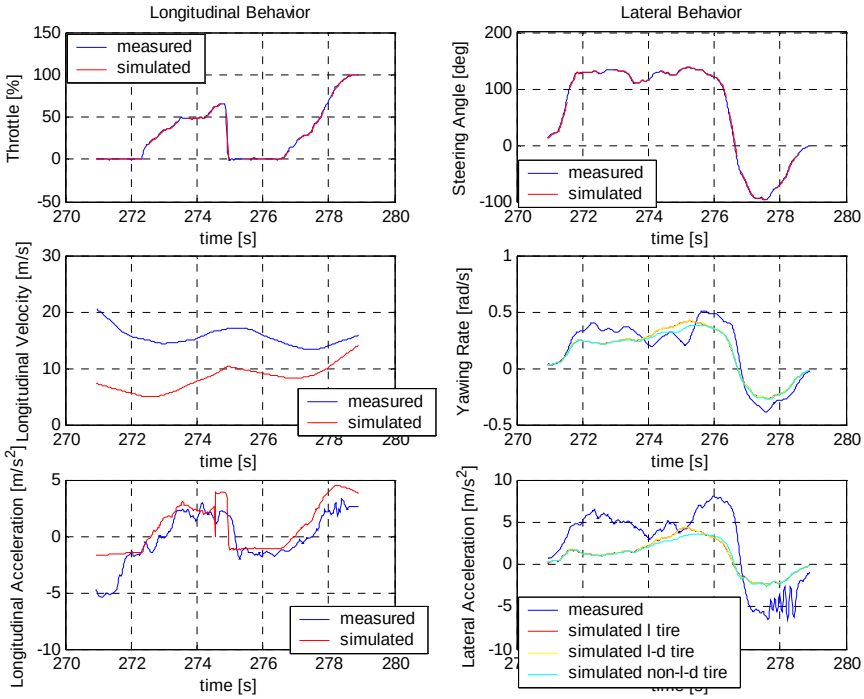

Figure 7.14: Experimental Test-Curve 3 Sim4, Simulated RWD.

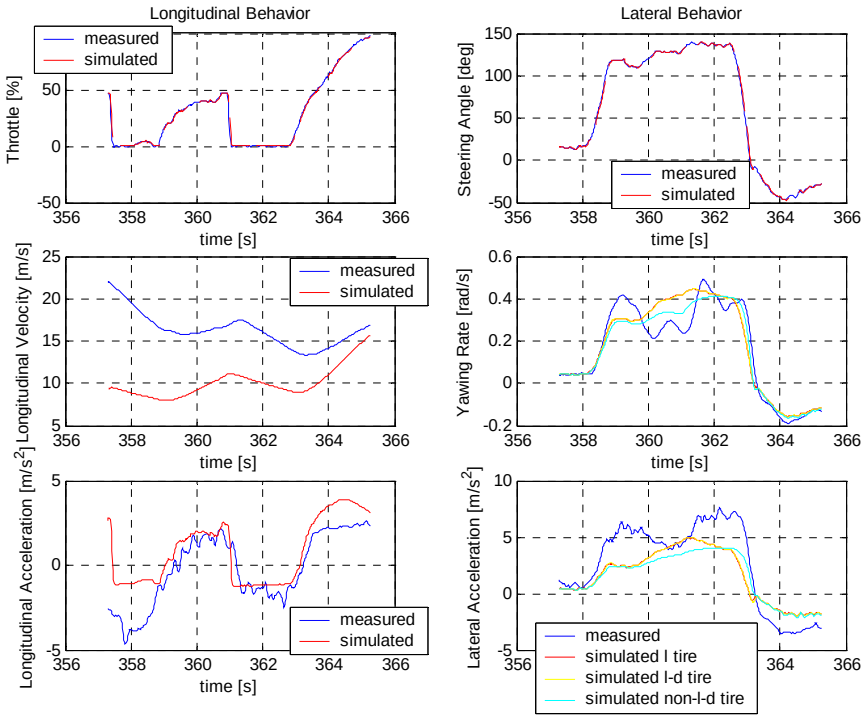

Figure 7.15: Experimental Test-Curve 3 Sim5, Simulated RWD.

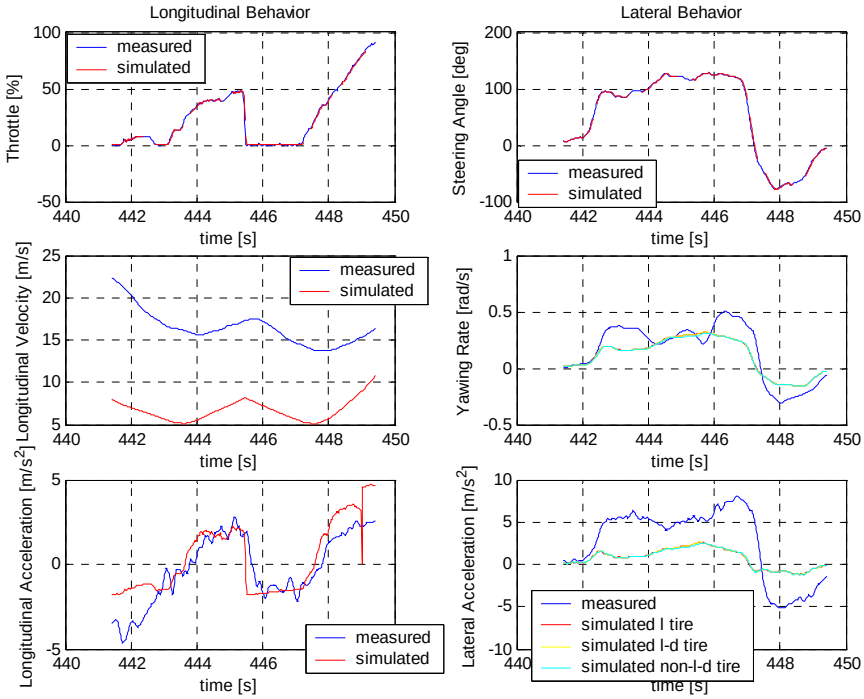

Figure 7.16: Experimental Test-Curve 3 Sim6, Simulated RWD.

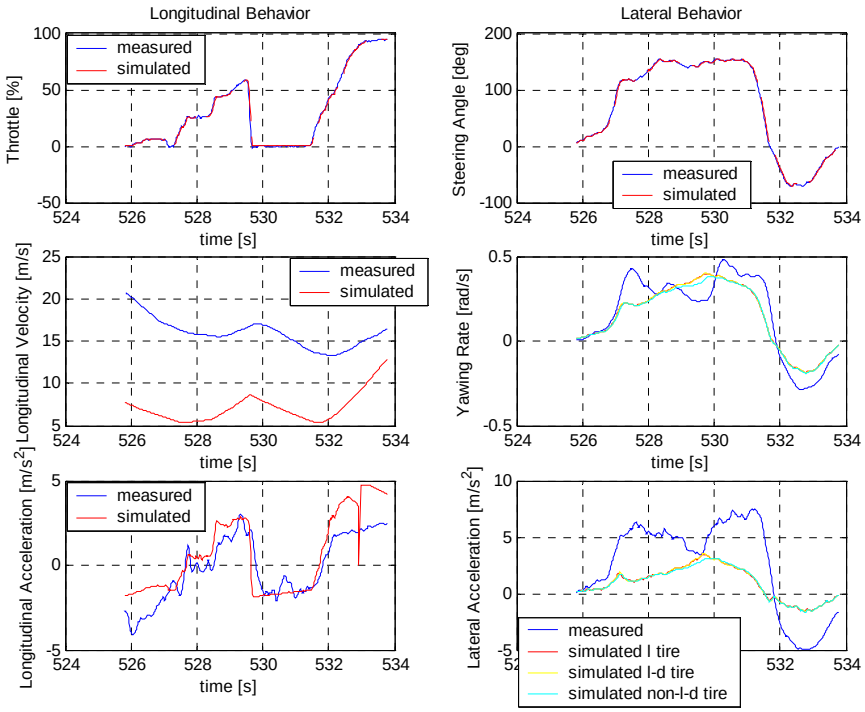

Figure 7.17: Experimental Test-Curve 3 Sim7, Simulated RWD.

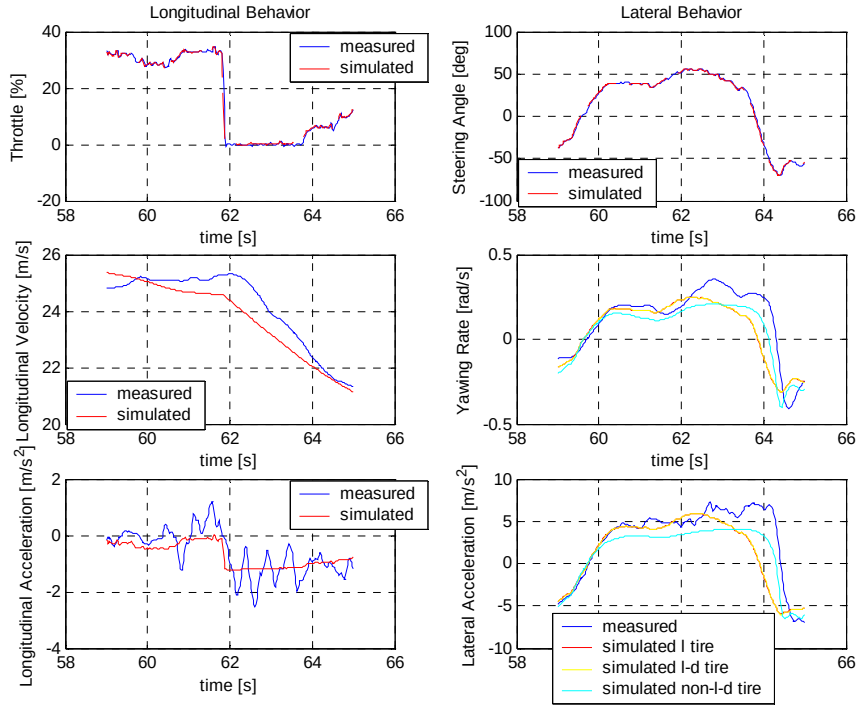

Figure 7.18: Experimental Test-Curve 7 Sim1, Simulated RWD.

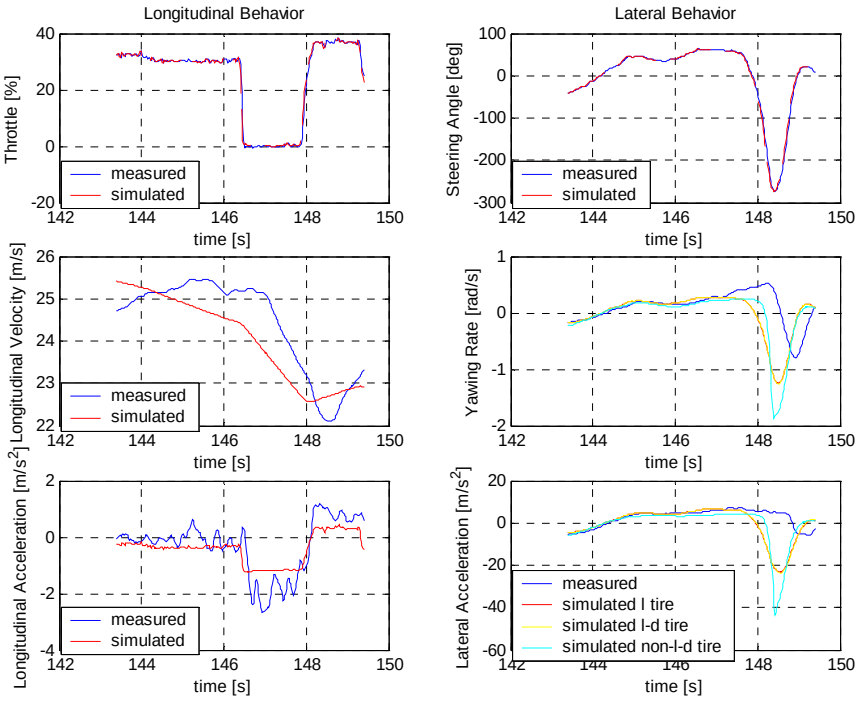

Figure 7.19: Experimental Test-Curve 7 Sim2, Simulated RWD.

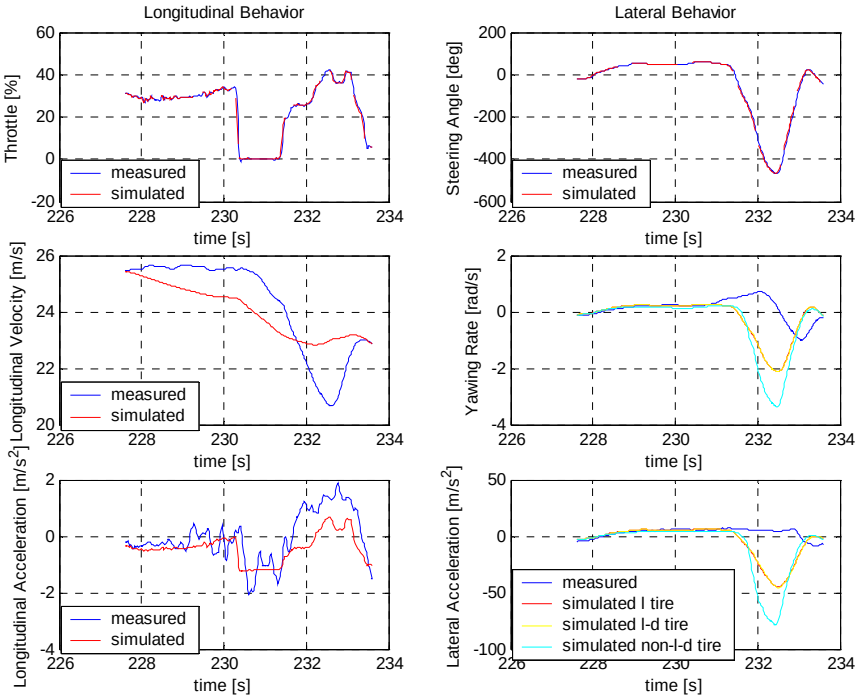

Figure 7.20: Experimental Test-Curve 7 Sim3, Simulated RWD.

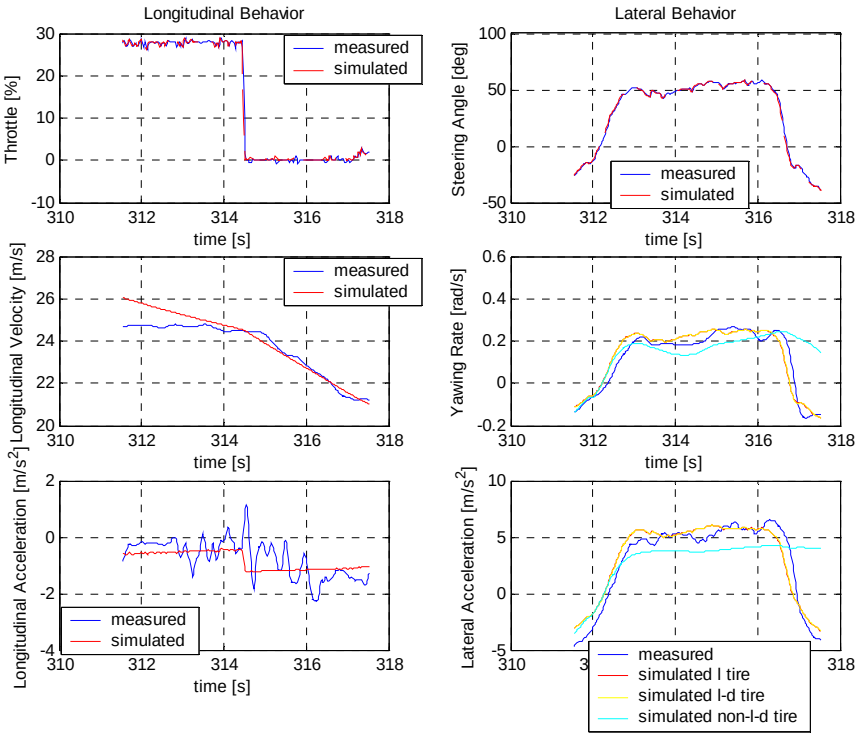

Figure 7.21: Experimental Test-Curve 7 Sim4, Simulated RWD.

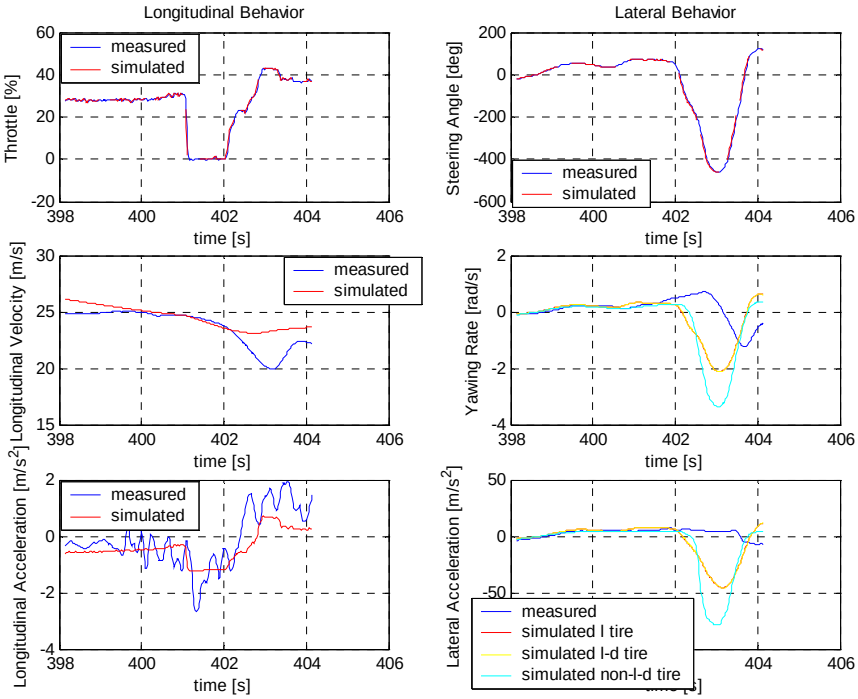

Figure 7.22: Experimental Test-Curve 7 Sim5, Simulated RWD.

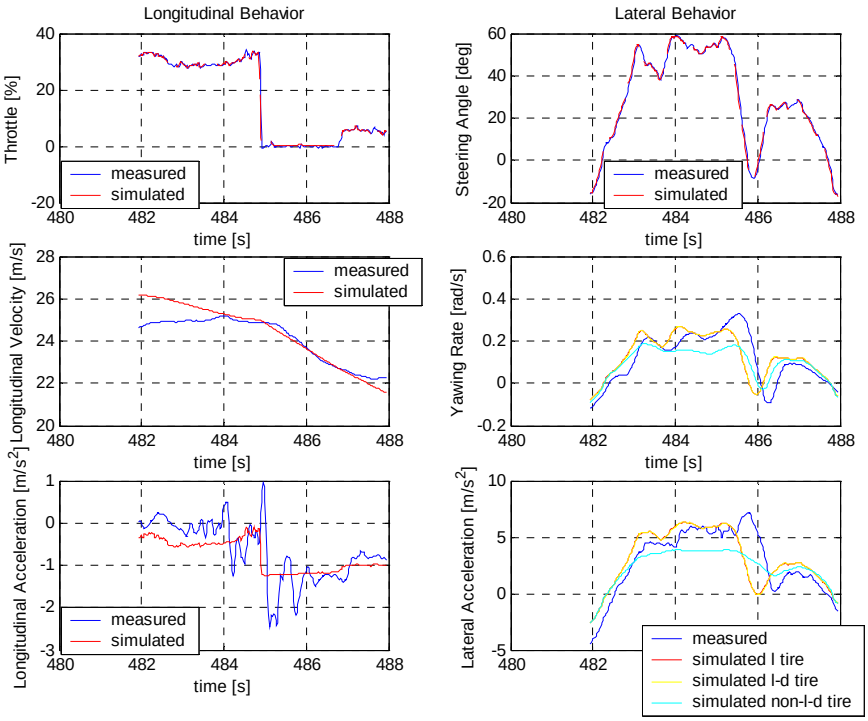

Figure 7.23: Experimental Test-Curve 7 Sim6, Simulated RWD.

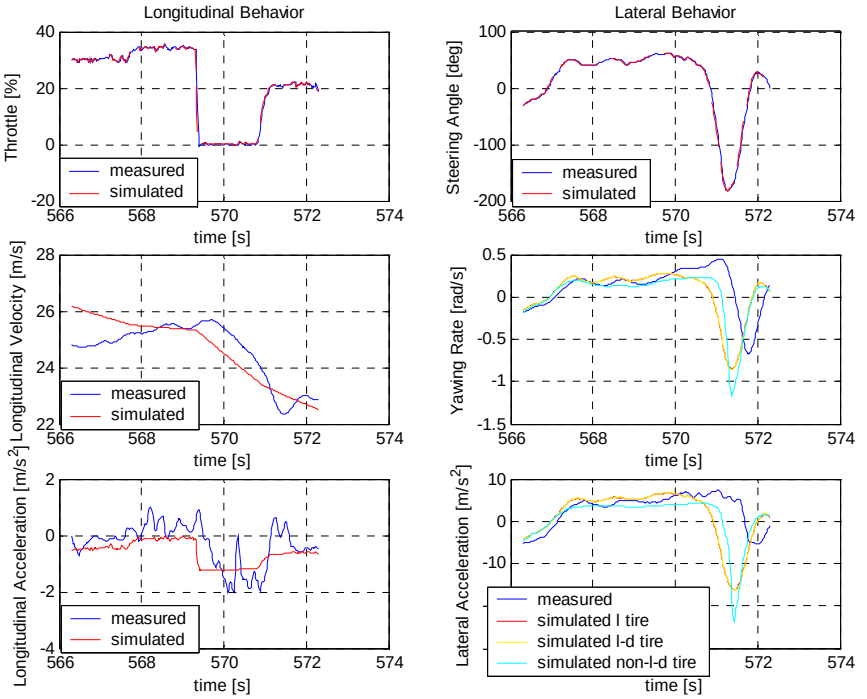

Figure 7.24: Experimental Test-Curve 7 Sim7, Simulated RWD.

Concluding, one can say that the simulated longitudinal dynamics corresponds very well to the measured data. Again the calculated values follow the measured data very well. The longitudinal velocity is also well reproduced.

The noise about the longitudinal acceleration, which according to the measured data is due to some extent dynamics, is simulated in the model as semi-constant value. This could be different if oscillatory phenomena would have considered.

Similarly good results are given for the simulated lateral dynamics which shows only small errors for the acceleration variable

In summary one can say that *with sufficient excitation of the respective dynamics, the longitudinal and lateral dynamics were very well reproduced.*

The simulation model has proved itself suitable for calculation of the relevant drive dynamics variables given steering angle and throttle opening.

Chapter 8

8 Conclusions and Recommendations for Future Research

This work has proposed some foundation of mathematics, analytical methods, and design strategies necessary to describe some characteristics of an automobile, so exploitable for any application. Although the mathematics and simulations presented herein can prove an useful intuitive understanding of generalized performance and control characteristics of the vehicle. Understanding the nature of what has been done here is essential in any future development of a vehicle simulation, even if a simple modelling has been proposed . Having said this, we can now consider some of the natural spin-offs of this research that must be considered in any future development efforts.

8.1 Conclusion

One of the objectives of this work has been to develop a vehicle model that could be used to predict the dynamics for steering and throttle regulation manoeuvres. The dynamics for the complete vehicle have been presented but with many assumptions. In fact, in this study only a non linear function for the lateral forces at the tyres has been constructed. For all, the principal characteristics of the vehicle dynamics have been performed.

8.1.1 Practical Use

One of the most important aspects of a computational study is its practical usefulness. In other words, how the study can be used by other engineers and researchers. This study can be helpful in many ways. First and foremost, it can be used as a basis for future studies of optimization concepts applied to vehicle dynamics. This study may be referenced to show that optimal paths can be generated by setting up the constrained "*optimization problem*" using the unconstrained optimization algorithm of Matlab, *fmins.*

Further, this research can be used as a preliminary study for the development of a new "*tyre testing procedure*". An accelerated tyre wear test path can be generated using the tyre force maximization optimization routine. Often time, tyre manufacturers want to compare the wear of different tyre constructions. By implementing this concept along with a feedback steering controller, an automated testing procedure can be developed to make tyre wear testing more efficient and accurate. Test vehicles are subjected to automatically follow generated paths using the feedback steering controller, augmenting the ability of the test drivers. Further, automatic testing improves repeatability by consistently maintaining the same vehicle path while different sets of tyres are being tested. As such, simulation such as those presented in this study can be used as a tool to perform comparison tests on different vehicle specifications to determine the effects of changing a certain parameter on the optimal path of the vehicle.

8.1.2 Improvement on Overall Approach

There are two issues that can be improved upon for this research, computation time and model prediction accuracy. It is difficult to improve upon both issues at the same time since they are strictly interrelated. Using a faster processor to perform the optimization simulation, one can use higher degrees-of-freedom models or more accurate integration routines, to increase the prediction accuracy.

A more efficient search algorithm can also be used to make the convergence rate of the simulation faster. Genetics algorithm is a very attractive method to pursue. This method is relative new to the field of engineering. There have been a few studies on using this

method in engineering applications [43]. The concept of genetics algorithm, however, is relatively difficult to understand and even more difficult to implement in the simulation algorithm.

Finally, a way to increase the speed of the simulation is to write the entyre simulation program in Matlab script, C or C++ code. This entails efficiently writing loops, matrix operations, algebraic operations, input/output of files, and other mathematical manipulations in C or C++. Working into only an environment, such as the Matlab/Simulink, the computational time could decrease rapidly. In fact, in our software, mdl-file, we recall during each loop of integration S-function (which are written in m-file). For this reason the process needs more time to converge. Unfortunately, in this way we need also to implement a numeric method to solve the differential equations.

8.2 Future Research

The research presented in this work has convinced us that the single track model is a good option in the choice-design of the ground vehicles. In fact we have seen a part of the dynamic performance, for all it was so quite complicated. We have also shown some of the more significant issues, such as the adherence condition concept, non linear linkage between the variables (such as it happens in the realty).

8.2.1 Optimal Control Methods

In the future an optimization method to vehicle dynamics could be applied to this study, specifically to generate some optimal paths. In this case, the final goal could be to minimize travel time, and to maximize tyre forces. Moreover, a parametric study, could demonstrate the effectiveness of the optimization algorithm. These optimal paths could be generated using optimization routine, such as the unconstrained optimization algorithm of Matlab, *fmins*.

8.2.2 Parallel Processing Computation

To improve the computation speed of the optimization routine, a method such as the parallel processing computation can be used to evaluate the optimization algorithm. This method is consisted of using the UNIX platform workstation to run two processors to evaluate the algorithm. This, however, would require some difficulties to implement the algorithm. This method of computation will increase the speed of obtaining the optimal solution. Furthermore, with an increase in computation speed, more complicated vehicle and tyre models can be used.

8.2.3 Using Different Vehicle and Tyre Models

A further study can be performed to determine the effects of different vehicle and tyre models. For the vehicle model, other degrees of freedom could be included, rolling motion, pitching motion, and suspension effects. Obviously, other important dynamic characteristics, such as the two masses motion have not taken into account. According to before mathematical developments both could be presented and solved, also to perform a three-dimensional vehicle and not plane-motion as we made.

As for the tyre model, a more current model can be used such as the Pacjeka tyre model. This model requires using actual tyre data and fitting it with a form of least square function.

At this time, according to the former, it may be considered another non linear behaviour for the tyre model in the longitudinal direction. However, in this case, the solutions required could be performed only by a numerical methods. Moreover, it should be investigated in terms of ground slip in that direction.

Another focus of future work is experimental validation of the complete model while it is moving on a discontinuous terrain, taking into account the vertical dynamics also. This means taking into account a suspension model in order to have good information about oscillatory phenomena. As known, these come from to common perturbations always present at the wheels.

Lastly, include vehicle dynamic controllers such as traction control and yaw control into the simulation to see the effects of these systems applied to determining an optimal

path. Another very interesting field of work surrounds to continuation of control algorithms for the "*ABS*" concept [44]. In fact, we have suggested the single track model but a double track model may provide distinct advantages in automatic field [45]. The dynamics for the braking manoeuvres have not been presented. However, it could be interesting to include a brake model in order to investigate a braking-test in a turn.

Finally, work must be completed on the physical design of the real vehicle, with all its topics. Many ideas concerning the typical problems of the vehicle have been considered during this research. We hope that sometime in the future, this little model of the ground-vehicle family will intrigue engineers and others to the same extent as it made with the author. We believe it has already made a good start.

Appendix A

```
%=========================================================
% Vehicle_Dynamics_data m-file
% Vehicle: Renault Mégane Coupé 16V 150 HP
% input: Gas data, Vehicle data
% output: Engine Map
%=========================================================

%=========================================================================
%                          GAS DATA                     %
%=========================================================================

% General data
   g = 9.806                  ;% [m/s^2] Gravitational Acceleration

% Gas data
   r0    = 8315.4             ;% [J kgmole/kg/K] Universal gas Constant
   mw    = 28.97              ;% [kg/kgmole] Air Molecular Weight
   rair  = r0/mw              ;
   pcr   = 0.528              ;% [/] Critical Pressure ratio
   rk    = 1.4                ;% [/] Specific Heats ratio

% Ambient data
   pair  = 101300             ;% [Pa] Atmospheric Pressure
   tair  = 300                ;% [K] Ambient Temperature
   umid  = 50                 ;% [%] Relative humidity
   rhoair=pair/rair/tair      ;% [Kg/m3] Air Density


%=========================================================================
%                          VEHICLE DATA                 %
%=========================================================================

% Road data
   grade=[0, 0.02, 0.04, 0.06, 0.08, 0.10]                  ;

% Transmission data

% Renault DATA Megane
   etad=.8;
   taud = 3.8                                               ;% dif. gear ratio
   etacv=[0.80, 0.91, 0.93, 0.92, 0.95];
   taucv=[3.7273,2.0476,1.3214,0.9667,0.7949]               ;% JB1 type
   % taucv=[3.3636,1.8636,1.3214,0.9667,0.7949]
   % taucv=[3.0909,1.8636,1.3214,0.9667,0.7381]             ;% JB3 type
   % taucv=[3.7273,2.0476,1.3214,0.9714,0.7561]             ;% JB5 type
   % taucv=[3.3636,1.8636,1.3214,1.0294,0.8205]

 % Geometrical data
   rr =.300                                                 ;% [m] Rolling Effective Radius
   J=1623.8                                                 ;% [kgm^2] Inertia around z axle
   L=2.468                                                  ;% [m] Wheelbase Vehicle
   L1=0.9552                                                ;% [m] semi-Wheelbase front Vehicle
   L2=L-L1                                                  ;% [m] semi-Wheelbase rear Vehicle
   Lsensor=0.30                                             ;% [m] Distance from rear axle to the sensor position
   d=0.25                                                   ;% [m] Relaxation length (or delay length)
   ratio_steer=20;

 % Tyre data
   C1=84085                                                 ;% [Ns/rad] Cornering Stiffness of fornt tyre
   C2=87342                                                 ;% [Ns/rad] Cornering Stiffness of rear tyre
   mu=.9                                                    ;% [/] Coefficient of road adhesion
   h1=0.450                                                 ;% [m] Legth between centre of gravity and ground
   h2=h1                                                    ;% [m] Legth between point of application Faero and ground

   if(C1*L1<C2*L2)
      disp('Understeering Vehicle');          % Understeering/Oversteering Behaviour
   else disp('Oversteering Vehicle');
```

```
   end
% Rigid driveline
   mc=2.8                                                ;% [kg] Crank Mass
   mcr=.3                                                ;% [kg] Connecting Rod Big End Mass
   rc=.03                                                ;% [m] Rc: Crank Radius
   ncyl=4                                                ;% [/] Cylinder Number
   ifw=.3                                                ;% [kgm^2] Flywheel Inertia
   icgi=((mc+mcr))*rc^2*ncyl                             ;% [kgm^2] Crank Gear Inertia
   iengine=icgi+ifw                                      ;% [kgm^2] Total Engine Inertia

   Ieach_wheel=0.08                                      ;% [kgm^2] Wheel Inertia
   iwheel=Ieach_wheel*[(etad)/(taud)]^2                  ;% [kgm^2] Equivalent Wheel Inertia

   mv_sprung=1202                                        ;% [kg] Sprung Mass of Vehicle
   mv_unsprung_front=105                                 ;% [kg] Unsprung front Mass of Vehicle
   mv_unsprung_rear=55                                   ;% [kg] Unsprung rear Mass of Vehicle
   mv=mv_sprung+mv_unsprung_front+mv_unsprung_rear       ;% [kg] Total Mass of Vehicle
   ichassis=(mv*rr^2)*[(etad)/(taud)]^2                  ;% [kgm^2] Equivalent Vehicle Inertia

% Aereodynamics data
   cx = .328                                             ;% [/] Drag Coefficient

   Af=1.6 + 0.00056 * (mv-765)                           ;% [m^2] Frontal Area after J.Y.Wong "Theory of Groung Vehicle"
   sez=Af;

% Engine data
   thvec=[0 20 30 40 50 60 70 80 85 100];
   nevec=[0.8 1.2 1.6 2.0 2.4 2.8 3.2 3.6 5.0 5.4 5.8]*10^3;

   engine_map=[ 26.8204  -29.5025  -32.8550  -35.5371  -38.2191  -40.9012  -43.5832  -46.9358  -49.6178  -52.2999  -55.9819;
                145.1599   78.4498   56.9934   45.2537   29.5025   19.4448    6.7051   -1.3410   -8.7166  -15.7512  -21.4564;
                165.2752  139.4663  119.3509   99.2356   81.8023   69.7331   56.9934   45.2537   32.1845   22.1269   12.0692;
                177.0149  175.3328  161.5931  146.8419  129.4086  111.9753  101.9177   89.1780   79.7908   65.3691   56.9934;
                177.0149  187.0726  189.0841  185.3905  175.3328  159.5816  149.5239  139.4663  126.7266  115.6574 101.9177;
                179.0264  195.4482  196.4597  199.1418  195.4482  185.3905  175.3328  171.6508  156.8996  142.1483 129.4086;
                179.0264  199.1418  205.5058  205.5058  205.5058  201.8238  196.4597  189.0841  179.0264  166.9572  51.5355;
                179.0264  201.8238  206.5174  209.1994  213.8930  216.5750  213.8930  211.8815  199.1418  187.0726 169.6393;
                179.0264  201.8238  209.1994  213.8930  219.2571  219.2571  219.2571  219.2571  209.1994  196.4597 179.0264;
                 179.0264  201.8238   209.1994  213.8930  219.2571  223.9507  223.9507  223.9507  213.8930  205.5058185.3905
                 ];

    figure(1)
   omega_engine=0:500:5000;
   plot(omega_engine,engine_map,'-')
   hold on
   title('Engine map')
   hold on
   xlabel('n_e [rpm]')
   ylabel('T_e [N m]')
   legend('th=0','th=20%','th=30%','th=40%','th=50%','th=60%','th=70%','th=80%','th=90%','th=100%',0)

   figure(2)
   omega_engine=0:500:5000;
   plot(omega_engine/5000,engine_map/223.9507,'-')
   hold on
   title('Adimensionless Engine map')
   hold on
   xlabel('n_e/n_emax [/]')
   ylabel('T_e/T_emax [/]')
   legend('th=0','th=20%','th=30%','th=40%','th=50%','th=60%','th=70%','th=80%','th=90%','th=100%',0)

   %close all
   tstep=0.02;
   tstop=120;
   disp('tstop 120')
```

Appendix B

```
%=============================================================
% gear_box_change m-file
% Vehicle: Renault Mégane Coupé 16V 150 HP
% input: Engine Speed, Actual Gear, Slope Throttle
% output: New Gear
%=============================================================


function [sys,x0,str,ts] = gear_box_change(t,x,u,flag)

%
% Dispatch the flag. The switch function controls the calls to
% S-function routines at each simulation stage of the S-function.
%

switch flag,

  %==========================
  % Initialization %
  %==========================
  % Initialize the states, sample times, and state ordering strings.

case 0
   [sys,x0,str,ts]=mdlInitializeSizes;

  %==================
  % Outputs %
  %==================
  % Return the outputs of the S-function block.

  case 3
    sys=mdlOutputs(t,x,u);

  %==========================
  % Unhandled flags %
  %==========================
  % There are no termination tasks (flag=9) to be handled.
  % Also, there are no continuous or discrete states,
  % so flags 1,2, and 4 are not used, so return an emptyu
  % matrix

  case { 1, 2, 4, 9 }
    sys=[];

  %=============================================================
  % Unexpected flags (error handling)%
  %=============================================================
  % Return an error message for unhandled flag values.

  otherwise
    error(['Unhandled flag = ',num2str(flag)]);

end

%
%=============================================================================
% mdl-InitializeSizes
% Return the sizes, initial conditions, and sample times for the S-function.
%=============================================================================
%

function [sys,x0,str,ts] = mdlInitializeSizes()

sizes = simsizes;
sizes.NumContStates  = 0;
sizes.NumDiscStates  = 0;
sizes.NumOutputs     = 1;      % dynamically sized
```

```
sizes.NumInputs      = 3;   % dynamically sized
sizes.DirFeedthrough = 1;   % has direct feedthrough
sizes.NumSampleTimes = 1;

sys = simsizes(sizes);
str = [];
x0  = [];
ts  = [-1 0];   % inherited sample time

% end mdl-InitializeSizes

%
%=============================================================================
% mdl-Outputs
% Return the output vector for the S-function
%=============================================================================
%

function sys = mdlOutputs(t,x,u)
if (u(3)>=0)
   if (u(1)>5000)                    % 5000 rpm  Default Value
   switch (u(2))
      case {1,2,3,4}
         disp(strcat('Change Velocity',num2str(u(2)+1))),sys(1)=u(2)+1;
      otherwise
         disp('Already in 5th Gear'),sys(1)=u(2);
      end
   elseif (u(1)==5000)               % 5000 rpm  Default Value
       disp('Velocity Engine equal to 5000')
      sys(1)=u(2);
   else
       disp('Velocity Engine lower than 5000')
      sys(1)=u(2);
   end
else
   if (u(1)<2000)                    % 2000 rpm  Default Value
   switch (u(2))
      case {2,3,4,5}
         disp(strcat('Change Velocity',num2str(u(2)+1))),sys(1)=u(2)-1;
      otherwise
         disp('Already in 1th Gear'),sys(1)=u(2);
      end
   elseif (u(1)==2000)
       disp('Velocity Engine equal to 2000')
      sys(1)=u(2);
   else
       disp('Velocity Engine upper than 2000')
      sys(1)=u(2);
   end
end
end
```

Appendix C

```
%=========================================
% Analytical Solution for Steering Pad test
% Vehicle: Renault Mégane Coupé 16V 150 HP
% input: Steering wheel angle
% output: Lateral velocity, Yaw Rate
%=========================================

close all;

tstep=0.002;
tstop=1;
 J=1623.8                                          ;% [kgm^2] Inertia around z-axis (Izz)
 L=2.468                                           ;% [m] Wheelbase Vehicle
 L1=0.9552                                         ;% [m] semi-Wheelbase front Vehicle
 L2=L-L1
 C1=84085                                          ;% Cornering Stiffness of front tyre
 C2=87342                                          ;% Cornering Stiffness of rear tyre

 % Transmission data
   % Renault Megane DATA
   etad=.8;
   etacv=[0.845, 0.904, 0.93, 0.948, 0.957];
   taud = 3.87                                     ;% dif. gear ratio
   taucv=[3.7273, 2.0476, 1.3214, 0.9667, 0.7949]  ;% JB1 type


  % Rigid driveline
   mc=2.5                                          ;% [kg] Crank Mass
   mcr=.35                                         ;% [kg] Connecting Rod Big End Mass
   rc=.04                                          ;% [m] Crank Radius
   ncyl=4                                          ;% [/] Cylinder Number
   ifw=.2                                          ;% [kgm^2] Flywheel Inertia
   icgi=((mc+mcr))*rc^2*ncyl                       ;% [kgm^2] Crank Gear Inertia
   iengine=icgi+ifw                                ;% [kgm^2] Total Engine Inertia

   Ieach_wheel=0.08                                ;% [kgm^2] Wheel Inertia
   iwheel=Ieach_wheel*[(etad)/(taud)]^2            ;% [kgm^2] Equivalent Wheel Inertia

   mv_sprung=1202                                  ;% [kg] Sprung Mass of Vehicle
   mv_unsprung_front=105                           ;% [kg] Un-sprung front Mass of Vehicle
   mv_unsprung_rear=55                             ;% [kg] Un-sprung rear Mass of Vehicle
   mv=mv_sprung+mv_unsprung_front+mv_unsprung_rear ;% [kg] Total Mass of Vehicle

u=20;
delta=0.035

if(C1*L1<C2*L2)
       disp('Understeering Vehicle');              % Under-steering/Over-steering Behaviour
   else disp('Oversteering Vehicle');
   end

   % A Matrix of coefficients
      a11=((C1+C2)/(mv*u));
      a12=[((C1*L1)-(C2*L2))/(mv*u)]+u;
      a21=((C1*L1)-(C2*L2))/(J*u);
      a22=((C1*L1^2)+(C2*L2^2))/(J*u);
      A=-[a11  a12;  a21 a22];

   % Particular Solution Evaluation
     vp=[((C1*L2*L)-(mv*L1*u^2))*C1*u*delta]/[mv*J*u^2*det(A)];
      rp=[C1*C2*L*u*delta]/[mv*J*u^2*det(A)];
      beta_p=vp/u;
      Rp=(1/delta)*[L-[([(C1*L1)-(C2*L2)]/(C1*C2))*mv*u*u/L]];
      alfa_1p=delta-[(vp+(rp*L1))/u];
      alfa_2p=-(vp-(rp*L2))/u;
      if (alfa_1p>alfa_2p) disp('True only if the vehicle is understeering');
         else disp('alfa_1p<alfa_2p because the vehicle is oversteering');          end
```

```
   % General Solution Evaluation
   eig(A)
   ut=(L/2)*sqrt([(C2*L2)-(C1*L1)]/[mv*L1*L2])
   if (u>ut) disp('in fact eigenvalues are complex and conjugate, transient osc. smorz.'); end
   parte_im=imag(eig(A));
   omega=parte_im(1,1)                                    ; %Puls [rad/s]
   parte_re=real(eig(A));
   eta=parte_re(1,1)                                      ;%Smor [s^-1]
   T=2*pi/omega                                           ;%Per [s]
   z1=-[vp;rp]                                            ;% Eigenvectors z1 and z2
   z2=(1/omega)*[A-eta*eye(size(A))]*z1;

;%Initial conditions: v(0)=0; r(0)=0

   % B Martrix
   b11=C1/(mv);
   b21=C1*L1/(J);
   B=[b11; b21];

   C=[1 0;0 1];
   D=[0;0];
   t=0:tstep:tstop;

   U=delta*ones(1,length(t));       % input step
   v_long=20*ones(1,length(t));    % input step

Sys=ss(A,B,C,D);
y=lsim(Sys,U,t,'foh');

figure(1)    % Numerical Solution in matrix form
plot(t,y)
legend('v','r')
close all

Wp=[vp;rp];
Solv=[];
Solr=[];
for k=0:tstep:1
Solv_temp=[exp(eta*k)]*[[z1(1)*cos(omega*k)]+[z2(1)*sin(omega*k)]]+Wp(1)
Solr_temp=[exp(eta*k)]*[[z1(2)*cos(omega*k)]+[z2(2)*sin(omega*k)]]+Wp(2)
Solv=[Solv;Solv_temp];
Solr=[Solr;Solr_temp];
end

figure(1)
plot(t,Solv)
hold on
grid on
plot(t,Solr,'r')
hold on
title('Lateral velocity')
legend('Lateral velocity','Yawing velocity')

figure(2)
alfa1=U'-((V+(R*L1))/u);
alfa2=-((V-(R*L2))/u);
plot(t,alfa1)
title('Slip Angles')
hold on
alfa2=-((V-(R*L2))/u);
plot(t,alfa2,'r')
grid on
hold on
legend('Slip Angle front','Slip Angle rear')

figure(3)
alfa1=U'-((V+(R*L1))/u);
F1=C1*alfa1;
```

```
plot(t,F1)
title('Lateral forces')
hold on
alfa2=-((V-(R*L2))/u);
F2=C2*alfa2;
plot(t,F2,'r')
grid on
hold on
legend('Lateral front force','Lateral rear force')
```

References

[1] N. W. Ressler, and D. J. Patterson, M. W. Soltis, , “Integrated Chassis and Suspension Controls – Present and Future World of Chassis Electronic Controls”, *IEEE International Congress on Transportation Electronics Proceedings*, 1988.

[2] F. Gustafsson, “Estimation and Change Detection of Tyre – Road Friction Using the Wheel Slip”, *Proceedings of the 1996 IEEE International Symposium on Computer-Aided Control System Design*, Dearborn, MI, September, 1996.

[3] J. Leih, “Semiactive Damping Control of Vibrations in Automobile”, *Transactions of the ASME Journal of Vibrations & Acoustics*, Volume 115, July 1993.

[4] G. Yu, and I. K. Sethi, “Road-Following with Continuous Learning”, *Proceedings of the Intelligent Vehicles '95. Symposium*, 1995.

[5] M. Werner, and C. Engels, “A Nonlinear Approach to Vehicle Guidance”, *Proceedings of the Intelligent Vehicles '95. Symposium*, 1995.

[6] E. Freund, and R. Mayr, “Nonlinear Path Control in Automated Vehicle Guidance”, *IEEE Transactions on Robotics and Automation*, Volume 13, No. 1, February 1997.

[7] A. Y. Maalej, D. A. Guenther, and J. R. Ellis, “Experimental Development of Tyre Force and Moment Models”, *International Journal of Vehicle Design*, Volume 10, Number 1, 1989.

[8] L. Palkovics, “The Dynamics of Vehicles on Roads and on Tracks”, Supplement to Vehicle Dynamics, *Proceeding of the 15th IAVSD Symposium held in Budapest, (Hungary, August 25-29, 1997)*, Volume 29, 1998.

[9] http://www.adams.com/

[10] K. Yi and K. Hedrick, "Active and Semi-Active Heavy Truck Suspensions to Reduce Pavement Damage," *Society of Automotive Engineers (SAE) Paper, No. 892486*, November 1989.

[11] H. Hatwal, and E. C. Mikulcik, "Some Inverse Solutions to an Automobile Path Tracking Problem with Input Control of Steering and Brakes", *Vehicle System Dynamics*, Volume 15(1986), 1986.

[12] J. P. M. Hendrikx, J. J. J. Meijlink, and R. F. C. Kriens, "Application of Optimal Control Theory to Inverse Simulation of Car Handling", *Vehicle System Dynamics*, Volume 26(1996), 1996.

[13] J. S. Arora, “Introduction to Optimum Design”, McGraw-Hill, Inc., New York, 1989.

[14] D. E. Smith and J. M. Starkey, "Effects of Model Complexity on the Performance of Automated Vehicle Steering Controllers: Model Development, Validation and Comparison", *Vehicle System Dynamics*, Volume 24(1995), 1995.

[15] J. P. Pauwelussen and H. B. Pacejka, "Smart Vehicles", Swets & Zeitlinger Publishers, 1995.

[16] G. Roppenecker, “Fahrzeugdynamik: Grundlagen der Modellierung und Regelung”, AT Automatisierungstechnik 42, S. 429-441, 1995.

[17] “Vehicle Dynamics Terminology”, SAE J670e, Society of Automotive Engineers (SAE), Inc., Warrendale, PA, July 1976.

[18] W. F. Milliken and D. L Milliken, “Race Car Vehicle Dynamics”, Society of Automotive Engineers (SAE), Warrendale, PA, 1995.

[19] T. D. Gillespie, “Fundamentals of Vehicle Dynamics”, Society of Automotive Engineers (SAE), Inc., Warrendale, PA, 1992.

[20] M. Guiggiani, “Dinamica del veicolo”, CittàStudi Edizioni, Torino, 1998.

[21] M. Mitschke, “Dynamik der Kraftfahrzeuge”, Band A: Antrieb und Brehsung 3. Auflage, Springer, Berlin, 1995. (Relax length)

[22] J. Y. Wong, “Theory of Ground Vehicles”, John Wiley and Sons, Inc., New York, 2001.

[23] G. Genta, “Meccanica dell'autoveicolo”, Levrotto e Bella, 1997.

[24] G. Genta, Motor Vehicle Dynamics, World Scientific Publishing , Singapore, 1997.

[25] S. Bruni, “Appunti di Meccanica del Veicolo”, Dipartimento di Ingegneria Meccanica, Politecnico di Milano, 2002.

[26] J. Fredrikkson, and B. Egardt, “Integrated Powertrain: The Engine as an Actuator”, Control and Automation Laboratory, Department of Signals and Systems, Chalmers University of Technology, SE-412 96 Göteborg, Sweden.

[27] U. Kiencke and L. Nielsen, "Automotive Control Systems", Society of Automotive Engineers (SAE), Inc., Warrendale, PA, 2000.

[28] M. Mitschke, “Dynamik der Kraftfahrzeuge”, Band C: Fahrverhalten, Springer-Verlag, Berlin, 1995.

[29] A. R. Guido e L. Della Pietra, “Lezioni di meccanica delle macchine”, CUEN, Napoli 1989.

[30] ISO 3888, “Road Vehicles – Test procedure for a serve lane change manoeuvre”, 1975.

[31] ISO 4138, “Road vehicles – Steady state circular test procedure– Open-Loop test procedure”, 1996.

[32] ISO 7401, “Road vehicles – Lateral transient response test method”, 1988.

[33] ISO 7975, “Road vehicles – Braking in a turn – Open-Loop test procedure”, 1985.

[34] ISO 9816, “Road vehicles –Dropped throttle in a turn”, 1998.

[35] ISO 8855, “Road vehicles – Vehicle dynamics and road holding ability – Vocabulary”, 1991.

[36] ISO 9816, “Passenger Cars – Power–off reactions of a vehicle in a turn – Open loop test method”, 1993.

[37] A. Porcel, “Contribution à la commande multivariable des systèmes complexes rapides, instables ou pseudostables. Application au contrôle de stabilité de véhicules par approche «12 forces»,” Laboratoire de Modélisation Intelligence Processus et Systèmes (MIPS), Equipe de Modélisation et Identification en Automatique et Mécanique (MIAM), Ecole Supérieure des Science Appliquées pour l’Ingénieur (ESSAIM), Mulhouse, Décembre 2003.

[38] M. G. Vigier, “Pratique des Plans d’Expérience, Méthodologie Taguchi”.

[39] G. Asch and al, “Acquisition de Données du Capteur à l’Ordinateur”.

[40] Brűel and Kjaer, “Accéléromètres Piézoélectrique”, Théorie d’Applications, 1979.

[41] J. Radix, , “Misures de Navigation”, Publication Techniques d’Ingénieur, 1990.

[42] A. Porcel, C. Runde, M. Basset, and G. L. Gissinger, “Neuro-Fuzzy Approach to Real Time Total Velocity Estimation of a Passenger Car Covering Critical Situations ”, IFAC Workshop, Ohio, USA, Proc. 29-36, 1998.

[43] Gen, M., Genetic Algorithms and Engineering Design, Wiley & Sons, New York, 1997.

[44] G. L. Gissinger et N. Le Fòrt-Piat, “Systèmes automatisés: Contrôle-commande de la voiture”, Lavoisier, Paris, 2002.

[45] G. L. Gissinger et N. Le Fòrt-Piat, “Systèmes automatisés: La voiture intelligente”, Lavoisier, Paris, 2002.